AD-A035 512 STEVENS INST OF TECH HOBOKEN N J DAVIDSON LAB F/G 13/10
AMPHIBIOUS HYDROFOIL LIGHTER PRELIMINARY DESIGN VERIFICATION.(U)
MAY 76 C J HENRY N00014-75-C-0384
UNCLASSIFIED SIT-DL-76-1890 NL

1 OF 2
AD-A
035 512

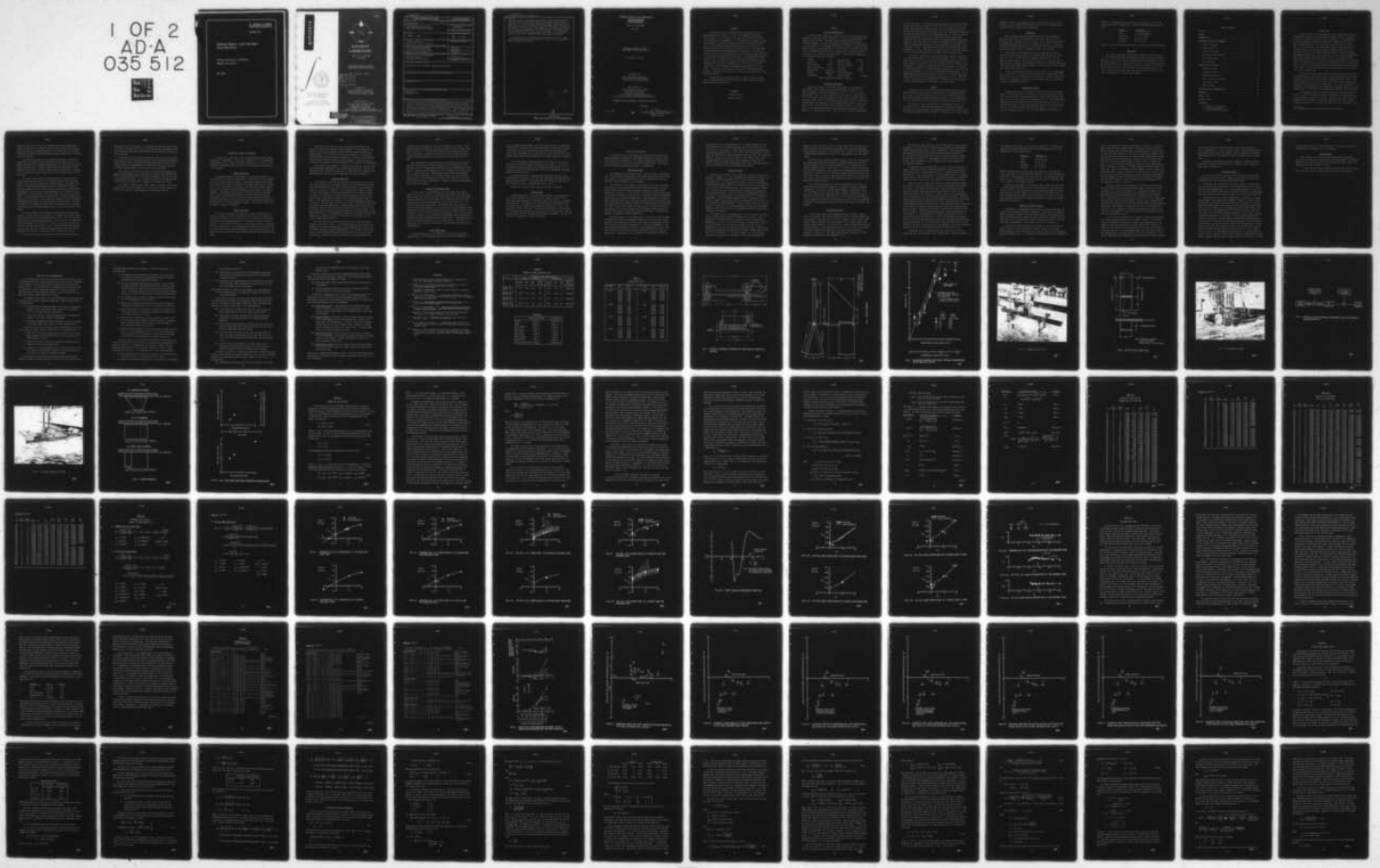

AMPHIBIOUS HYDROFOIL LIGHTER PRELIMINARY DESIGN VERIFICATION

STEVENS INSTITUTE OF TECHNOLOGY
HOBOKEN, NEW JERSEY

MAY 1976

R-1890

DAVIDSON LABORATORY

Report SIT-DL-76-1890
May 1976

AMPHIBIOUS HYDROFOIL LIGHTER PRELIMINARY DESIGN VERIFICATION

by Charles J. Henry

Prepared for

U.S. Army Mobility Equipment
Research and Development Center
Fort Belvoir, Virginia 22060

Administered by

Office of Naval Research (616T)
Department of the Navy
Arlington, Virginia 22217
Under Contract No. N00014-75-C-0384
DL Projects 4254/163,165,166,167,168,169,170,187

STEVENS INSTITUTE OF TECHNOLOGY

CASTLE POINT STATION
HOBOKEN, NEW JERSEY 07030

UNCLASSIFIED

SECURITY CLASSIFICATION OF THIS PAGE (When Data Entered)

REPORT DOCUMENTATION PAGE		READ INSTRUCTIONS BEFORE COMPLETING FORM
1. REPORT NUMBER SIT-DL-76-1890	2. GOVT ACCESSION NO.	3. RECIPIENT'S CATALOG NUMBER
4. TITLE (and Subtitle) AMPHIBIOUS HYDROFOIL LIGHTER PRELIMINARY DESIGN VERIFICATION		5. TYPE OF REPORT & PERIOD COVERED FINAL REPORT 6. PERFORMING ORG. REPORT NUMBER
7. AUTHOR(s) CHARLES J. HENRY		8. CONTRACT OR GRANT NUMBER(s) N00014-75-C-0384
9. PERFORMING ORGANIZATION NAME AND ADDRESS Davidson Laboratory Stevens Institute of Technology Castle Point Station, Hoboken, New Jersey 07030		10. PROGRAM ELEMENT, PROJECT, TASK AREA & WORK UNIT NUMBERS
11. CONTROLLING OFFICE NAME AND ADDRESS U.S. Army Mobility Equipment Research and Development Center Belvoir, Virginia 22060		12. REPORT DATE MAY 1976 13. NUMBER OF PAGES 142
14. MONITORING AGENCY NAME & ADDRESS (if different from Controlling Office) Office of Naval Research (616T) Dept. of the Navy Arlington, Virginia 22217		15. SECURITY CLASS. (of this report) Unclassified 15a. DECLASSIFICATION/DOWNGRADING SCHEDULE

16. DISTRIBUTION STATEMENT (of this Report)

Approved for Public Release; Distribution Unlimited.

17. DISTRIBUTION STATEMENT (of the abstract entered in Block 20, if different from Report)

18. SUPPLEMENTARY NOTES

19. KEY WORDS (Continue on reverse side if necessary and identify by block number)

Amphibians
Hydrofoil Craft

20. ABSTRACT (Continue on reverse side if necessary and identify by block number)

In order to provide verification that the proposed design of an amphibious hydrofoil lighter will meet its hydrodynamic performance specifications, a series of tests were carried out using scaled models of the vehicle and its components. It was shown that the proposed simple control system is effective in providing control in head and following seas. Tandem hydrofoil tests were carried out to verify design lift characteristics and, in particular, the choice of foil spacing was shown to yield optimum lift-drag character-

DD FORM 1 JAN 73 1473 EDITION OF 1 NOV 65 IS OBSOLETE
S/N 0102-014-6601 |

UNCLASSIFIED

SECURITY CLASSIFICATION OF THIS PAGE (When Data Entered)

20. (Cont'd)

istics at take-off. The model was operated in the foil borne mode with light ship and design load conditions, in calm water, head seas and following seas, using the proposed automatic height control. Directional stability and turning characteristics were analyzed. Roll motions at zero speed in beam seas were found acceptable. The behavior of the model was observed while transiting a seven foot periodic surf zone in light ship and design load conditions at 5 and 11 knots. It was found that entering and exiting at 5 knots present no problems. Entering the surf zone at 11 knots will cause some water to be taken over the bow.

Recommendations for further studies are given in order to assure that the proposed design modifications will yield a final design which meets required specifications.

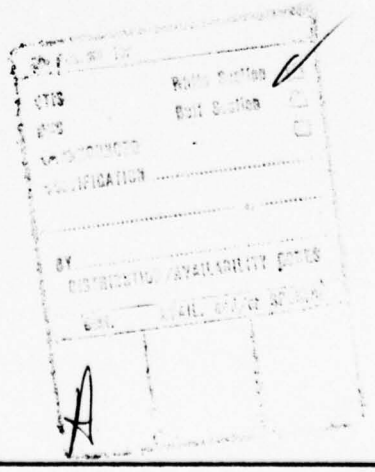

STEVENS INSTITUTE OF TECHNOLOGY
DAVIDSON LABORATORY
CASTLE POINT STATION
HOBOKEN, NEW JERSEY

Report SIT-DL-76-1890

May 1976

AMPHIBIOUS HYDROFOIL LIGHTER
PRELIMINARY DESIGN VERIFICATION

by Charles J. Henry

Prepared for

U.S. Army Mobility Equipment
Research and Development Center
Fort Belvoir, Virginia 22060

Administered by

Office of Naval Research (616T)
Department of the Navy
Arlington, Virginia 22217
Under Contract No. N00014-75-C-0384
(DL Project 4254/163,165,166,167,168,169,170,187)

Approved:

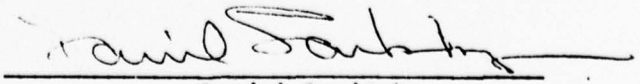

Daniel Savitsky
Deputy Director

vii + 131 pp.

ABSTRACT

In order to provide verification that the proposed design of an amphibious hydrofoil lighter will meet its hydrodynamic performance specifications, a series of tests were carried out using scaled models of the vehicle and its components. It was shown that the proposed simple control system is effective in providing control in head and following seas. Tandem hydrofoil tests were carried out to verify design lift characteristics and, in particular, the choice of foil spacing was shown to yield optimum lift-drag characteristics at take-off. The model was operated in the foil borne mode with light ship and design load conditions, in calm water, head seas and following seas, using the proposed automatic height control. Directional stability and turning characteristics were analyzed. Roll motions at zero speed in beam seas were found acceptable. The behavior of the model was observed while transiting a seven foot periodic surf zone in light ship and design load conditions at 5 and 11 knots. It was found that entering and exiting at 5 knots present no problems. Entering the surf zone at 11 knots will cause some water to be taken over the bow.

Recommendations for further studies are given in order to assure that the proposed design modifications will yield a final design which meets required specifications.

KEYWORDS

Hydrofoil Craft

Amphibious Craft

SUMMARY

Overall Characteristics

A series of model tests was carried out to verify that the amphibious hydrofoil lighter described in Reference 1 will meet its hydrodynamic performance specifications. The model closely represented the prototype vehicle in geometric, dynamic and hydrodynamic characteristics, consisting of a planing hull, fixed submerged hydrofoils with flaps, a foilborne height control system, rudder and wheels for land operation. The vehicle also contains a waterborne propulsion system; however, only the skegs and ventilation plates were included in the towed model. The principal characteristics of the proposed design are as follows:

Length	79'	Hydrofoil Span	34'-6"
Hull Beam	30'	Hydrofoil Chord	6'
Beam at Wheels	44'-2"	Hydrofoil Spacing	45'
Draft (Stationary)	8'-5"	Flap Span	34'-6"
Gross Weight	413,000 lb	Flap Chord	1'-6"
Payload	120,000 lb	Draft (Foilborne)	4'
Installed HP	7200	Take-Off Speed	17 knots

Maximum Speed Fully Loaded 35 knots

Height Control System

Based on the results of the model test program, the recommended foilborne height control system consists of manual control of the aft flap position together with manual and automatic control of the port and starboard forward flaps. A simple automatic control system is recommended for each of the forward flaps consisting of a height sensor, hydraulic actuator, flap and a manual input. The proposed height sensors consist of a vertically hinged twisted flap supported by a strut located between the main strut and wheel on each side of the hull at the forward foil location. The twisted vertical flap should extend from the hull baseline to the hydrofoil and its operation is described as follows. Since this flap is free to rotate about

its vertical hinge, it will continually seek an angle such that the hydrodynamic moment about the hinge is zero. Due to a constant twist per unit length, the zero-moment angular position will ideally be proportional to the submerged span-length of the twisted flap since then the side forces on the upper and lower halves of the submerged portion will cancel and the resultant hinge moment will be zero. Tests of the height sensor output showed that this ideal principle of operation closely represents the actual operation. Over the range of practical flying heights for the proposed vehicle, the height sensor output will be proportional to height and will be independent of speed. Additional manual control inputs forward and manual adjustment of the aft flap angle are needed to adjust fore and aft hydrofoil lift for varying load conditions or to adjust flying height and trim.

The hydraulic actuators in the forward automatic control system provide the necessary power to move the forward hydrofoil flaps in response to deviations in flying height as sensed by the forward height sensors. The model actuators and control system were designed and built so that the rate of change of flap angle with height (gain) could be adjusted. As a result of these model tests it is recommended that a constant value of gain can be used in the prototype for all load conditions and foilborne speeds. It is recommended that additional analyses be carried out to finalize the detailed specifications of this simple automatic height control system. These additional studies should include analyses of foilborne roll motions as well as pitch and heave motions in calm water and irregular seas.

Rudder

Directional stability (ability to maintain heading without control) and minimum turning circle radii were estimated for the amphibious hydrofoil lighter in the displacement mode as well as for foilborne operation. The displacement mode analyses were based on model tests with wheels down while the foilborne analyses were based on available empirical relations.

The results of these analyses show that the proposed vehicle is directionally stable in both the displacement and flying mode. Adequate turning circle characteristics can be obtained by using either (a) fore and aft centerline rudders extending from hull to hydrofoils with constant chord

lengths of 6 feet, or (b) steerable flaps on the aft main struts (or on all four struts). Turning circle characteristics with the proposed single tapered centerline rudder were not acceptable.

Propulsion

Model resistance measurements were obtained for the displacement mode with wheels down, for the foilborne mode in calm water and for the foilborne mode in head and following irregular seas. The results were used to estimate prototype drag for similar operating conditions. In the displacement mode with wheels down and fully loaded, the installed horsepower should give a maximum speed in excess of 11 knots in calm water.

The increase in mean drag in Sea State 2, head seas over that in calm water for foilborne operation, is dependent upon the mean heave and trim of the craft. By making minor changes in mean heave and trim (by means of manual changes in fore and aft flap position), the speed loss in head seas can be made less than 7 percent as desired. At constant mean heave and trim the speed loss at constant power will be 10 percent or less, depending on mean flying conditions.

In the foilborne mode, hydrofoil suction creates a significant depression of the water surface above the foils which will be accentuated at the aft foil due to fluid acceleration by the propellers. Further study of this problem is recommended in order to insure no loss of power resulting from propeller ventialtion or emersion.

Wave-Induced Motions

Heave accelerations at the bow and center of gravity, heave displacement at the center of gravity, pitch angle and drag were measured for the model while foilborne in head and following irregular seas representing Sea State 2, for the light ship and fully-loaded conditions. These measurements were carried out for a range of control gains and mean flap positions. As mentioned previously, it was demonstrated that one control system gain can be used for all load conditions and foilborne speeds, in calm water or in head or following Sea State 2. For the light condition in head seas at

30 knots, the RMS prototype motion levels are expected to be within the ranges given in the following table, depending somewhat on mean heave and trim:

MOTION	RMS LEVEL
Pitch	0.4 to 0.8 degrees
Heave at CG	0.4 to 1.1 feet
Bow Accel.	0.2 to 0.3 g's
CG Accel.	0.1 to 0.2 g's

Bow-up trim or a lower flying height tend to increase all RMS motion levels.

Surf Tests

Surf transit tests were carried out entering the water and exiting with the light ship and design load condition, where the wave period corresponded to 7.2 sec full scale and the breaker height corresponded to 7 feet. The beach slope was 1:6. Based on these tests it is concluded that exiting or entering the surf zone at speeds up to 5 knots presents no difficulties for the fully loaded or light ship conditions. At higher speeds the vehicle will begin to take some green water over the bow particularly in the fully loaded condition, when entering the water.

TABLE OF CONTENTS

Abstract ii

Summary iii

INTRODUCTION 1

EXPERIMENTAL MODELS AND APPARATUS 4

Control Flap Tests 4

Tandem Foil Tests 4

Foilborne Wave Tests 5

Stability and Turning Tests 6

Surf Transit Tests 6

Beam Sea Tests 7

ANALYSIS AND DISCUSSION 8

Control Flap Tests 8

Tandem Foil Tests 9

Foilborne Wave Tests 10

Stability and Turning Tests 12

Surf Transit Tests 14

Beam Sea Tests 15

CONCLUSIONS AND RECOMMENDATIONS 16

REFERENCES 20

TABLES (1-2)

FIGURES (1-10)

APPENDICES

A. Tandem Foil Test Results
B. Foilborne Wave Tests
C. Stability and Turning Tests

INTRODUCTION

A feasibility analysis of an amphibious lighter capable of carrying a 60-short-ton payload from ship-to-shore and onto a beach at a speed of 35 knots in calm water was carried out in Reference 1.* A wheeled vehicle with fixed submerged hydrofoils was selected in comparison with several other candidate concepts, and a preliminary design analysis was carried out. It was estimated that the amphibious hydrofoil lighter could carry the 60-ton payload at the required speed and could maintain 32.5 knots in Sea State 2 using a simple automatic height control in the foilborne mode. The purpose of this study is to further verify that this design concept does meet the hydrodynamic performance specifications. A series of six test phases were carried out for this purpose using a scaled model of the proposed vehicle. The model and the results are described and discussed in this report. Also, a 16mm silent color movie has been prepared showing the model operating in Sea State 2 in the foilborne mode and showing the model transiting a surf zone in the hullborne mode.

The automatic height control system for the proposed vehicle includes some modifications of the existing passive control system which has operated successfully and reliably on three smaller submerged hydrofoil craft. The modifications are the use of a hydraulic actuator for the main flaps and a twisted surface-piercing flap as height sensor. The first test phase of the experimental program gave data to characterize the angular output of the new height sensor, in relation to the submerged span length of the height sensor.

In the proposed vehicle, the spacing between the fore and aft hydrofoils was carefully selected to take full advantage of the wavemaking interference between the fore and aft foils at take-off speed. The lift on the forward hydrofoil creates a free-surface wave which, with proper spacing, develops an upwash at the aft foil which improves its lift-drag ratio. The

*All references noted in this report are listed on page 20.

second test phase was carried out to determine the lift-drag characteristics of the aft foil in the tandem hydrofoil configuration over a range of speed, trim angle and hydrofoil spacing. At the same time, the lift characteristics for both of the model hydrofoils were established for flap angle as well as for trim.

In the third test phase of this experimental program, a dynamically scaled model was tested in the foilborne mode in calm water as well as in head and following seas representing Sea State 2, for the light ship and the design load conditions, in order to demonstrate the effectiveness of the height control system. A range of control gains was tested and it was shown that the vehicle can operate successfully with no automatic control of the aft flaps.

A series of captive model tests were carried out to provide hydrodynamic force characterization in the hullborne mode so that directional stability and turning characteristics could be analyzed. Using these results, it is shown that the proposed vehicle is directionally stable at hullborne speeds and the minimum turning circle diameter for various speeds was analyzed. For the case of foilborne operation, the same results were predicted using semi-empirical lift characteristics for the strut side force rates. In each of these analyses, both the light ship and the design load conditions are considered. It was found that acceptable turning performance can be obtained by using flaps on the main struts for steering. A single aft rudder is not adequate but forward and aft rudders may be an acceptable alternative where each rudder extends from hull to foils, with 6 foot chord length.

In order to demonstrate the amphibious performance of the proposed vehicle, a series of tests were carried out in regular waves with the model entering and exiting a simulated seven-foot surf zone. Both the light ship and the design load condition were tested. No difficulty is anticipated for either load condition in exiting at 11 knots, nor in entering at the same speed for the light ship condition. At 11 knots the design load condition will take some water over the bow which should present no problem for the proposed vehicle and at five knots, no water is shipped over the bow.

In the final test phase, the motions of the model were measured in

beam seas at zero forward speed. In irregular seas representing Sea States 2, 3 and 4, the statistics of the roll and heave motions were obtained. The results show that the vehicle can survive these sea conditions in the wallowing condition.

Conclusions of this study are summarized in the final section of this report, which show that the proposed vehicle meets the desired hydrodynamic specifications using a simple straightforward design which should yield a reliable vehicle. Recommendations for some further study are discussed, which will further enhance or insure the vehicle's performance.

This study was carried out for the U.S. Army Mobility Equipment Research and Development Center, Fort Belvoir, Virginia, administered by the Office of Naval Research, Dept. of the Navy, Arlington, Virginia under Contract No. N00014-75-C-0384. Mr. Frank Stora of Fort Belvoir observed some of the tests and provided helpful suggestions throughout this study.

The author is indebted to Mr. John K. Roper, originator of the design concept, for his helpful suggestions in carrying out the test programs and for his contributions to understanding and interpreting the data.

EXPERIMENTAL MODELS AND APPARATUS

All tests were carried out using a 1/13-scale model of the proposed vehicle and its appendages. The overall characteristics of the model and prototype are listed in Table 1 and shown schematically in Figure 1. The equipment and apparatus used in each of the six test phases are described in this section.

Control Flap Tests

The proposed sensor for the automatic height control system in the foilborne mode is a twisted, free-swinging, surface-piercing flap supported by a fixed strut as shown in Figure 2. The twisted flap has a helicoidal surface with pitch equal to 18.46 deg/ft (20 deg/in model scale). The purpose of this test phase was to determine the relationship between angular position of the control flap and submergence, and to observe any speed dependence. Accordingly, measurements of control flap position were made over a range of submergences and speed in Davidson Laboratory Tank No.1. During these tests the fixed strut shown in Figure 2 was mounted below a flat plate inclined at 18.2 degrees to simulate the deadrise portion of the bottom of the hull where the sensor is mounted. The results of these tests are shown in Figure 3 and Table 2.

Tandem Foil Tests

In order to characterize the model foil system and particularly to define the changes in aft foil loading due to the wake of the forward foil, a series of tandem foil tests were carried out in calm water using a 1/13-scale model of the proposed hydrofoils. The tandem foil setup is shown in Figure 4. The fore and aft foils have the same geometry which is described in Figure 5 and Table 1. The cross-sectional shapes of the model struts and foils were simplified for ease of manufacture to straight sections over the middle half-chord length with rounded leading edge and wedge shaped trailing edge.

The fore and aft foils and struts were mounted on an H-beam such that their longitudinal position could be adjusted. The trim angle of the H-beam also was easily adjusted, and the four flap angles could be set at desired angles. The aft struts and foils were mounted on a lift-drag balance and the pivot of the H-beam was attached to a second lift-drag balance which measured forces on fore and aft foils together. The vertical position of all this apparatus could be adjusted to the desired foil submergences.

This apparatus was mounted on a carriage in DL Tank No.3 and towed over a range of speed, submergence, trim, spacing and flap angles. The four balance outputs were recorded and analyzed on a tank-side digital computer. The detailed results of these tests are described and listed in Appendix A.

Foilborne Wave Tests

A scaled model of the hull was constructed of wood and the struts and foils were mounted as well as skegs, propeller ventilation plates and wheels which could be mounted in the down or retracted position, as illustrated in Figure 1. A picture of the model in the foilborne mode is shown in Figure 6. Four height sensors of the type described above were mounted, as shown in Figure 1. A bracket for the pitch gimbal was mounted in the hull such that the pitch pivot could be moved to any of the CG positions listed in Table 1. This apparatus was attached to a free-to-heave apparatus as seen in Figure 6. Yaw, sway and roll motions were rigidly restrained and the model was towed at constant forward speed. Various ballast weights were added to the model in order to obtain the inertial properties listed in Table 1. The pitch gimbal and heave masts were instrumented so that pitch and heave motions could be monitored. One accelerometer was mounted in the model to measure bow acceleration in heave and another was mounted on the heave mast to sense vertical acceleration at the CG.

All four flaps were automatically controlled with identical control systems illustrated in Figure 7. As the angular position of a control flap changes due to changes in submergence, the corresponding height signal from the angular transducer changes proportionately. This signal is amplified by the gain factor which could be adjusted independently for each of the four flap controls. The resulting error signal drove the flap servo-motor to

change the main flap angle in response to the height error signal. There were basically two adjustments that could be made in each of the four flap control systems, viz., (1) the relative position of the control and main flap, which adjusts the height for zero error signal, and (2) the rate of change of main flap position per unit deflection of the control flap or gain.

This automatically controlled model and apparatus were towed from a carriage in DL Tank No.3 as shown in Figure 6. Tests were made in calm water as well as in irregular head and following seas corresponding to Sea State 2. Control system parameters were first adjusted in calm water, then run in irregular head seas. Then several control system configurations, which were found acceptable for calm water and head seas, were tested in following seas. This procedure was carried out for the light ship weight and for the design load, with wheels up. Several runs from this test phase are included in the movie.

Stability and Turning Tests

With the model in the displacement mode with wheels down, measurements of the drag, side force, roll moment and yaw moment were made over a range of speed, roll angle, yaw angle, rudder angle and turning rate. These tests were carried out in DL Tank No.2 on the rotating arm for the light ship condition and the design load condition, with the model free in trim and heave which were also observed. The forward flaps were locked full down since the height control will call for full flaps when operating in the displacement mode, and the aft flaps were set at six degrees down for all of these tests, since this flap angle was found suitable in the foilborne tests. The tests were carried out to provide the hydrodynamic force representation required to predict straight course directional stability and steady turning equilibrium conditions such as minimum turning diameter. The results of these tests and the details of the stability and turning analyses are given in Appendix B.

Surf Transit Tests

Successful operation of the proposed vehicle requires successful passage through a surf zone between open sea conditions and the beach. In

order to demonstrate the capability of the proposed vehicle in negotiating this phase of its operation, the model was towed in DL Tank No.3, entering into and exiting from a regular wave. One wave period was used in all tests, which corresponded to 7.2-sec full scale. This period falls in the middle-to-short-period range of observed surf periods reported in Reference 2.

The existing beach for absorbing waves in DL Tank No.3 was used for this phase of the test program. The slope of this beach is 1:6, which is relatively steep but not outside of representative beach slopes. The resulting surf zone width was about 3/4 of the vehicle length and the breaker height was about seven feet.

The model was towed at constant speed through the surf zone, with freedom to pitch and heave. The light ship and design load conditions were tested with wheels down. The forward flaps were locked full down and the aft flaps were fixed at six degrees down for all tests.

Several runs from this test phase are included in the movie.

Beam Sea Tests

Although Sea State 2 is the design wave condition, the proposed vehicle must be capable of surviving in seas of greater severity. It is anticipated that beam seas at zero forward speed of the vehicle is a nearly worst condition. Consequently, roll and heave motions were measured for this condition in irregular seas representing Sea States 2, 3 and 4. The apparatus is shown in Figure 8. The tests were carried out in DL Tank No.3 for the design load and the light ship conditions with wheels down. The results of these tests are tabulated and described in Appendix C. Several runs from this test phase are included in the movie.

ANALYSIS AND DISCUSSION

The results of the six test phases were analyzed to verify the estimated hydrodynamic performance of the proposed amphibious hydrofoil lighter design described in Reference 1. The analysis procedures are described in this section and the results are discussed in general terms. Specific details of results and analyses are given in the Appendices.

Control Flap Tests

The measured control flap deflection is shown in Figure 3 and Table 2, for a range of speed and submergence. The speed range covers that for foilborne operation of the proposed vehicle while the submergence varies from very small flap submergence to fully submerged.

From symmetry, in the absence of free-surface, ventilation and separation effects, the expected angular position would be one-half times the pitch of the helicoidal surface times the submergence, as shown by the dashed line in Figure 3. It is seen that in the middle range of submergences, the expected ideal control flap position is reasonably close to the ideal expected value but at small submergence and at large submergence, the measured position deviates from ideal. The observed behavior can be explained by (1) spray forces at small submergence acting on the lower helicoidal face to push the control flap to larger angles than ideal, and by (2) flow separation at the lower end of the strut perhaps at the flap hinge, tending to draw the control flap to smaller angles than that ideally expected. Some speed dependence is observed at extreme submergences.

From these results it is concluded that: (1) the ideal rate of change of control flap angle with submergence (one-half times pitch) gives a good estimate of the observed rate for the middle range of submergences, (2) control flap angle at constant submergence has little speed dependence in the middle range of submergences, and (3) at extreme submergences, control flap position varies with speed and deviates significantly from the ideal expected value. Accordingly, it is concluded that the proposed twisted flap

height sensor gives a reliable output if it is made long enough so that spurious behavior at extreme submergences occurs when the main flap is at or near its limit stops. A longer flap with less pitch should decrease the submergence ranges where spurious behavior was observed while at the same time expanding the middle submergence range where near ideal output was observed. Further testing of this device might better be done in the Davidson Laboratory Water Channel where atmospheric pressure can be modeled thereby more closely approximating full-scale ventilation effects, and where flow conditions can be observed more readily.

Tandem Foil Tests

The results and analysis of the tandem foil tests are presented and described in Appendix A. It was found that both forward and aft foils of the model exhibited evidence of stall or loss of lift due to boundary layer separation. This phenomenon is expected to occur in the prototype at substantially higher values of lift coefficient than for the model due to the larger value of Reynolds number. The results presented in Reference 3 indicate that the prototype hydrofoils should achieve a maximum lift coefficient between 1.1 and 1.2 while the observed maximum lift coefficient for the model appears to be between 0.6 and 0.8 in Figures A-1 through A-8. The various other characteristics of the model lift and drag are compared with expected values from References 3, 4 and 5, and it is concluded that these references provide reliable results for the prediction of prototype lift and drag, combined with observed Froude number dependent terms from this study. The recommended prediction procedure is summarized in Appendix A.

The forward foil lift is composed of lift due to camber, trim, flap angle and Froude number effects or wave-making. Lift due to camber is represented by a zero lift angle of attack which can be obtained from Reference 6. Lift due to trim and flap angle are determined from the results of Reference 3 for infinite fluid together with the results of Reference 4 for free-surface effects at high Froude number. The effect of finite Froude number was estimated from the present results together with the results of Reference 7. Lift due to camber, trim, flap angle and wave-making is expected to be the same on forward and aft hydrofoils.

However, the aft foil will also feel the wake effect from the forward foil, which has been divided into high Froude number and wave-induced components in the expression for aft foil lift coefficient. The empirical coefficients in these two contributions to aft foil lift were evaluated from the present results.

One of the primary purposes stated for these tests was to substantiate the advantageous choice of foil spacing at take-off speed where the wave-induced upwash at the aft foil due to forward foil lift should yield the maximum lift-drag ratio for the aft foil. It is seen in Figure A-9 that the design take-off condition is very close to the estimated spacing for maximum upwash and in Figure A-15 it is very close to the estimated spacing for maximum aft foil lift. At the same time, Figure A-16 shows nearly constant drag for various spacings so that the desired maximum value for the aft foil lift-drag ratio has been achieved.

The recommended procedure for predicting hydrofoil drag of the proposed vehicle as described in Appendix A is composed of profile drag based on Reference 3 plus various induced drag components. Induced drag due to lift from camber and trim, and flap angle, is based on Reference 5, while that due to Froude number dependent lift is estimated from the present results. On the aft foil, induced drag due to lift from forward foil downwash is also assumed to be given by the results of Reference 5 since the mechanism producing an induced velocity should not effect the rate at which drag is developed.

Foilborne Wave Tests

The 1/13-scale model of the proposed amphibious hydrofoil lighter which is described in the previous section was towed at constant speed while free to move in pitch and heave and with the automatic height control system. Vehicle response characteristics were observed over a range of speeds and control system parameters, in calm water and in head and following seas representing Sea State 2. Both load conditions described in Table 1 were tested. A detailed description and tabulation of the test results are given in Appendix B. Several runs from these tests have been included in the movie demonstrating the model of the proposed vehicle.

The results of these tests show that the proposed vehicle can operate acceptably in calm water and in head or following waves using the proposed simple automatic height control on the forward flaps. To achieve acceptable operating qualities over a range of load and speed, adjustment of (1) the forward flap null positions, and (2) fixed aft flap angle, should be available to the pilot. It would appear at this time that one fixed value of control system gain for the forward flaps may be acceptable for all operating conditions.

In addition to the foilborne tests, a series of runs were made at low speed in calm water with the light ship condition in order to study take-off characteristics. Based on these tests, it is concluded that with the forward flaps in the full-down position in the hullborne mode, with the aft flaps adjusted by the pilot and with the resulting bow-up trim, a take-off speed of 17 knots is well within the capabilities of the proposed design.

Many of the runs in calm water exhibited a long-period lightly-damped oscillation in pitch and heave which is similar to the phugoid oscillation of aircraft. Even though this oscillation is usually stable, the long-period can lead to sufficiently large transient motions so that the hull re-enters the water after take-off. In waves, there is some evidence that this oscillation can also be excited by wave impacts on the bow. These test results indicate that the damping of the phugoid oscillation can be increased by decreasing the forward control gain, or by increasing the mean trim. Lightly-damped short-period oscillations in pitch and heave were also observed and eliminated by adjusting control settings. Finally, the forward control gain will have a significant effect on roll motions of the craft, which were not investigated. Based on these observations of response characteristics of the model, it is concluded that (1) automatic height control aft is not required for calm water operation or in waves, (2) acceptable pitch-heave dynamics and equilibrium conditions can be achieved through appropriate selection of control gain for the forward flaps and the above-mentioned pilot adjustments, and (3) a dynamic analysis of the prototype in the flying condition should be carried out to estimate the required forward control gain.

Measurements of wave-induced motions and accelerations for fully-loaded and light ship conditions in the foilborne mode in head and following

seas representing Sea State 2 are described in Appendix C. The RMS prototype motions depend on mean heave and trim and are expected to be in the ranges shown in the following table:

MOTION	RMS LEVEL
Pitch	0.4 to 0.8 deg
Heave	0.4 to 1.1 ft
Bow Accel.	0.2 to 0.3 g
CG Accel.	0.1 to 0.2 g

Based on the observed increase in mean drag between calm water and head seas in Sea State 2 with the light ship condition, it is estimated that the speed loss at constant power will be 10 percent or less, depending on mean heave and trim. By adjusting mean heave and trim in waves, the speed loss can be reduced to values below 7 percent.

During this test phase, it was observed that a significant depression is created above each hydrofoil due to suction pressures on the upper surface of the foils. This depression will be augmented by propeller induced acceleration of the fluid above the aft foil of the full-scale vehicle. It would therefore seem desirable to fly with bow-up trim in order to increase water depth over the aft foil in order to minimize the chances of propeller ventilation or emersion.

Stability and Turning Tests

Measurements of hydrodynamic forces acting on the model described previously were analyzed as described in Appendix C. Using empirical relations based on these measurements, the directional stability, turning equilibrium conditions and the dynamic stability of these turning equilibrium conditions were predicted for the model with a single aft rudder as shown in Figure 9a. Test speeds corresponded to the full-scale range of 3 to 11 knots.

The model was found to be statically unstable in yaw angle about the center of gravity, as are many marine vehicles. However, the yaw rate damping moment is stabilizing and large so that the vehicle is directionally stable on straight course. In analyzing directional stability, the theoretical

results of Reference 9 were used for added mass of the hull. The turning radius with the original rudder design is unacceptably large which also results from the large stabilizing yaw rate damping moment. Further analysis shows that there should be no difficulty in obtaining acceptable turning qualities with either one of two practical design modifications, namely, (1) installation of an additional bow rudder, or (2) use of flaps on the four main struts for steering instead of rudders. Also, if rudders are used, its side area should be changed such that the rudder extends from hull to foils as shown in Figure 9b, in order to obtain the optimum rudder side force rate. Use of an additional bow rudder appears to be the simpler design modification. However, steering with strut flaps is not overly complicated, requires smaller steering power, is less susceptible to damage and will give somewhat better turning qualities. The proposed rudder geometry for fore and aft rudders is shown in Figure 9b while the proposed strut flap rudders are shown in Figure 9c.

Calculations carried out in Appendix C verified that the predicted turning diameter, using the proposed rudder design, by means of a simplified model of the turning conditions, are in substantial agreement with estimates based on the more accurate model obtained from data analysis. Using empirical results of Reference 10 for representing side forces on struts, the directional stability and turning radius for the foilborne mode were analyzed. Using strut-flap rudders, a large range of stable flying conditions is obtained for both the light ship and the design load condition. The turning circle diameter is estimated to be 2.6 vehicle lengths for a light ship, or 3.0 lengths for the design load condition, where a flying condition of one degree trim and 3.9-ft zero-trim foil submergence was assumed for both load conditions.

All of the turning calculations are based on simplifying assumptions. Roll angle has been neglected in all estimates. Forces on the hull and skegs were neglected in the simplified model used to analyze strut-flap rudders in both the displacement mode and foilborne mode. However, roll angles in turns should be very small because of the large roll stiffness provided by the hull in the displacement mode, and by the height control in the foilborne mode. Estimates based on the simplified model were in substantial agreement with corresponding estimates based on the model obtained

from the data analysis so that the neglect of hull and skeg forces is valid. Consequently, it is felt that the trends in turning characteristics predicted here are reliable and, further, that the magnitude of predicted turning qualities is representative of those to be expected on the prototype.

Prototype drag estimates described in Appendix C indicate that the prototype is capable of making more than 11 knots when fully loaded with wheels down in calm water.

Surf Transit Tests

The results of the surf transit tests are descriptive and are best illustrated by viewing the movie. Runs were made entering the water and exiting with the light ship and design load conditions.

No problems were encountered in the exiting phase. Runs were made with various wave phases at the time of first beach impact and all exiting conditions progressed smoothly with no water being shipped. All runs with the light ship condition were made at a speed of 11 knots (full-scale speed) while for the design load condition speeds of 5, 11 and 16 knots were run.

Entering the surf-zone from the beach gave no difficulty at 5 knots. At high speeds, some difficulty was observed. However, it should be kept in mind that (1) the model was entirely open while the vehicle will have a watertight weather deck so that water over the bow presents no great problem, and (2) the beach used in the model studies had a severe slope (1:6) which dictates a large bow-down attitude as the vehicle enters the first wave crest. Thus, the model operation represents at least a worst case for investigating prototype surf operation. Since the model negotiated the surf zone successfully, prototype operation should be found acceptable. On entering the surf zone with the light ship condition at 11 knots, the model took some water over the bow but easily rose over the second crest and continued out to sea. With the heavier condition at the same speed, the bow rises less rapidly and more water is taken over the bow. With the worst timing of entry, it is possible that green water will be shipped over the bow at 11 knots. However, entering the surf zone at 5 knots with the design load, it appears that only spray or spray sheets will fall on deck. The bow

extension plate added to the model helped very little at 11 knots and is not recommended as necessary for the prototype.

Beam Sea Tests

Heave motions, roll motions and wave heights were digitized and analyzed to find the root mean square values of each signal. The observed RMS levels are plotted in Figure 10 for the three sea states tested, and these runs have been included in the movie.

It is seen that the motion levels are not severe and the movies show that little water will be taken on deck up to the sea state tested.

CONCLUSIONS AND RECOMMENDATIONS

A 1/13-scale model of the design concept defined in Reference 1 for an amphibious hydrofoil lighter was subjected to various tests as described in this report, in order to verify that the vehicle can meet the design specifications. It is concluded that the proposed vehicle can carry a 60-ton payload at 35 knots, maintaining a speed of at least 32.5 knots in head seas with an installed power of 7200 HP. Specific observations and conclusions based on these tests are as follows:

The proposed height sensor, a twisted flap piercing the water surface, was tested over a range of speed and submergence. Based on these tests, it is concluded that:

1) The ideal rate of change of control flap angle with submergence (one-half times pitch) gives a good estimate of the observed rate for the middle range of submergences.

2) Control flap angle at constant submergence has little speed dependence in the middle ranges of submergences.

3) At extreme submergences, control flap position varies with speed and deviates significantly from the ideally expected value.

Tandem foil tests were carried out using a scaled model of the actual foils, flaps and struts. Based on these tests, it is concluded that:

4) Model foil lift results showed evidence of stall at a lift coefficient between 0.6 and 0.8 while stall of the prototype is expected between 1.1 and 1.2.

5) The desired maximum lift-drag ratio has been achieved with the design foil spacing at take-off speed.

6) Prototype lift and drag characteristics should be predicted using the procedure outlined herein, based on available empirical results and on the results of these measurements.

The dynamically scaled model of the proposed amphibious hydrofoil lighter was towed at constant speed while free to move in pitch and heave,

with the proposed automatic height control. Based on these tests, it is concluded that:

7) The proposed vehicle can operate acceptably in calm water and in head and following seas representing Sea State 2, using the proposed height control system forward only.

8) To achieve acceptable operating qualities over a range of load and speed conditions, adjustments available to the pilot should include (a) forward flap null position, and (b) fixed aft flap angle. It presently appears that one gain for the height control system can be used for a wide range of speed and load conditions.

9) The proposed take-off speed of 17 knots is well within the power and lifting capabilities of the design.

10) Damping of the observed phugoid-oscillation can be increased by decreasing forward control gain and by increasing the mean trim.

11) Wave-induced motions in Sea State 2 are small and the RMS acceleration at the bow in head seas was observed to be 0.2g for the fully loaded condition at 35 knots.

12) The speed loss in head seas can easily be made less than 7 percent by means of small changes in mean heave or trim. The speed loss at constant heave, trim and power will be 10 percent or less, depending on mean heave and trim.

13) Hydrofoil suction creates a significant depression above the foils which will be accentuated at the aft foil by fluid acceleration due to propeller thrust. Running with a small bow-up trim should alleviate any resulting propeller ventilation or emersion.

Directional stability, turning equilibrium conditions and dynamic stability of these equilibrium conditions were estimated using measurements of forces and moments on the model as well as empirical relations for strut added mass and theoretical estimate of hull added mass. Based on these measurements and analyses, it is concluded that for hull-borne operation:

14) The proposed vehicle is statically unstable in yaw angle about the center of gravity, as is true of many marine vehicles.

15) Lateral plane damping derivatives are large leading to a high degree

of directional stability.

16) The proposed aft rudder does not give acceptable turning performance due to the overpowering effects of the stabilizing damping derivatives.

17) Acceptable turning performance will be achieved by using either (a) fore and aft rudders extending from hull to foils, or (b) strut-flap rudders on all four struts.

For foilborne operation using strut-flap rudders, it is concluded that:

18) The proposed vehicle is directionally stable with acceptable turning performance.

Surf transit tests were carried out entering the water and exiting with the light ship and design load conditions, where the period of the wave was 7.2 seconds and the breaker height was 7 feet. The beach slope used was 1:6. Based on these tests, it is concluded that:

19) In the light ship or design load condition, exiting the surf zone presents no difficulties at speeds up to 11 knots.

20) Entering the surf zone, the model test conditions and setup represents a nearly worst condition for judging prototype operation.

21) With the design load condition at 5 knots, some spray or spray sheet will come over the bow when entering the first wave, but no green water should come over the bow.

22) On entering the surf zone with the light ship condition at 11 knots, the model took some water over the bow from the first crest, but easily negotiated the second crest and continued out to sea.

23) With the design load condition at 11 knots, water will be shipped over the bow when entering the first wave crest but should not present too great a problem for the prototype.

The model was subject to irregular beam seas with the design load condition at zero speed and with RMS wave elevation up to 2.1 feet (significant height 8.5 feet between Sea States 4 and 5). Based on these tests, it is concluded that:

24) The proposed vehicle can easily survive in waves up to at least

sea state 5 with acceptable motion levels and with little water taken on deck.

The overall conclusion is that the proposed design described in Reference 1 for an amphibious hydrofoil lighter will have acceptable operational qualities with only slight changes as follows:

25) The height control sensor should extend from the hull baseline to the hydrofoil.

26) Steering should be controlled by four strut flaps rather than a single aft rudder or fore and aft rudders.

In the further development of this craft, the confidence gained from these model tests indicates that the next development phase should be a manned model supported by some preliminary analyses and tests. In particular, the following development tasks are recommended:

27) Height Sensor Test — A small model of the extended height sensor should be tested in a variable pressure water channel, in order to assure that the ideal output rate is achieved over a wide range of submergence.

28) Dynamic Analyses — Simulation of vehicle behavior should be carried out to study dynamic stability and response over a range of foil-borne speed and load conditions, in order to specify an acceptable range of gain for the height control system. Degrees of freedom should include sway, heave, roll, pitch and yaw. No further model tests are required to support this task.

29) Manned Model Design — Based on Items 27 and 28 and on the concept design in Reference 1, a manned model should be designed for further testing of this concept. A scale ratio between 1:2.9 to 1:3.2 seems reasonable at this time.

30) Manned Model Testing — The manned model design from Item 29 should be constructed and tested over a range of speed, load and environmental conditions.

Based on this recommended development program, a final prototype design can be established with confidence that the prototype operational qualities will be found acceptable.

REFERENCES

1. "60-Ton Amphibious Lighter Conceptual Design," M. Rosenblatt and Son, Inc., MR&S Report No.2106-1, March 1972.

2. Dalzell, J.F., "The Simulation of Vehicle Performance in Surf-1," Journal of Terramechanics, Vol.10, No.2, 1973.

3. "Data Sheets - Aerodynamics," Royal Aeronautical Society, Technical Department, London, 1965.

4. Wadlin, K. and Christopher, K., "A Method for Calculation of Hydrodynamic Lift for Submerged and Planing Rectangular Lifting Surfaces," NASA Technical Report R-14.

5. Glauert, H., The Elements of Aerofoil and Airscrew Theory, Cambridge University Press, 1959.

6. Abbott, I. and VonDoenhoff, A., Theory of Wing Sections Including a Summary of Airfoil Data, Dover Publications, New York, 1959.

7. Sottorf, W., "Experimental Investigations Concerning the Problems of Hydrofoils," DT NSRDC Translation 299, June 1966.

8. Milne-Thomson, L.M., Theoretical Aerodynamics, MacMillan and Co., New York, 1958.

9. Kim, C., Henry, C. and Chou, F., "Hydrodynamic Characteristics of Prismatic Barges," Stevens Institute of Technology, Report OE-71-7, September 1971.

10. Breslin, J., "The Hydrodynamic Characteristics of Several Surface-Piercing Struts, Part II: The Side Force Developed in the Absence of Ventilation," Davidson Laboratory Report SIT-DL-56-597, January 1956.

TABLE 1

SUMMARY OF MODEL CHARACTERISTICS

Configuration	OVERALL WEIGHTS AND INERTIAS							
	MODEL (1/13 Scale)				FULL SCALE			
	Weight lb	LCG in	VCG in	Pitch Inertia ft^2 - lb	Weight tons	LCG ft	VCG ft	Pitch Inertia ft^2-tons
Light Ship Wheels Up	121.6	30.0	4.32	283	120	32.5	4.7	46,900
Design Load Wheels Up	187.8	31.2	5.57	365	184	33.8	6.0	60,500
Light Ship Wheels Down	121.6	30.0	2.70	283	120	32.5	2.9	46,900
Design Load Wheels Down	187.8	31.2	4.56	365	184	33.8	4.9	60,500

DIMENSIONS

	Model (1/13 Scale)	Full Scale
Length	72.90 in	79.00 ft
Beam	27.70 in	30.00 ft
Foil Spacing	41.50 in	45.00 ft
Foil Span	32.00 in	34.67 ft
Foil Chord	5.50 in	5.96 ft
Flap Chord	1.38 in	1.49 ft
Strut Length	4.50 in	4.88 ft
Strut Chord	5.50 in	5.96 ft
Control Flap Pitch	20 deg/in	18.46 deg/ft

TABLE 2

CONTROL FLAP TESTS

Submergence ft	Speed kt	Deflection deg	Submergence ft	Speed kt	Deflection deg
0.271	17.04	4.50	1.354	17.04	11.25
	20.62	4.00		20.62	12.25
	24.23	4.25		24.23	12.50
	27.84	3.00		27.86	12.75
	31.40	3.50		31.40	12.75
	35.03	3.25		35.03	12.50
	17.04	4.50			
0.542	17.04	3.25	1.625	17.04	11.75
	20.62	4.50		20.62	12.00
	24.23	5.00		24.23	11.75
	27.86	5.25		27.84	11.75
	31.40	5.50		31.40	11.75
	35.03	5.50		35.03	11.75
0.812	17.04	5.25	1.896	17.04	12.50
	20.62	5.75		20.62	12.75
	24.23	6.25		24.23	12.50
	27.84	6.75		27.84	13.50
	31.40	6.75		31.40	13.75
	35.03	6.75		35.03	13.50
1.083	17.04	8.25	2.437	17.04	14.75
	20.62	8.50		20.62	14.25
	24.23	8.75		24.23	13.50
	27.84	9.00		27.84	13.25
	31.40	9.00		31.40	13.50
	35.03	9.00		35.03	13.50

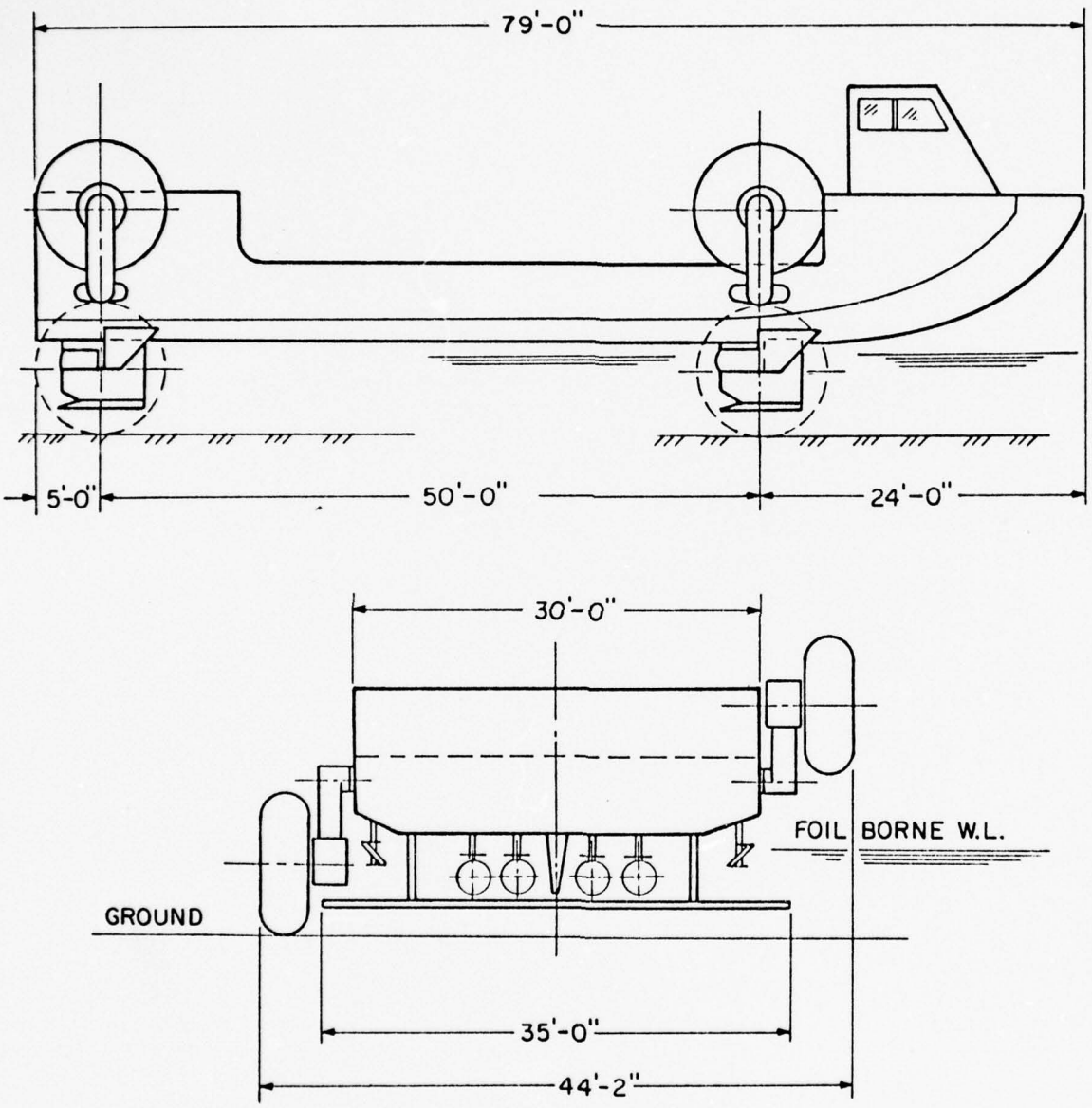

FIG. I. OVERALL SCHEMATIC DRAWING OF AMPHIBIOUS HYDROFOIL LIGHTER

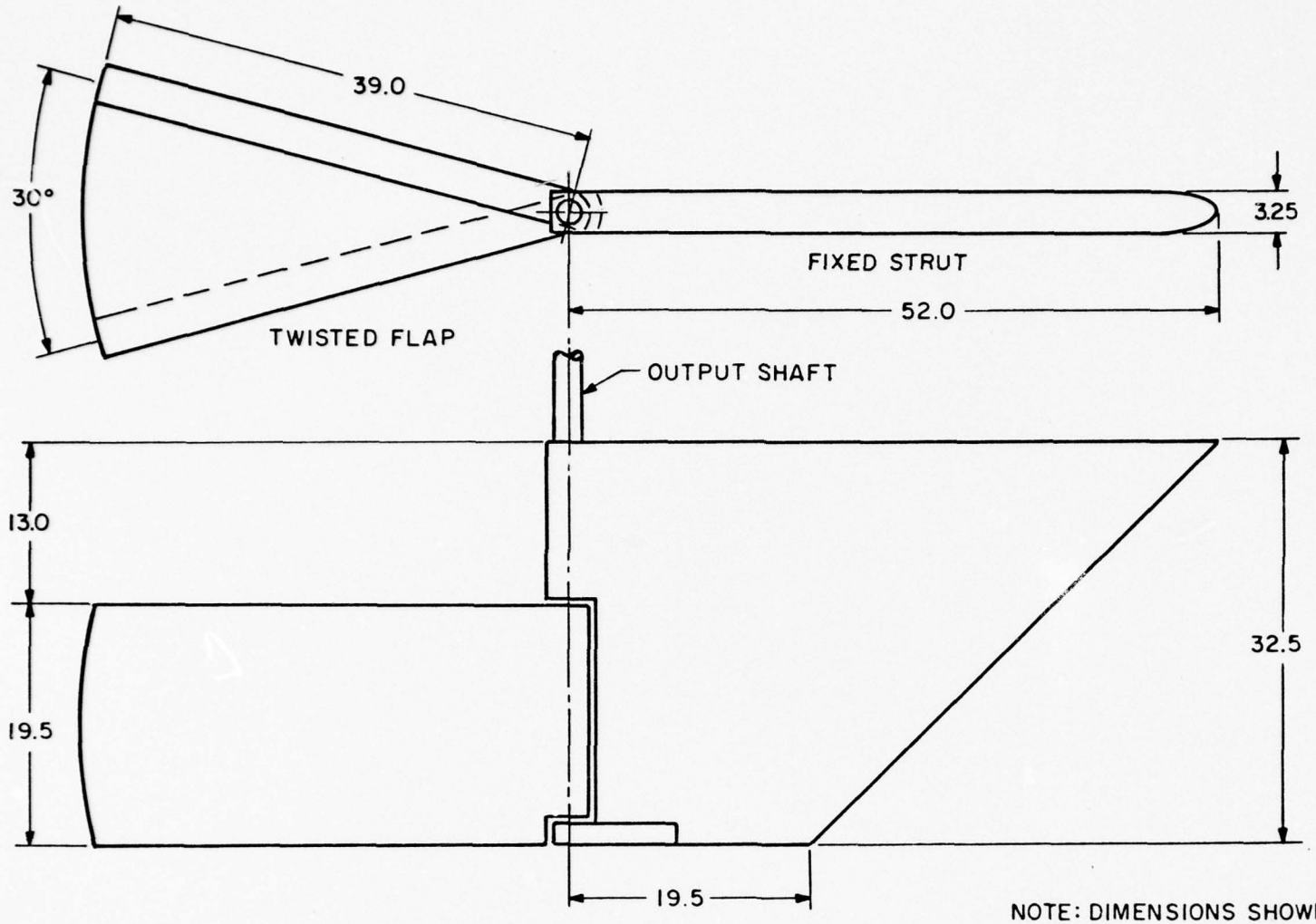

NOTE: DIMENSIONS SHOWN IN INCHES, FULL SCALE.
MODEL WAS 1/13 OF FULL SCALE.

FIG. 2. HEIGHT SENSOR

R-1890

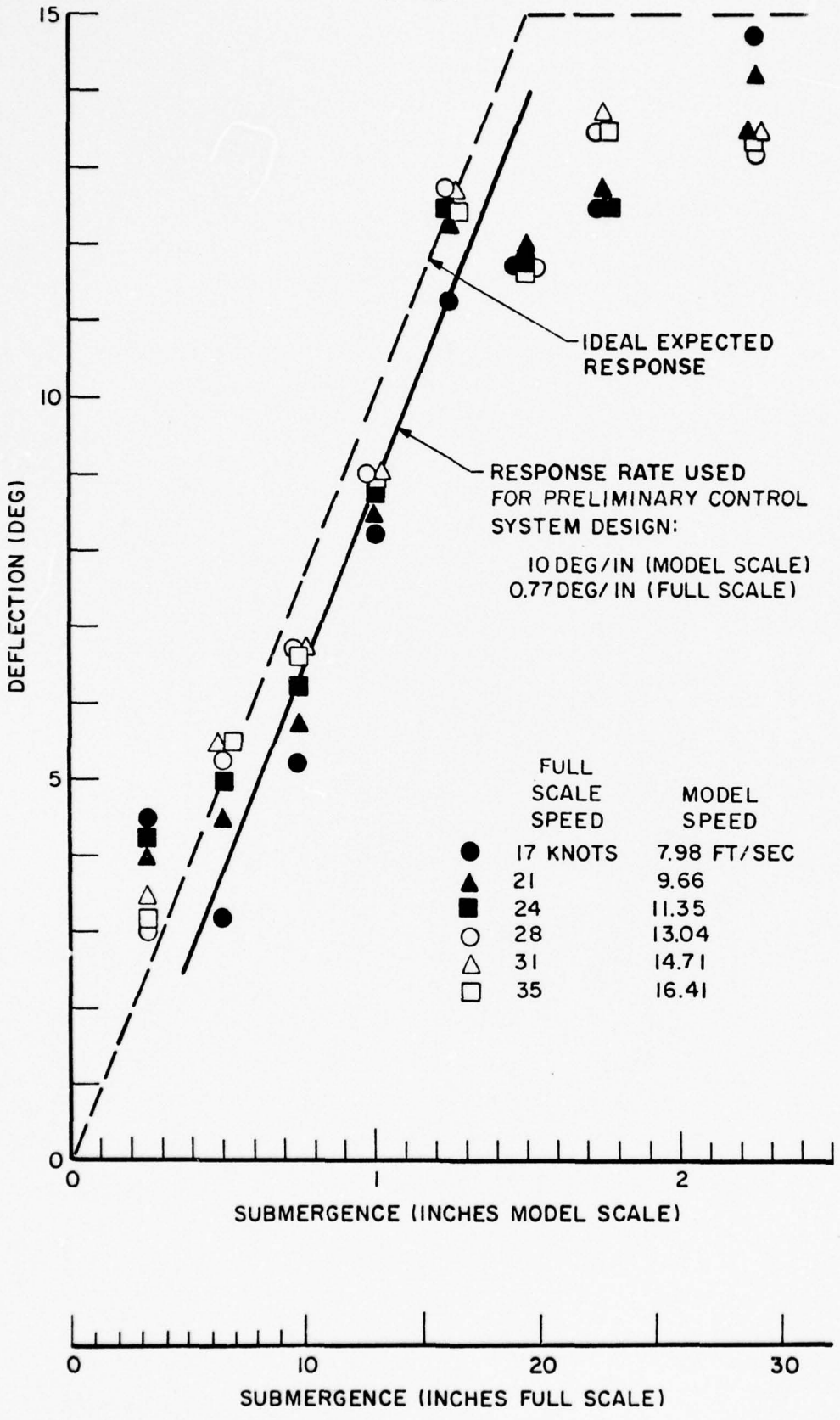

FIG. 3. MEASURED CONTROL FLAP ANGLE VERSUS SUBMERGENCE OVER RANGE OF SPEEDS

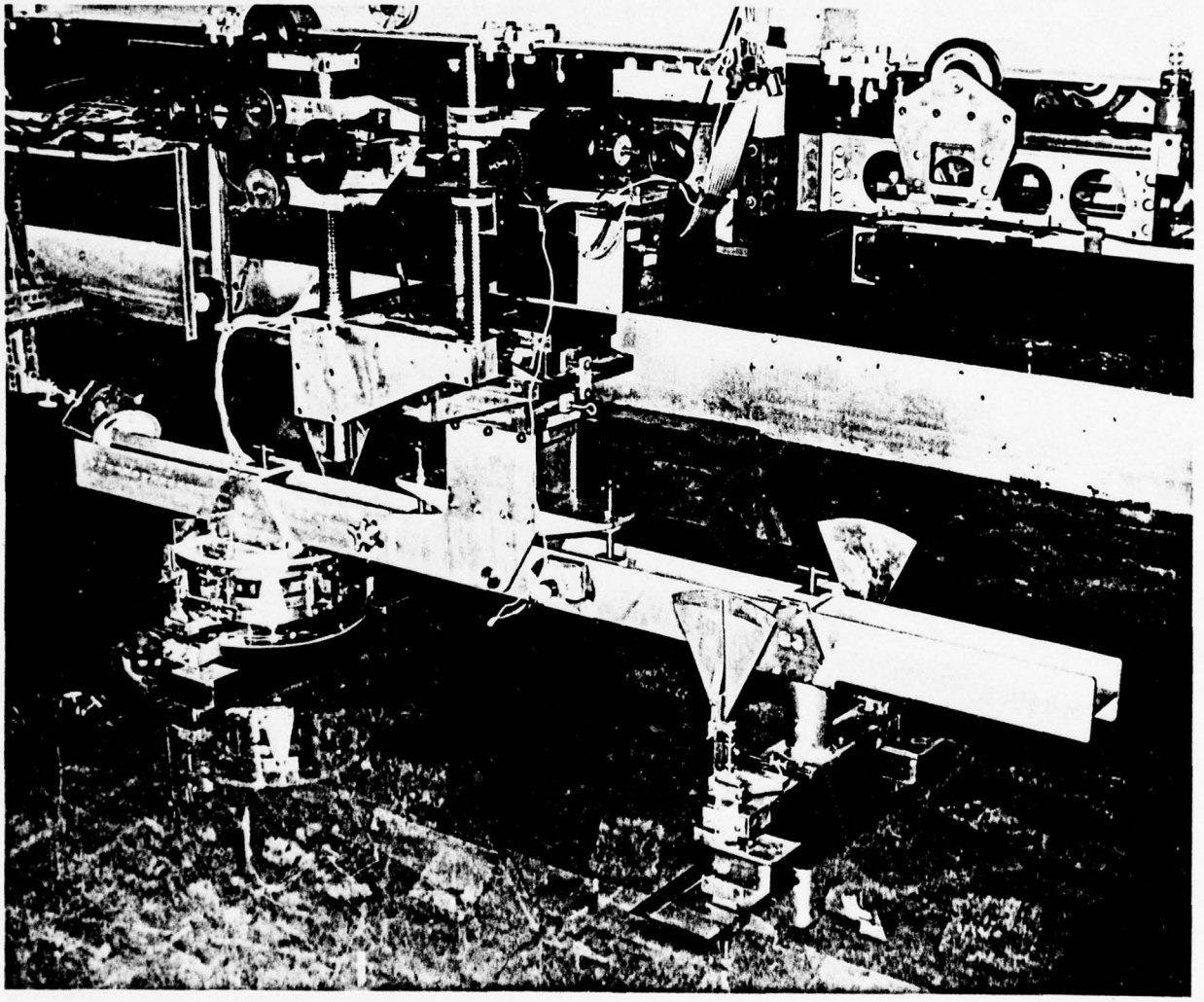

FIG. 4. TANDEM FOIL TEST SETUP

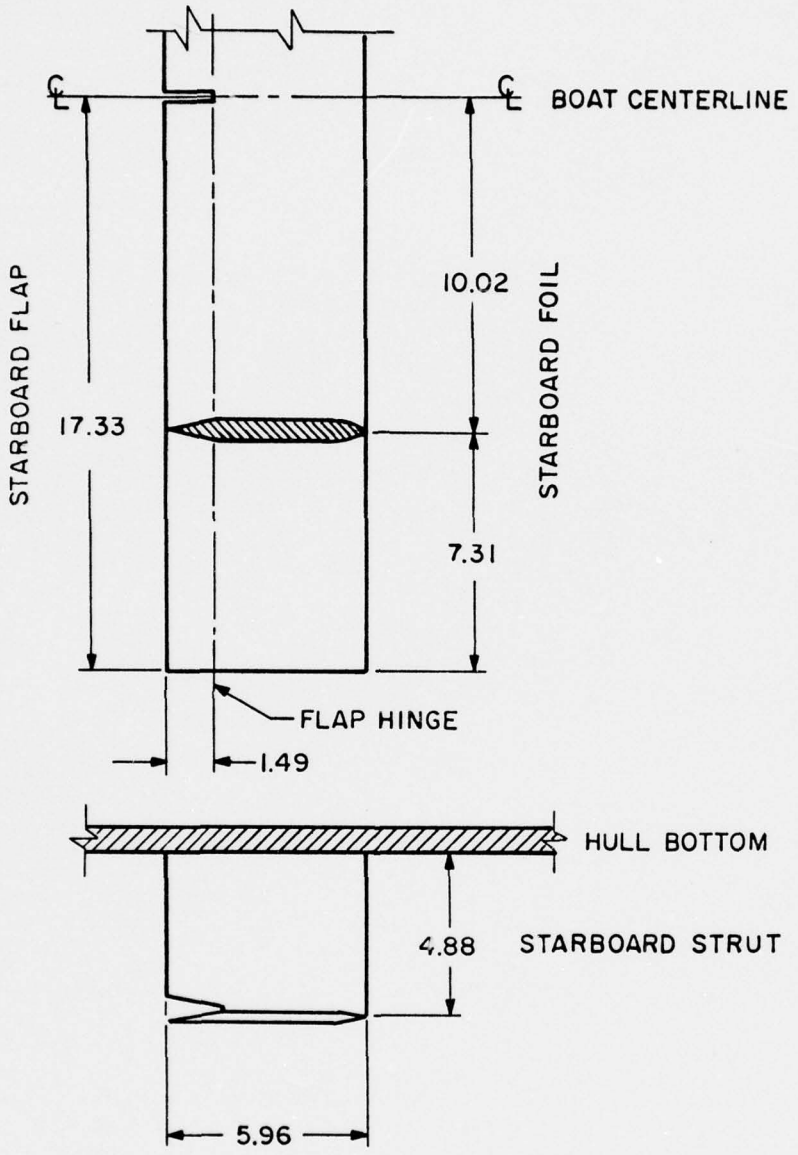

FIG. 5. STRUTS, FOILS AND FLAPS

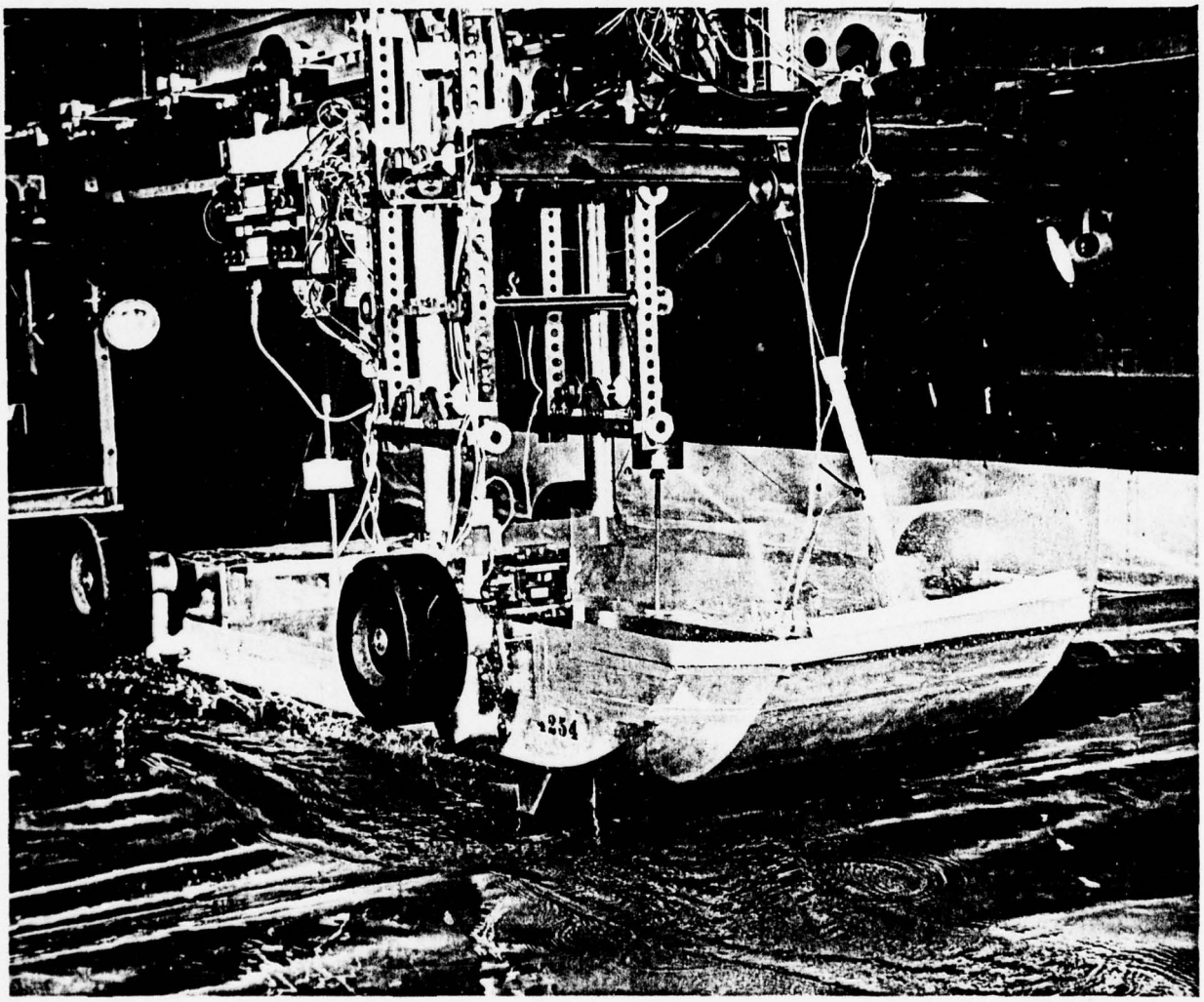

FIG. 6. FOILBORNE TEST SETUP

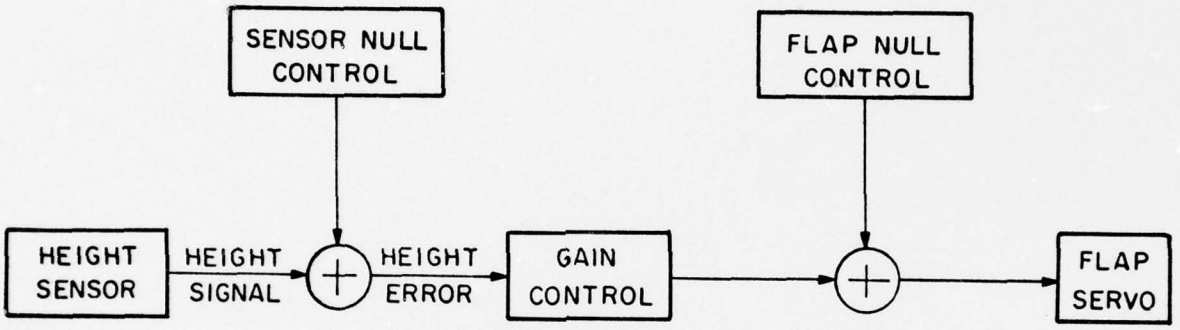

FIG. 7. CONTROL SYSTEM SCHEMATIC FOR MODEL STUDY OF CONTROL CHARACTERISTICS

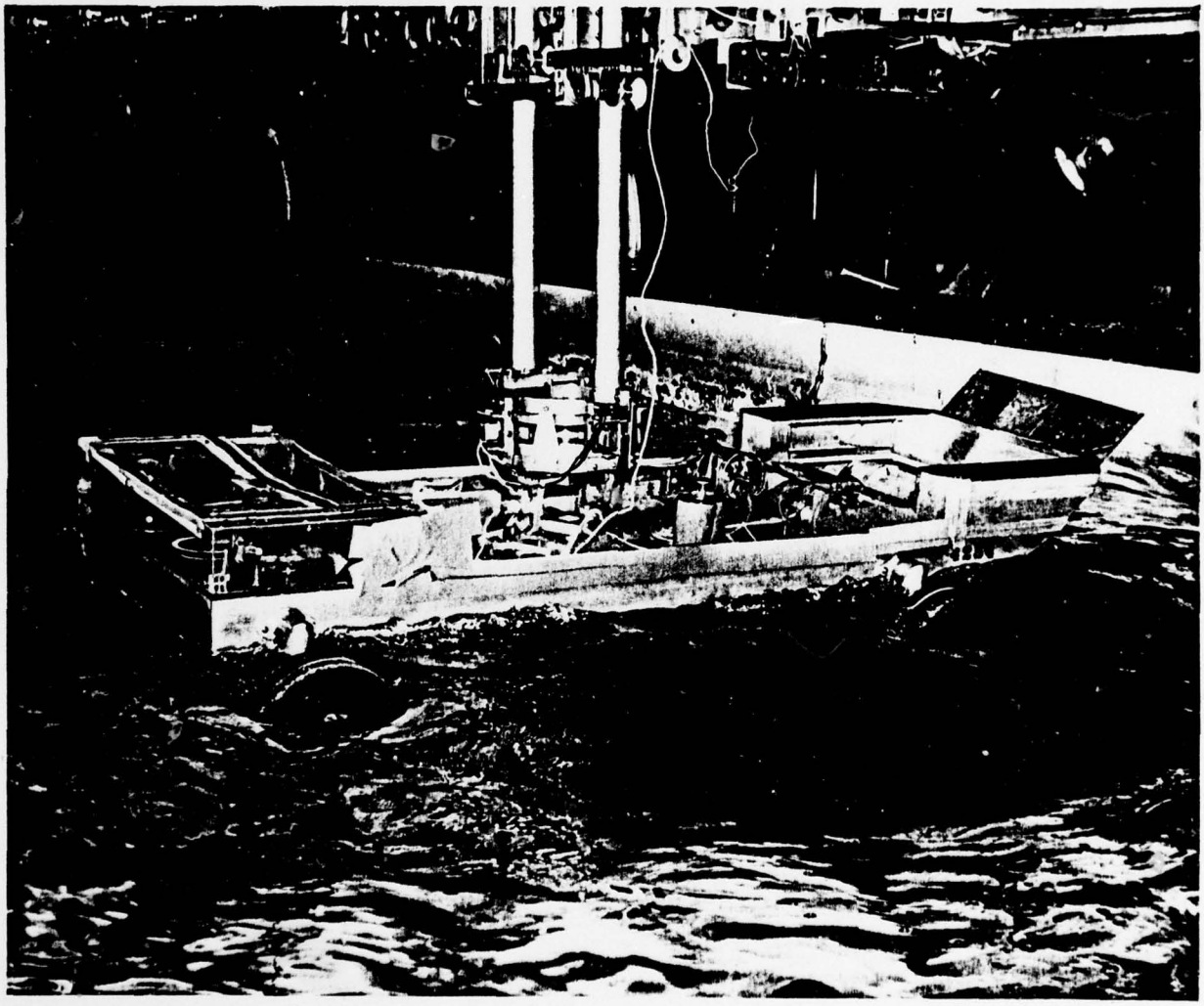

FIG. 8. ZERO SPEED BEAM SEA TEST SETUP

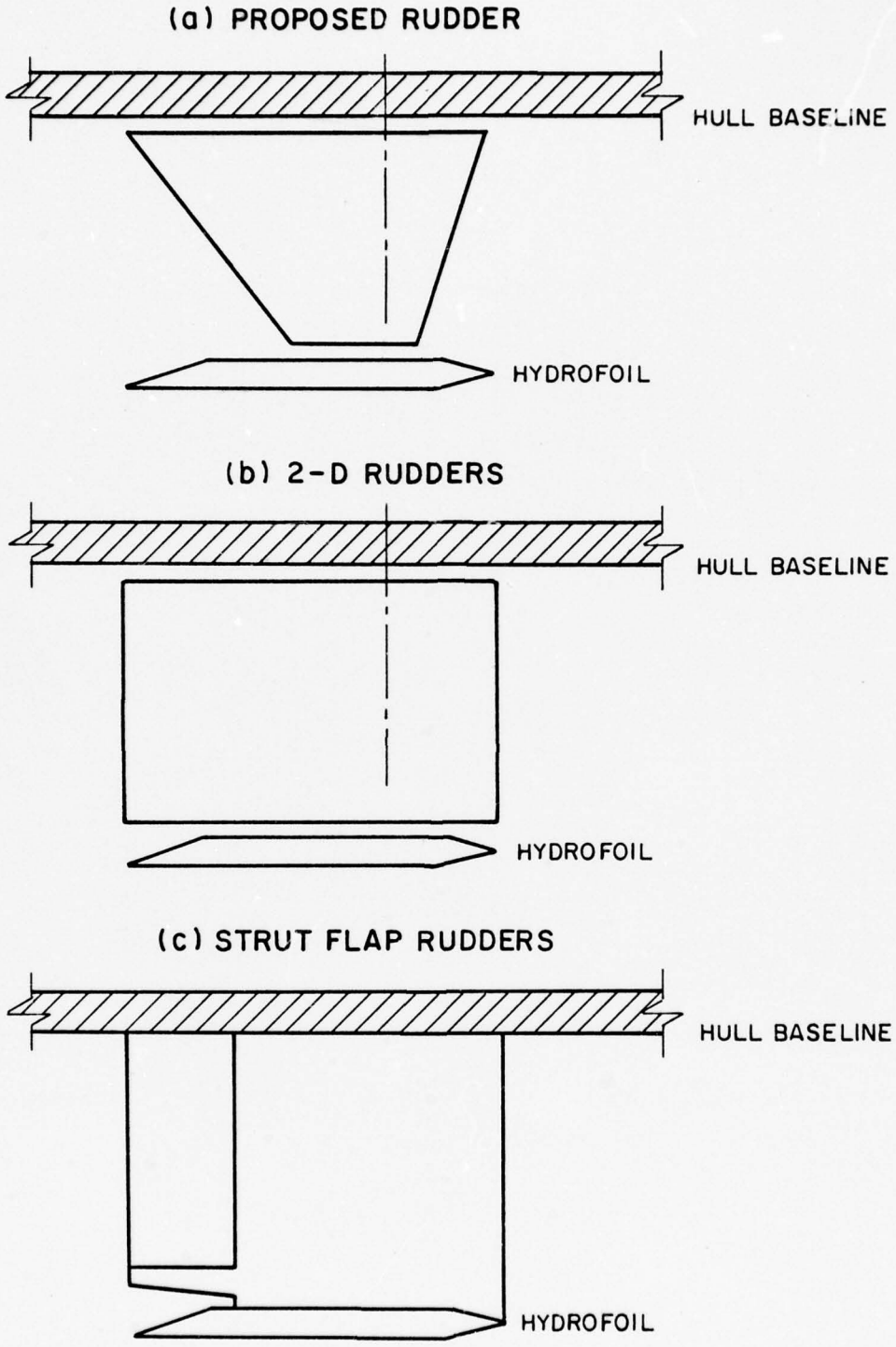

FIG. 9. RUDDER DESIGNS

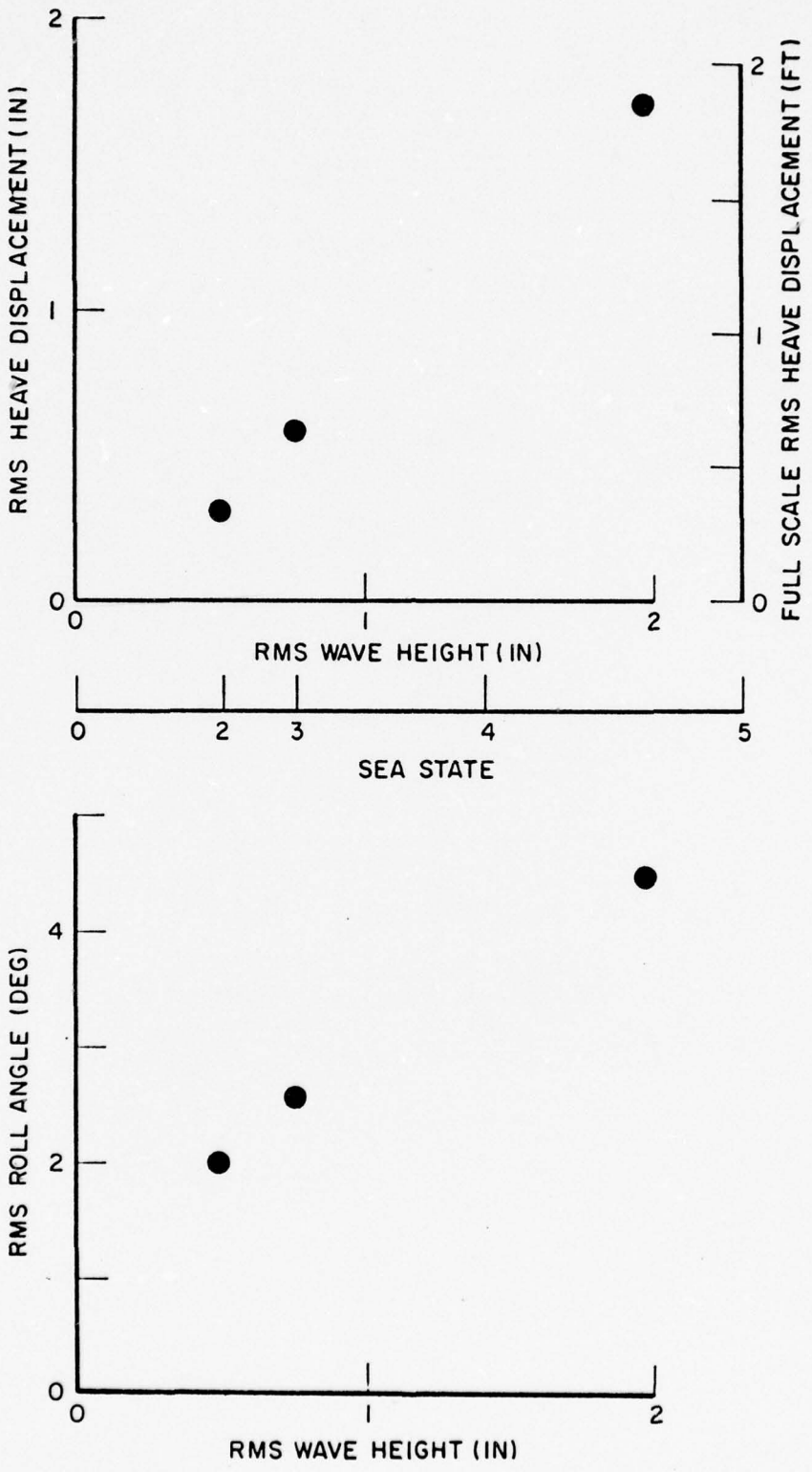

FIG. 10. ROLL AND HEAVE MOTIONS IN IRREGULAR BEAM SEAS

APPENDIX A

TANDEM FOIL TEST RESULTS

Lift and drag forces on the proposed tandem hydrofoil system were measured over a range of speed, trim angle, fore and aft flap angles and separation distance. Using the apparatus described previously, total lift, L, and drag, D, of the tandem foil system were measured as well as lift and drag on the aft foil. After correcting the aft foil measurements for trim angle τ, by means of

$$\begin{aligned} L_a &= N\cos\tau - R\sin\tau \\ D_a &= N\sin\tau + R\cos\tau \end{aligned} \qquad \text{(A-1)}$$

where N and R are forces normal and parallel to the chord plane of the aft foil, while L_a and D_a are forces normal and parallel to the free stream velocity, the lift and drag on the forward foil were found by subtraction as

$$\begin{aligned} L_f &= L - L_a \\ D_f &= D - D_a \end{aligned} \qquad \text{(A-2)}$$

The submergence at midchord was computed for each foil from

$$\begin{aligned} \zeta_f &= \zeta - \tfrac{1}{2}\xi\sin\tau \\ \zeta_a &= \zeta + \tfrac{1}{2}\xi\sin\tau \end{aligned} \qquad \text{(A-3)}$$

where ζ_f and ζ_a are the fore and aft foil submergence, ζ is the mean submergence midway between the foils and ξ is the foil spacing. All results were non-dimensionalized according to the following relations:

$$\begin{aligned} \zeta_f' &= \zeta_f/c \;,\; F_c^2 = V^2/gc \;,\; C_{Lf} = L_f/\tfrac{1}{2}\rho V^2 A \;,\; C_{DF} = D_f/\tfrac{1}{2}\rho V^2 A \\ \zeta_a' &= \zeta_a/c \;,\; F_\xi^2 = V^2/g\xi \;,\; C_{La} = L_a/\tfrac{1}{2}\rho V^2 A \;,\; C_{Da} = D_a/\tfrac{1}{2}\rho V^2 A \end{aligned} \qquad \text{(A-4)}$$

where c is the foil chord length, V is the forward speed, g is the gravitational constant, ρ is water density and A is the chord plane area of one foil. Trim angles and flap angles are in degrees.

The observed dimensionless lift and drag are listed in Table A-1 for the forward foil and in Table A-2 for the aft foil. Runs 32 through 81 and Runs 97 through 103 exhibit the variation in lift and drag with trim angle, flap angles, and speed at the design foil separation, while Runs 82 through 96 demonstrate their variation with foil separation at take-off speed. Also shown in these tables are predicted values of forward foil lift coefficient and aft foil lift and drag coefficients, as obtained by least squares curve fits of the corresponding measured data. The forward foil drag coefficient was not found amenable to least squares curve fitting, probably because too much scatter was introduced by the subtraction of small measured values in Eq.(A-2). Drag forces tended to be about 1/10 of the lift forces and their measurement accuracy was not correspondingly smaller.

The results of the least squares curve fitting are shown in Table A-3, where it is seen that the forward foil lift coefficient was fitted with six terms. The first five terms represent the high Froude number free-surface effect times the trim angle and flap angle terms. The last term is a free-surface correction due to wave-making which depends on Froude number based on chord length F_c as well as on depth ζ_f'. The value of each coefficient as determined by the least squared error technique is listed in Table A-3, together with some statistics of the fit. It is seen that 62 data points were used, that the ratio of unexplained mean squared variation to total variation is 0.103 percent and that the correlation of residual error with dependent variable is 3.5 percent. Fitted and measured values of forward foil lift coefficient are plotted versus flap angle in Figure A-1 through A-4, showing good agreement between empirical and observed values. Stalling of the forward foil is evident in these plots as well as in the need for higher order flap angle terms. The zero-lift flap angle at zero trim is seen to be about -5 deg. Flap angles were measured from a position with the lower flap surface parallel to the lower foil surface and the wedge angle at the trailing edge of the flap was 10.4 degrees, so that a flap angle of -5.2 degrees yields a

symmetric foil. The rate of change of lift coefficient with trim angle in infinite fluid was estimated from Reference 3 as 0.0640 per degree. Using Eq.(15) of Reference 4, the lift-curve slope is estimated to be

$$\frac{C_L}{h_f \tau} = \frac{A_R (a_1)_o}{A_R + \frac{1}{\pi}(a_1)_o h_f + 1} = 0.0635/\text{deg} \quad \text{at} \quad \zeta_f' = 0.659$$

where

$$h_f = \frac{(4\zeta_f')^2 + 1}{(4\zeta_f')^2 + 2} ,$$

where $A_R = 5.82$ is the aspect ratio of the foil and where $(a_1)_o = 5.18/\text{rad}$ is the estimated two-dimensional lift curve slope for the model foil cross-section as obtained from Reference 3. The empirical lift curve slope $a_1 = 0.04814$ appears to be about 25 percent low. This may be due to the small range of trim angle included in the measurements, to the extrapolation to low Reynolds number (3.5 to 7.1×10^5) in applying the results of Reference 3, to laminar flow conditions and separation on the model foil, or due to measurement error. It is felt that the value predicted by means of References 3 and 4 is reliable.

The linear flap angle term in the forward foil lift coefficient was also compared with that predicted by Reference 3. For the given model foil geometry the lift-curve slope due to flap angle was estimated to be .0349/deg which is 12 percent higher than a_2=.030829/deg shown in Table A-3. Again, an extrapolation in Reynolds number was required in using Reference 3 for model size, so that the agreement in lift-curve slope due to flap angle is considered satisfactory and use of this reference for predictions is recommended.

For the aft foil lift coefficient, the first six terms shown in Table A-3 are similar to the corresponding terms for the forward foil. The seventh term accounts for the downwash from the forward foil at high Froude number while the last four terms account for the wave-induced downwash from the forward foil. It is seen that 66 data points were included in the least squares curve fit, that the ratio of unexplained mean square variation to

total variation is 1.15 percent and that the residual correlation is 9.9 percent. The fitted and measured values of aft foil lift coefficient are plotted versus flap angle in Figures A-5 through A-8, indicating good agreement between empirical and observed values. Stalling of the aft foil is not so evident in the observed aft foil lift coefficient as with the forward foil because most of the plots at constant trim angle contain data only at two values of aft flap angle. However, in fitting the aft lift data it was found that the overall statistics improved significantly when the higher order flap angle terms were included. The lift-curve slope due to trim angle based on References 3 and 4 is the same for the aft foil as that of the forward foil, about 0.064 per degree, while the fitted value is $b_1 = 0.056934$ per degree, which is about 11 percent low. This result may be closer to the estimated value than that of the forward foil due to turbulence created by the forward foil which decreased the laminar separation on the aft foil. This explanation is in agreement with the higher value of lift-curve slope due to flap angle $b_2 = 0.037397$ per degree for the aft foil as compared to $a_2 = 0.030829$ per degree for the forward foil. The aft value is, in fact, 7 percent higher than 0.0349 the estimated value based on Reference 3. These results further substantiate use of References 3 and 4 for predictive purposes.

The terms in the aft foil lift coefficient representing the effect of the wave-induced downwash from the forward foil depend on the forward foil lift coefficient, the fore and aft foil submergence, the Froude number based on chord length, as well as on the Froude number based on separation distance F_ξ. At sufficiently large separations the wave-induced downwash should vary sinusoidally with F_ξ^{-2}. Since the tandem foils of this vehicle are separated by less than one wave length at all speeds from take-off and above, the regular wave train is augmented by a local effect which requires the higher order terms shown in Table A-3. The variation of upwash with separation distance, due to the forward foil wake as inferred by the least square fit results, i.e.,

$$f(F_\xi) = b_7 \sin F_\xi^{-2} + b_8 \cos F_\xi^{-2} + b_9 \sin 3F_\xi^{-2} + b_{10} \cos 3F_\xi^{-2}$$

is plotted in Figure A-9. The higher order terms were chosen to give a more peaked fitting function and are not physically realistic since they do not

decay with increasing separation distance. However, these functions are considered an appropriate simplification for the purposes of this study. More data at larger separations would be required to establish more realistic terms containing perhaps an exponential decay with separation distance.

The first term of the fitting function for the aft foil drag coefficient represents profile drag while the second through the sixth terms are various components of the induced drag. Each induced drag term is a product of the aft foil lift coefficient times a factor proportional to contributions to the downwash at the aft foil. The second term is the induced drag due to downwash produced by trim angle of the aft foil while the third term is that due to aft flap angle. The fourth term is the induced drag due to downwash from the forward foil at high Froude number while the fifth is that due to waves made by the forward foil. The last induced drag term represents wave drag of the aft foil. The seventh and eighth terms were added to improve the fit and are due to stalling of the aft foil. The profile drag coefficient is commensurate with the model Reynolds number and foil cross section. The coefficients of the induced drag terms are considerably higher than expected. The induced drag for one wing of a biplane with rectangular planform (the biplane is the high Froude number representation of a hydrofoil near the free-surface) is given in Reference 5 as

$$C_{D_i} = \frac{(1 + \Delta + \sigma)}{\pi A_R} C_L^2$$

where Δ is a correction factor for non-elliptical spanwise lift distribution (Δ=0.06) and σ is a correction factor due to the upper wing of the biplane (σ=0.44 at ζ'=0.659), thus, it is expected that the induced drag terms would be approximately

$$C_{D_i} = 0.082\ C_L^2$$

Thus, coefficients c_1, c_3 and c_4 appear too large by a factor of 2 while coefficients c_2 and c_5 seem to be about 50 percent higher than expected. This discrepancy may be due to the low Reynolds number and stalling of the aft foil, due to numerical effect of the non-linear flap terms on the least squared error technique, due to the effect of the viscous wake from the

stalled region of the forward foil or due to inappropriate fitting functions for the complex flow pattern of a tandem hydrofoil system with substantial stalling effects. It is felt that the established results of Reference 5 are more reliable than this one set of measurements containing several reasons to question the least square fitting results as mentioned above. Consequently, the results of Reference 5 are recommended for prototype predictions, for both forward and aft hydrofoils.

Based on the above reasoning, it is recommended that the following expressions be used for full-scale predictions of lift and drag of the proposed tandem hydrofoil system:

1) Forward Foil Lift Coefficient

$$C_{Lf} = (\tau-\tau_o)C_{L\tau}(\zeta_f') + \delta_f C_{L\delta}(\zeta_f') + C_{Lw}(\zeta_f', F_c^2)$$

2) Forward Foil Drag Coefficient

$$C_{Df} = C_{Do} + C_{Lf}\left[(\tau-\tau_o)C_{L\tau}(\zeta_f')c_1 + \delta_f C_{L\delta}(\zeta_f')c_2 + g(\zeta_f', F_c^2)C_{Lf}c_5\right]$$

3) Aft Foil Lift Coefficient

$$C_{La} = (\tau-\tau_o)C_{L\tau}(\zeta_a') + \delta_a C_{L\delta}(\zeta_a') + C_{Lw}(\zeta_a', F_c^2) + C_{Laf\infty} + C_{Lafw}$$

4) Aft Foil Drag Coefficient

$$C_{Da} = C_{Do} + C_{La}\left[(\tau-\tau_o)C_{L\tau}(\zeta_a')c_1 + \delta_a C_{L\delta}(\zeta_a')c_2 + g(\zeta_a', F_c^2)C_{La}c_5 + C_{Laf\infty}c_3 + C_{Lafw}c_4\right]$$

where τ_o = zero lift angle of attack

$C_{L\tau}(\zeta')$ = lift rate due to trim

$C_{L\delta}(\zeta')$ = lift rate due to flap

$C_{Lw}(\zeta', F_c^2)$ = lift coefficient due to Froude number effects

C_{Do} = profile drag coefficients

$c_i; i=1,2,3,4,5$ = coefficients of induced drag terms

$g(\zeta', F_c^2) = \exp(-2\zeta'/F_c^2)/F_c^2$

$C_{Laf\infty}$ = lift coefficient for aft foil due to forward foil downwash at high Froude number

C_{Lafw} = lift coefficient for aft foil due to wave-induced downwash from forward foil

The value of τ_o depends on the camber of the hydrofoils and a value of $\tau_o = -3.48$ degrees has been used in some previous design studies for this vehicle. The other coefficients above can be evaluated as follows:

Coefficient	Expression or Value	Source
$C_{L\tau}(\zeta')$	$\dfrac{h(\zeta')(a_1)_o K_3(\zeta') A_R}{A_R + 1 + \frac{1}{\pi}(a_1)_o h(\zeta')}$	Reference 4
$C_{L\delta}(\zeta')$	$\dfrac{h(\zeta')(a_2)_o K_3(\zeta') A_R}{A_R + 1 + \frac{1}{\pi}(a_2)_o h(\zeta')}$	Reference 4
$C_{Lw}(\zeta', F_c^2)$	$a_5' g(\zeta', F_c^2)$	Table 3
a_5'	$\frac{1}{2}(a_5 + b_5)$	Table 3
C_{Do}	0.00522	Reference 3
$c_1 = c_2$	$[1 + \Delta + \sigma(\zeta')]/\pi A_R$	Reference 5
Δ	0.06	Reference 5
$\sigma(\zeta')$	$\exp[-2.4(2\zeta'/A_R)^{.75}]$	Reference 5
c_5	0.138	Table 3
$C_{Laf\infty}$	$b_6 h(\zeta_f')[(\tau-\tau_o) C_{L\tau}(\zeta_f') + \delta_f C_{L\delta}(\zeta_f')]$	Table 3
b_6	-0.376	Table 3

(Cont'd)

Coefficient	Expression or Value	Source
C_{Lafw}	$C_{Lf}g(\zeta_f'+\zeta_a', F_c^2)(b_7 \sin F_\xi^{-2} + b_8 \cos F_\xi^{-2} + b_9 \sin 3F_\xi^{-2} + b_{10} \cos 3F_\xi^{-2})$	Table 3
b_7	4.6587	Table 3
b_8	1.2602	Table 3
b_9	0.10252	Table 3
b_{10}	1.1617	Table 3
$c_3 = c_4$	$-c_1$	
$(a_1)_o$	0.0990/deg	Reference 3
$K_3(\zeta')$	$1.1865/[1.1865 + w_6(\zeta')]$	Reference 4
where	$w_6(\zeta') = \frac{A_R}{\sqrt{(4\zeta)^2 + A_R^2 + 1}} \left(\frac{1}{(4\zeta)^2 + 1} + \frac{\sqrt{(4\zeta')^2 + A_R^2 + 1}}{A_R^2 + (4\zeta')^2} \right)$	
$(a_2)_o$	0.0527/deg	Reference 3

TABLE A-1

TANDEM FOIL TEST RESULTS

FORWARD FOIL LIFT AND DRAG

Run	Trim Angle	Flap Angle	Depth	F_c^2	C_{Lf} Meas.	C_{Lf} Fit	C_{Df}
32	0	0	0.659	18.22	0.149	0.150	0.0160
33	0	0	0.659	18.31	0.149	0.150	0.0156
34	0	0	0.659	4.32	0.139	0.143	
35	0	0	0.659	4.32	0.146	0.143	0.0186
36	0	0	0.659	10.13	0.152	0.142	0.0164
37	0	0	0.659	18.20	0.143	0.150	0.0192
38	0	10	0.659	4.32	0.405	0.378	0.0358
39	0	10	0.659	10.07	0.404	0.383	0.0281
40	0	10	0.659	18.20	0.393	0.385	0.0233
41	0	20	0.659	4.30	0.518	0.519	0.0631
42	0	20	0.659	10.07	0.528	0.524	0.0535
43	0	20	0.659	18.20	0.537	0.526	0.0483
45	0	-5	0.659	4.30	0.002	-0.002	0.0138
46	0	-5	0.659	10.07	-0.002	0.003	0.0089
47	0	-5	0.659	18.22	-0.001	0.005	0.0227
48	0	-10	0.659	4.30	-0.152	-0.161	0.0192
49	0	-10	0.659	6.88	-0.159	-0.158	0.0111
51	0	10	0.659	4.30	0.387	0.378	0.0560
52	0	10	0.659	6.88	0.379	0.381	0.0132
53	0	10	0.659	6.88	0.382	0.381	0.0378
54	0	10	0.659	6.88	0.382	0.381	0.0393
55	0	10	0.659	10.07	0.386	0.383	0.0383
57	0	10	0.659	18.22	0.382	0.385	0.0372
58	0	20	0.659	4.30	0.498	0.519	0.0766
59	0	20	0.659	6.88	0.512	0.522	0.0837
61	0	20	0.659	10.07	0.482	0.524	0.1099
62	0	20	0.659	10.07	0.519	0.524	0.0992
63	0	20	0.659	10.07	0.507	0.524	0.0628
64	2	0	0.511	4.30	0.212	0.215	0.0338
65	2	0	0.511	4.30	0.211	0.215	0.0315
66	2	0	0.511	6.88	0.219	0.218	0.0280
67	2	10	0.511	4.30	0.441	0.437	0.0503
68	2	10	0.511	6.88	0.448	0.440	0.0412
69	2	20	0.511	4.30	0.567	0.570	0.0824
70	2	20	0.511	6.88	0.576	0.573	0.0702
71	2	0	0.511	4.30	0.209	0.215	0.0420
72	2	0	0.511	6.88	0.214	0.218	0.0340
73	2	10	0.511	4.30	0.434	0.437	0.0662
74	2	10	0.511	6.88	0.437	0.440	0.0521
75	2	0	0.511	4.30	0.207	0.215	0.0418
76	2	0	0.511	6.88	0.210	0.218	0.0412

(Cont'd)

Table A-1 (Cont'd)

Run	Trim Angle	Flap Angle	Depth	F_c [a]	C_{Lf} Meas.	C_{Lf} Fit	C_{Df}
77	2	10	0.511	4.30	0.428	0.437	0.0835
78	2	10	0.511	6.88	0.429	0.440	0.0584
79	1	0	0.586	4.30	0.187	0.181	0.0264
80	1	0	0.586	6.88	0.181	0.184	0.0237
81	1	0	0.586	18.22	0.193	0.188	0.0201
82	2	0	0.562	5.50	0.231	0.222	0.0320
83	2	0	0.547	5.49	0.228	0.221	0.0309
84	2	0	0.531	5.49	0.225	0.219	0.0201
85	2	0	0.515	5.49	0.220	0.217	0.0165
86	2	0	0.499	5.49	0.215	0.215	0.0018
87	2	0	0.483	5.49	0.207	0.213	0.0457
88	2	0	0.467	5.49	0.180	0.211	0.0313
89	2	0	0.451	5.49	0.230	0.209	0.0088
90	2	0	0.436	5.49	0.216	0.207	0.0178
92	2	0	0.467	4.34	0.228	0.210	
93	2	0	0.499	4.34	0.219	0.214	0.0378
94	2	0	0.515	4.34	0.223	0.216	0.0323
95	2	0	0.531	4.34	0.222	0.218	0.0334
96	2	0	0.562	4.34	0.222	0.221	0.0311
97	0	10	0.659	18.22	0.386	0.385	0.0376
98	0	9	0.659	18.22	0.365	0.365	0.0325
99	0	8	0.659	18.22	0.342	0.345	0.0331
100	0	8	0.659	18.22	0.344	0.345	0.0314
101	0	8	0.659	18.22	0.343	0.345	0.0319
102	0	8	0.659	18.22	0.344	0.345	0.0330
103	0	8	0.659	18.22	0.346	0.345	0.0318

TABLE A-2

TANDEM FOIL TEST RESULTS

AFT FOIL LIFT AND DRAG

Run	Trim Angle	Flap Angle	Depth	F_c [a]	F_ζ [a]	C_{Lf} Fit	C_{La} Meas.	C_{La} Fit	C_{Da} Meas.	C_{Da} Fit
32	0	0	0.659	18.22	2.172	0.150	0.096	0.134	0.0181	0.0173
33	0	0	0.659	18.31	2.184	0.150	0.097	0.134	0.0183	0.0173
34	0	0	0.659	4.32	0.516	0.143	0.154	0.183		
35	0	0	0.659	4.32	0.516	0.143	0.178	0.183	0.0164	0.0174
36	0	0	0.659	10.13	1.207	0.142	0.136	0.130	0.0173	0.0174
37	0	0	0.659	18.20	2.169	0.150	0.122	0.134	0.0178	0.0173
38	0	0	0.659	4.32	0.516	0.378	0.224	0.235	0.0160	0.0166
39	0	0	0.659	10.07	1.199	0.383	0.101	0.121	0.0173	0.0172
40	0	0	0.659	18.20	2.169	0.385	0.062	0.112	0.0166	0.0166
41	0	0	0.659	4.30	0.513	0.519	0.240	0.267	0.0153	0.0157
42	0	0	0.659	10.07	1.199	0.524	0.094	0.110	0.0171	0.0170
43	0	0	0.659	18.20	2.169	0.526	0.038	0.098	0.0157	0.0158
45	0	0	0.659	4.30	0.513	-0.002	0.152	0.151	0.0172	0.0175
46	0	0	0.659	10.07	1.200	0.003	0.147	0.148	0.0171	0.0174
47	0	0	0.659	18.22	2.172	0.005	0.154	0.147	0.0173	0.0174
48	0	0	0.659	4.30	0.513	-0.161	0.131	0.116	0.0178	0.0171
49	0	0	0.659	6.88	0.821	-0.158	0.140	0.140	0.0228	
51	0	10	0.659	4.30	0.513	0.378	0.462	0.430	0.0431	0.0434
52	0	10	0.659	6.88	0.821	0.381	0.374	0.367	0.0451	0.0435
53	0	10	0.659	6.88	0.821	0.381	0.388	0.367	0.0451	0.0435
54	0	10	0.659	6.88	0.821	0.381	0.389	0.367	0.0451	0.0435
55	0	10	0.659	10.07	1.200	0.383	0.346	0.316	0.0458	
57	0	10	0.659	18.22	2.172	0.385	0.302	0.307	0.0423	0.0423
58	0	10	0.659	4.30	0.513	0.519	0.467	0.462	0.0412	0.0425
59	0	10	0.659	6.88	0.821	0.522	0.358	0.376	0.0417	0.0435
61	0	10	0.659	10.07	1.200	0.524	0.327	0.306	0.0431	0.0428
62	0	10	0.659	10.07	1.200	0.524	0.310	0.306	0.0427	0.0428
63	0	10	0.659	10.07	1.200	0.524	0.334	0.306	0.0439	0.0428
64	2	0	0.807	4.30	0.513	0.215	0.306	0.288	0.0304	
65	2	0	0.807	4.30	0.514	0.215	0.316	0.288	0.0257	0.0254
66	2	0	0.807	6.88	0.821	0.218	0.265	0.252	0.0255	0.0252
67	2	0	0.807	4.30	0.513	0.437	0.367	0.338	0.0248	0.0247
68	2	0	0.807	6.88	0.821	0.440	0.245	0.265	0.0256	0.0252
69	2	0	0.807	4.30	0.514	0.570	0.383	0.367	0.0247	0.0238
70	2	0	0.807	6.88	0.821	0.573	0.257	0.273	0.0242	0.0252
71	2	10	0.807	4.30	0.513	0.215	0.554	0.490	0.0596	0.0595
72	2	10	0.807	6.88	0.821	0.218	0.493	0.454	0.0586	0.0584
73	2	10	0.807	4.30	0.513	0.437	0.609	0.540	0.0598	0.0588
74	2	10	0.807	6.88	0.821	0.440	0.488	0.467	0.0582	0.0584
75	2	20	0.807	4.30	0.514	0.215	0.664	0.692	0.1020	0.1020
76	2	20	0.807	6.88	0.821	0.218	0.604	0.656	0.0998	0.1001
77	2	20	0.807	4.30	0.514	0.437	0.710	0.742	0.1015	0.1012
78	2	20	0.807	6.88	0.821	0.440	0.594	0.669	0.1000	0.1001

(Cont'd)

Table A-2 (Cont'd)

Run	Trim Angle	Flap Angle	Depth	F_c [a]	F_ξ [a]	C_{Lf} Fit	C_{La} Meas.	C_{La} Fit	C_{Da} Meas.	C_{Da} Fit
79	1	0	0.733	4.30	0.513	0.181	0.248	0.236	0.0211	0.0208
80	1	0	0.733	6.88	0.821	0.184	0.212	0.205	0.0211	0.0207
81	1	0	0.733	18.22	2.172	0.188	0.167	0.174	0.0205	0.0204
82	2	0	0.756	5.50	1.008	0.222	0.214	0.231	0.0242	0.0251
83	2	0	0.772	5.49	0.862	0.221	0.238	0.248	0.0261	0.0252
84	2	0	0.788	5.49	0.755	0.219	0.260	0.264	0.0260	0.0253
85	2	0	0.804	5.49	0.671	0.217	0.277	0.276	0.0250	0.0253
86	2	0	0.819	5.49	0.604	0.215	0.281	0.283	0.0254	0.0254
87	2	0	0.835	5.49	0.549	0.213	0.313	0.285	0.0253	0.0254
88	2	0	0.851	5.49	0.503	0.211	0.315	0.282	0.0262	0.0255
89	2	0	0.867	5.49	0.464	0.209	0.269	0.276	0.0252	0.0256
90	2	0	0.883	5.49	0.431	0.207	0.264	0.269	0.0306	
92	2	0	0.851	4.34	0.398	0.210	0.212	0.266		
93	2	0	0.819	4.34	0.477	0.214	0.303	0.283	0.0241	0.0255
94	2	0	0.804	4.34	0.531	0.216	0.297	0.290	9.0241	0.0254
95	2	0	0.788	4.34	0.597	0.218	0.285	0.289	0.0253	0.0254
96	2	0	0.756	4.34	0.796	0.221	0.238	0.260	9.0253	0.0253
97	0	8	0.659	18.22	2.172	0.385	0.267	0.268	0.0351	0.0359
98	0	9	0.659	18.22	2.172	0.365	0.291	0.289	0.0391	0.0391
99	0	10	0.659	18.22	2.172	0.345	0.307	0.310	0.0424	0.0424
100	0	10	0.659	18.22	2.172	0.345	0.308	0.310	0.0419	0.0424
101	0	10	0.659	18.22	2.172	0.345	0.306	0.310	0.0417	0.0424
102	0	10	0.659	18.22	2.172	0.345	0.303	0.310	0.0421	0.0424
103	0	10	0.659	18.22	2.172	0.345	0.308	0.310	0.0420	0.0424

44<

TABLE A-3

TANDEMFOIL TEST RESULTS

SUMMARY OF LEAST SQUARE FITS

1) FORWARD FOIL LIFT COEFFICIENT

$$C_{Lf} = \left[\frac{(4\zeta_f')^2 + 1}{(4\zeta_f')^2 + 2}\right]\left(a_o + a_1\tau + a_2\delta_f + a_3\delta_f^2 + a_4\delta_f^3\right) + a_5 \frac{e^{-2\zeta_f'/F_c^2}}{F_c^2}$$

$a_o = 0.17185$	$a_3 = -0.38686\times10^{-3}$	$n = 62$
$a_1 = 0.048414$	$a_4 = -0.48298\times10^{-5}$	$\sigma_e^2/\sigma_y^2 = 0.00103$
$a_2 = 0.030829$	$a_5 = -0.055222$	$r = 0.035$

2) AFT FOIL LIFT COEFFICIENT

$$C_{La} = \left[\frac{(4\zeta_a')^2 + 1}{(4\zeta_a')^2 + 2}\right]\left(b_o + b_1\tau + b_2\delta_a + b_3\delta_a^2 + b_4\delta_a^3\right) + b_5 \frac{e^{-2\zeta_a'/F_c^2}}{F_c^2}$$

$$+ b_6\left[\frac{(4\zeta_f')^2 + 1}{(4\zeta_f')^2 + 2}\right]\left(a_o + a_1\tau + a_2\delta_f + a_3\delta_f^2 + a_4\delta_f^3\right)$$

$$+C_{Lf} \frac{e^{-2(\zeta_f'+\zeta_a')/F_c^2}}{F_c^2}\left(b_7 \sin F_\xi^{-2} + b_8 \cos F_\xi^{-2} + b_9 \sin 3F_\xi^{-2} + b_{10} \cos 3F_\xi^{-2}\right)$$

$b_o = 0.17481$	$b_6 = -0.37623$	$n = 66$
$b_1 = 0.056934$	$b_7 = 4.6587$	$\sigma_e^2/\sigma_y^2 = 0.0115$
$b_2 = 0.037397$	$b_8 = 1.2602$	$r = 0.099$
$b_3 = -0.13612\times10^{-2}$	$b_9 = 0.10252$	$r_{C_{Lf}} = -0.0077$
$b_4 = 0.22872\times10^{-4}$	$b_{10} = 1.1617$	
$b_5 = -0.091872$		

(Cont'd)

Table A-3 (Cont'd)

3) AFT FOIL DRAG COEFFICIENT

$$C_{Da} = c_o + C_{La}\left\{c_1 b_1 \tau\left[\frac{(4\zeta_a')^2+1}{(4\zeta_a')^2+2}\right] + c_2\left[\frac{(4\zeta_a')^2+1}{(4\zeta_a')^2+2}\right]\left(b_o+b_2\delta_a+b_3\delta_a^2+b_4\delta_a^3\right)\right.$$

$$+ c_3 b_6\left[\frac{(4\zeta_f')^2+1}{(4\zeta_f')^2+2}\right]\left(a_o+a_1\tau+a_2\delta_f+a_3\delta_f^2+a_4\delta_f^3\right)$$

$$+ c_4 C_{Lf}\frac{e^{-2(\zeta_f'+\zeta_a')/F_c^2}}{F_c^2}\left(b_7 \sin F_\xi^{-2}+b_8\cos F_\xi^{-2}+b_9\sin 3F_\xi^{-2}+b_{10}\cos 3F_\xi^{-2}\right)$$

$$\left. + c_5 C_{La}\frac{e^{-2\zeta_a'/F_c^2}}{F_c^2}\right\} + c_6\delta_a^2 + c_7\tau\delta_a$$

c_o = 0.014261	c_4 = -0.17106	n = 61
c_1 = 0.17682	c_5 = 0.13817	σ_e^2/σ_y^2 = 0.00125
c_2 = 0.12671	c_6 = 0.84237×10^{-4}	r = 0.0332
c_3 = -0.17180	c_7 = -0.12491×10^{-3}	$r_{C_{La}}$ = 0.0116
		$r_{C_{Lf}}$ = -0.0503

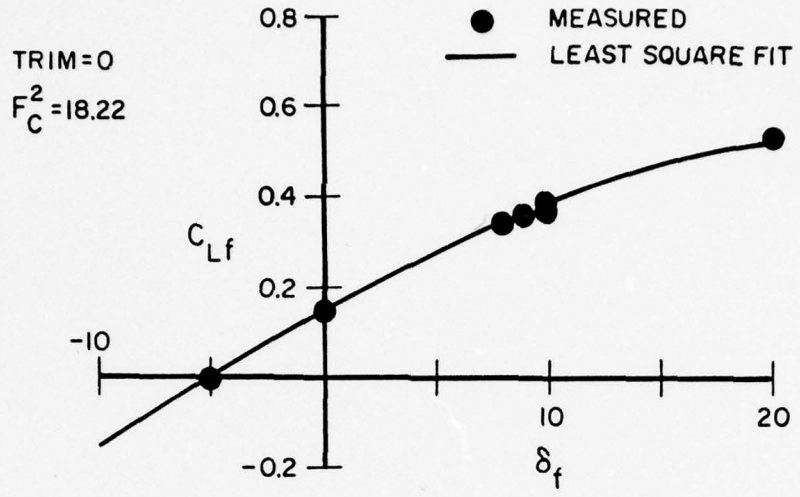

FIG. A-1. FORWARD FOIL LIFT COEFFICIENT AT 35 KNOTS AND ZERO TRIM

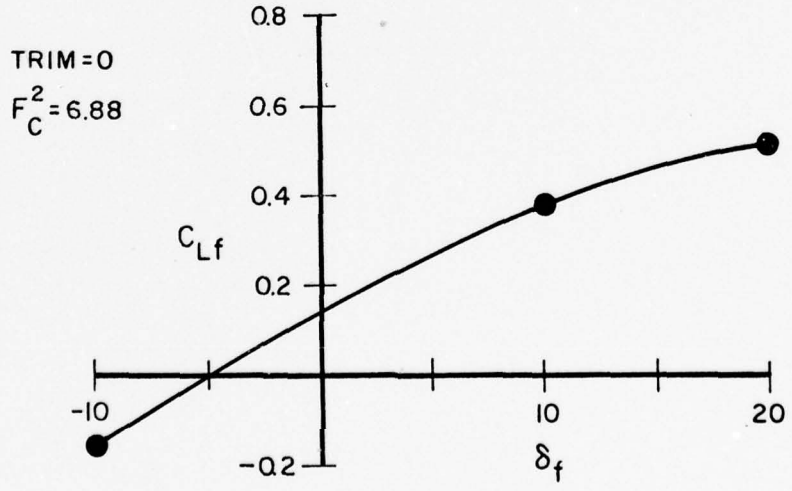

FIG. A-2. FORWARD FOIL LIFT COEFFICIENT AT 21.5 KNOTS AND ZERO TRIM

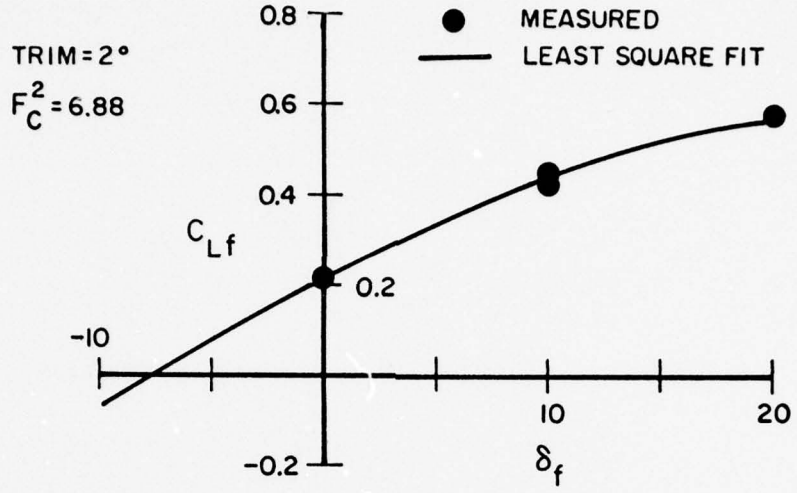

FIG. A-3. FORWARD FOIL LIFT COEFFICIENT AT 21.5 KNOTS AND TWO DEGREES TRIM

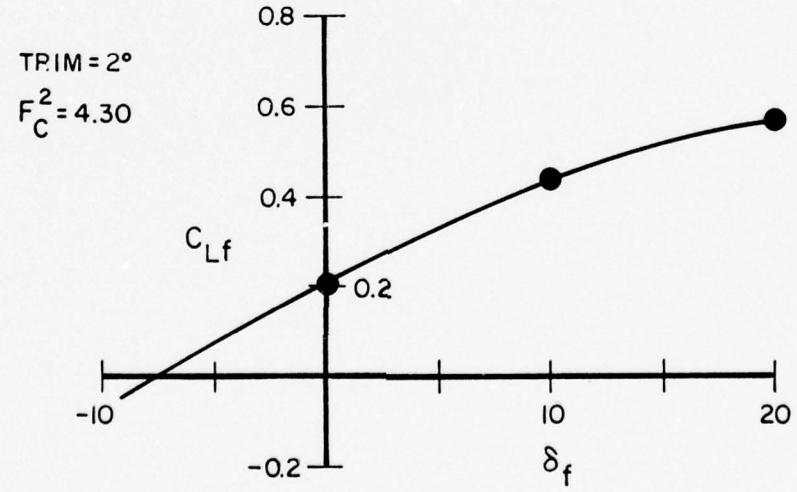

FIG. A-4. FORWARD FOIL LIFT COEFFICIENT AT 17 KNOTS AND TWO DEGREES TRIM

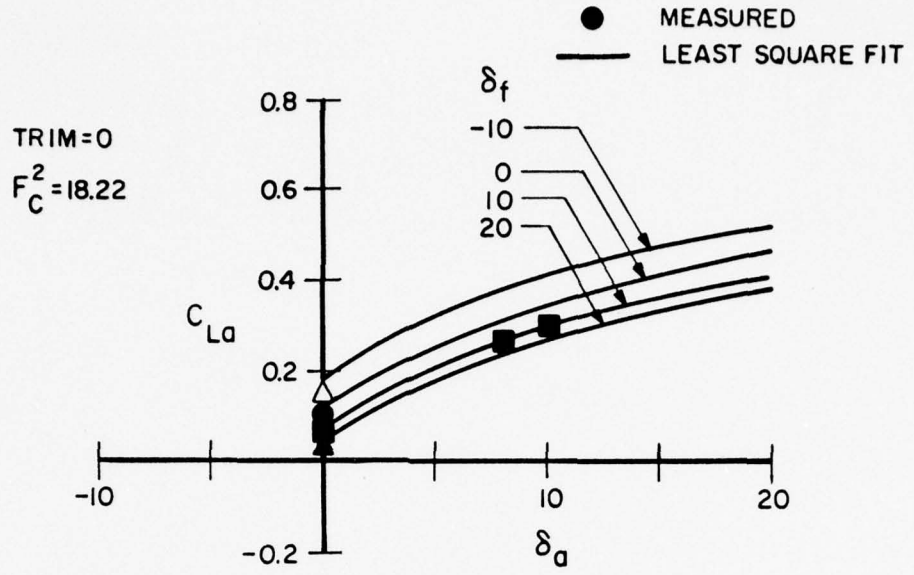

FIG. A-5 AFT FOIL LIFT COEFFICIENT AT 35 KNOTS AND ZERO TRIM

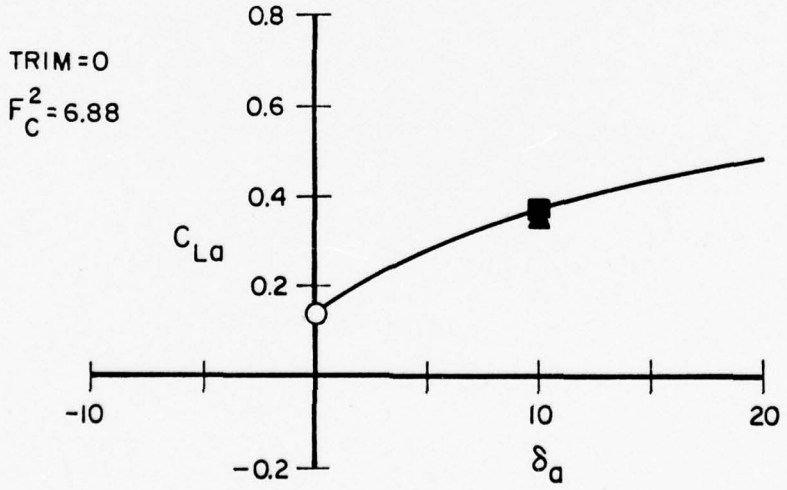

FIG. A-6. AFT FOIL LIFT COEFFICIENT AT 21.5 KNOTS AND ZERO TRIM

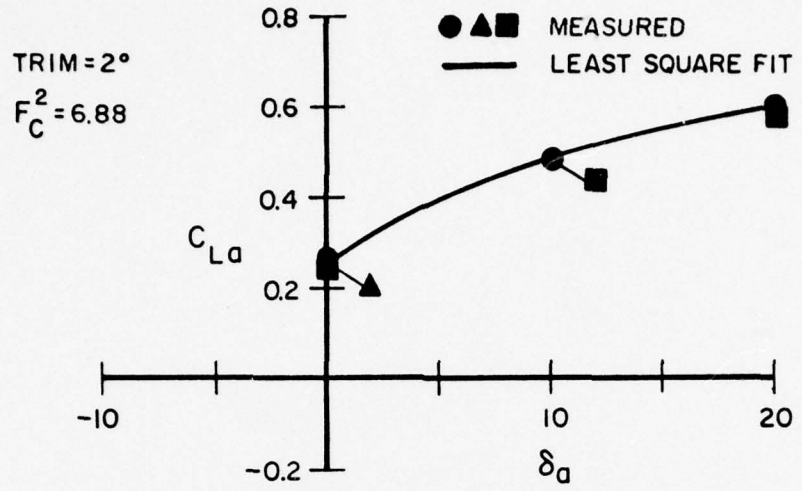

FIG. A-7. AFT FOIL LIFT COEFFICIENT AT 21.5 KNOTS AND TWO DEGREES TRIM

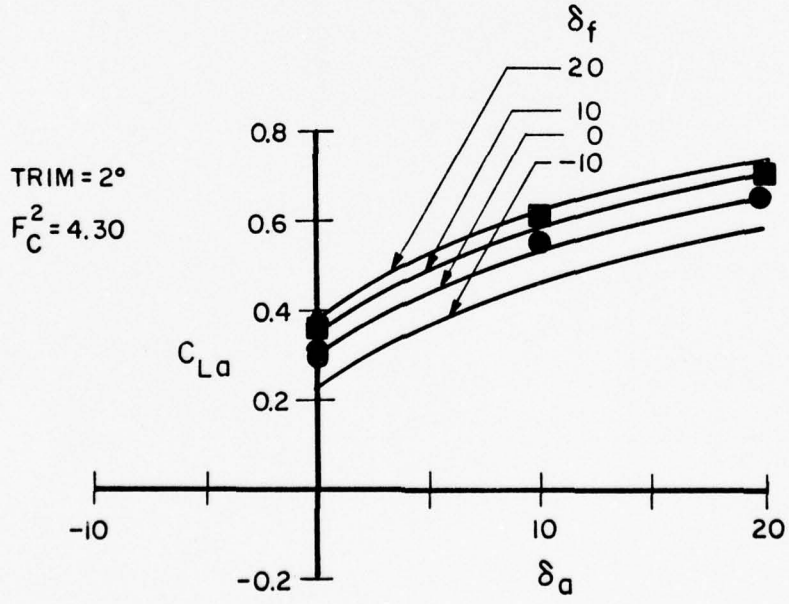

FIG. A-8. AFT FOIL LIFT COEFFICIENT AT 17 KNOTS AND TWO DEGREES TRIM

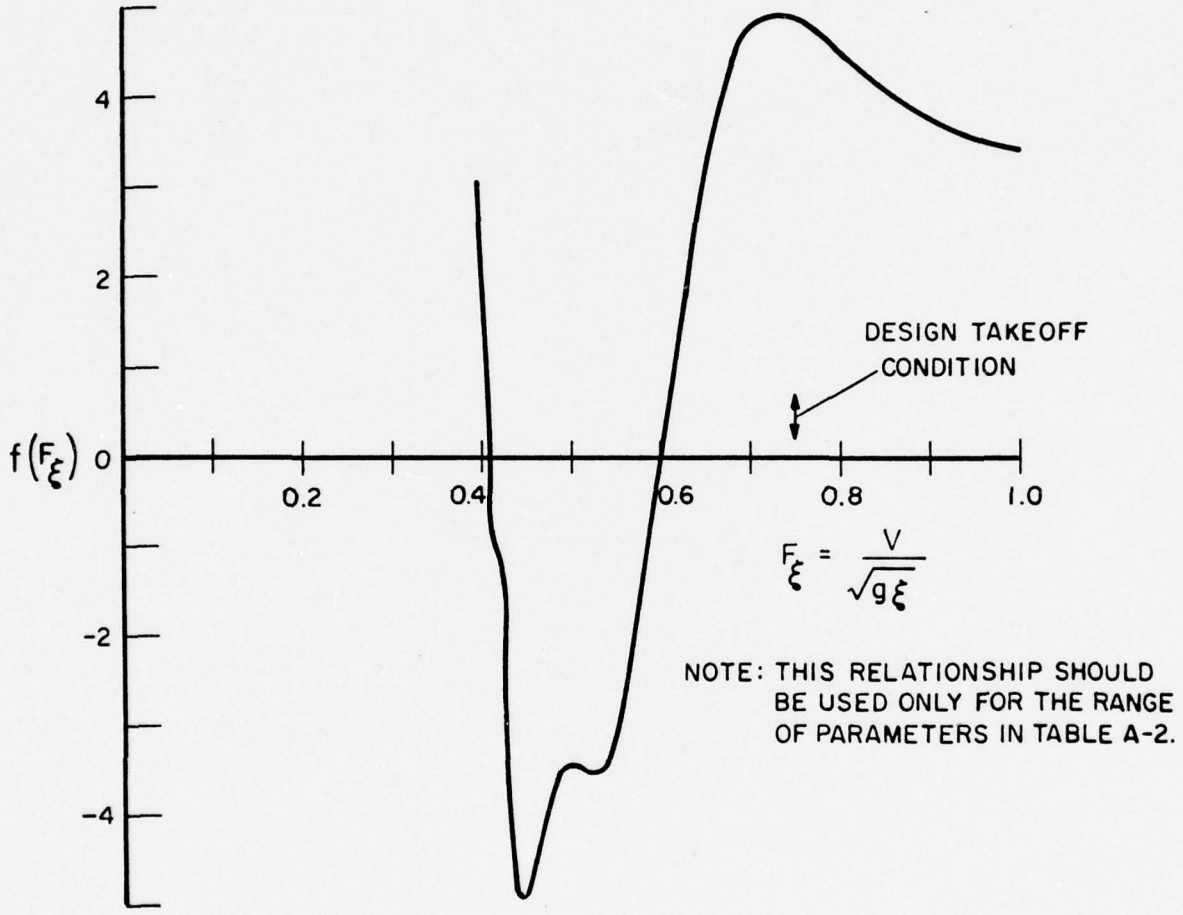

FIG. A-9. WAVE-INDUCED DOWNWASH FUNCTION

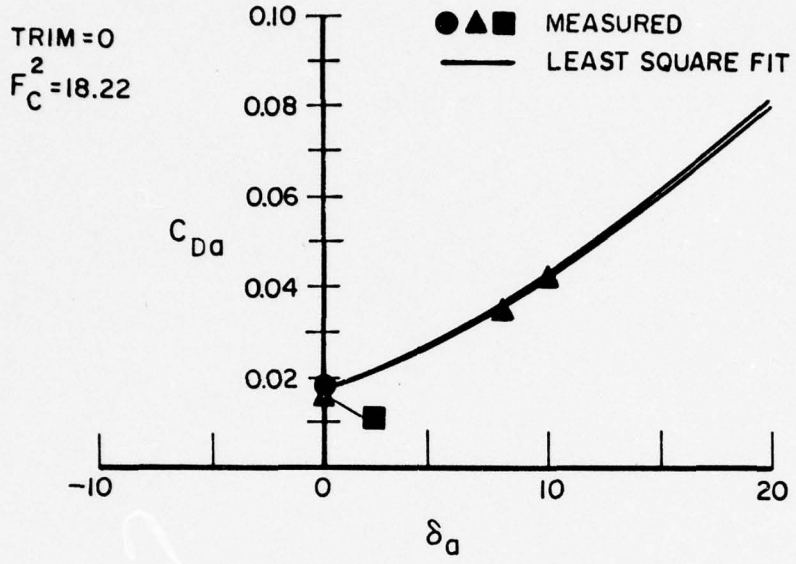

FIG. A-10. AFT FOIL DRAG COEFFICIENT AT 35 KNOTS AND ZERO TRIM

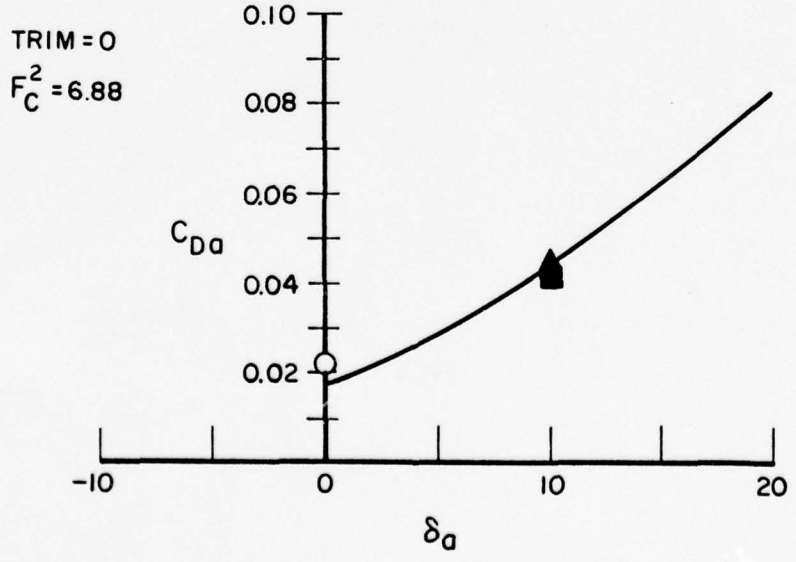

FIG. A-11. AFT FOIL DRAG COEFFICIENT AT 21.5 KNOTS AND ZERO TRIM

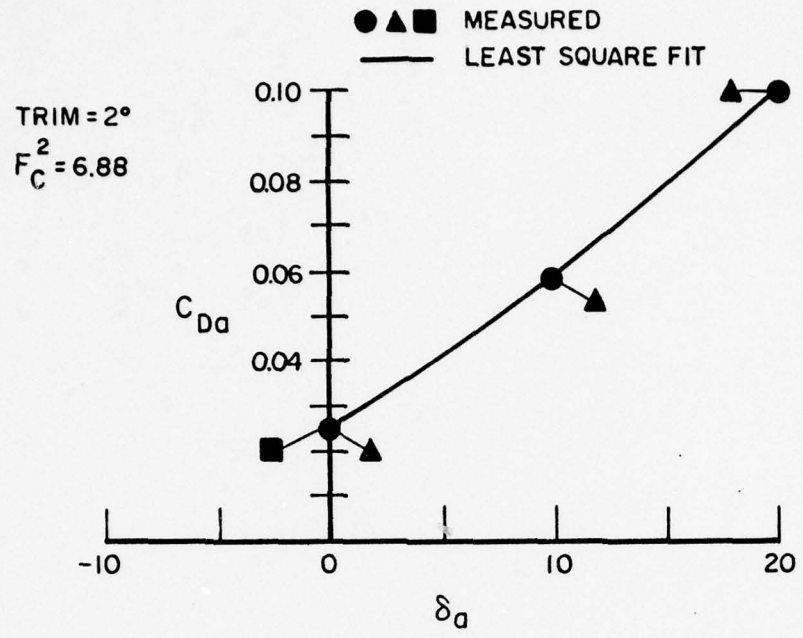

FIG. A-12. AFT FOIL DRAG COEFFICIENT AT 21.5 KNOTS AND 2° TRIM

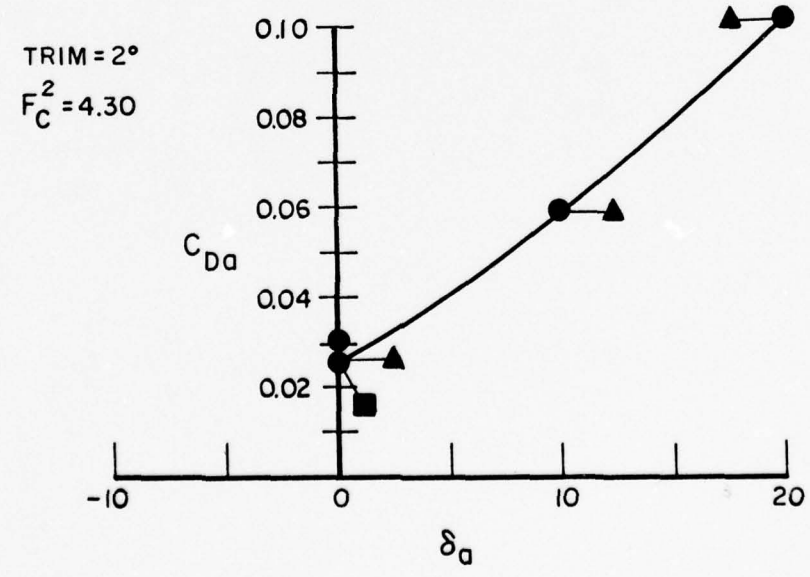

FIG. A-13. AFT FOIL DRAG COEFFICIENT AT 17 KNOTS AND 2° TRIM

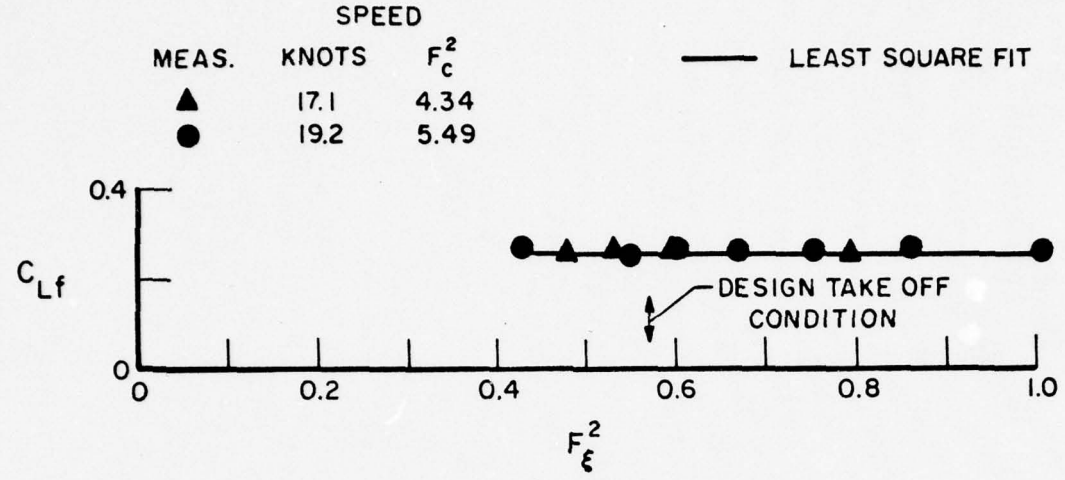

FIG. A-14. FORWARD FOIL LIFT VERSUS SEPARATION AT TWO DEGREES TRIM

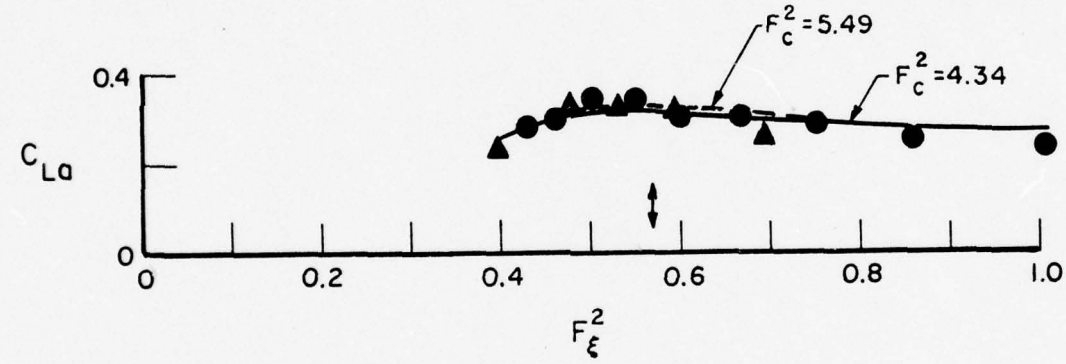

FIG. A-15. AFT FOIL LIFT VERSUS SEPARATION AT TWO DEGREES TRIM

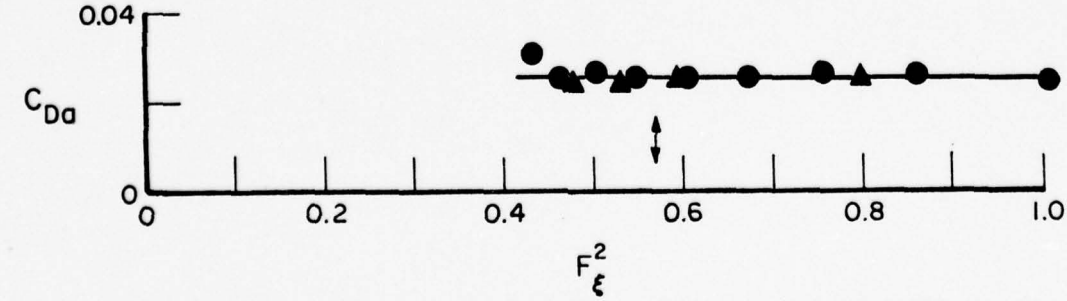

FIG. A-16. AFT FOIL DRAG VERSUS SEPARATION AT TWO DEGREES TRIM

APPENDIX B

FOILBORNE WAVE TESTS

The scaled model of the proposed hydrofoil amphibious lighter which is described on pages 5 and 6 was towed at constant speed unrestrained in pitch and heave, and with the automatic height controls, in calm water and in waves. Recordings were made of drag, heave, pitch, heave acceleration at the bow and vertical acceleration at the center of gravity, for various speeds and control settings. Tests were made in head seas and following seas representing sea state 2 for the full-scale vehicle. Both the light condition and the design load condition were tested.

The test results are summarized in Table B-1. For each run, the load configuration is indicated as well as the null position of each main flap, and the gain of each flap control system. The measured speed is indicated next, then the averages of the recorded samples for the drag force, heave displacement at the center of gravity and the pitch angle. The root mean square (RMS) signal level was calculated for the deviation from the mean of each motion signal, for those runs carried out in waves.

In addition to foilborne tests,a series of hullborne runs were carried out for low speed in calm water for the light ship condition. (See Runs 97 through 113.) The forward flaps were fixed at 5 degrees up, which is the zero lift flap angle at zero trim. The aft flaps were fixed at several values as indicated. The observed mean of the drag, heave and trim have been plotted for these runs in Figure B-1. It is seen that up to a speed of 8.5 knots, there is no effect of the aft flap angle on any results. Between 8.5 and 13 knots, the aft flap angle begins to reduce the bow-down trimming moment but heave and drag are still uneffected. As speed increases from 13 to 17 knots, a bow-up trim develops for aft flap angles of zero or less and drag begins to drop with more up-flap aft. Finally, between 17 and 21 knots, the heave position begins to rise, the bow-up trim increases and substantial reductions in drag occur with increasing up-flap aft.

The observed sinkage with increasing speed is caused by suction forces due to increased water velocities passing around and under the hull while

the bow-down trim develops in particular due to suction load on the convex bow sections. At speeds below 8.5 knots, insufficient dynamic lift is developed on the hydrofoils to overcome these suction forces and moments. These results would change little even if the forward flaps were full down. Between 8.5 and 13 knots, the pitching moment due to aft flap angle is sufficient for dynamic lifting forces to begin to effect trim, but the actual lift force is not sufficient to change the downward trend in heave displacement. Also in these speed ranges, the contribution to drag from increased flap angle is not noticeable due to the much higher drag of the hull. Up to 17 knots, the hydrofoil lift due to trim is still insufficient to cause a rise in the heave displacement. However, above 17 knots greater lift is developed due to greater speed as well as greater bow-up trim so that the heave displacement begins to rise with speed. As less of the weight is supported by the hull and more by hydrofoil lift, drag increases more slowly with speed and, in fact, drag falls off between 17 and 21 knots with the aft flap at -5 degrees. Take-off speed for the model corresponded to 22 knots full scale.

The trends observed in Figure B-1 are expected to be the same for the prototype. However since the maximum lift coefficient for the model was 0.7 while that for the prototype is 1.1 due to the higher Reynolds number, the observed effects of flap angle on heave, trim and drag will occur at lower speeds. Furthermore, with the hull in the displacement mode, the forward height sensors will call for full flap down on the forward foils which will increase the bow-up trim so that the anticipated maximum lift coefficient will be achieved. Consequently, take-off speed should be at 17 knots as anticipated for the prototype. It is significant that with -5 degrees of flap aft, the drag maximum shown in Figure B-1 is 21 lb at 8 ft/sec which corresponds to a full-scale power of 2420 HP. This power requirement will be reduced by (1) additional unloading of the hull by means of forward flap angle, and (2) reduction of full-scale drag estimate due to scale effect. Consequently, the full-scale installed power of 6400 HP should be more than sufficient for take-off requirements.

The take-off characteristics of the model were necessarily different than anticipated for the prototype because (1) the model take-off speed was higher than the prototype due to the lower maximum lift coefficient noted

in the foregoing, and (2) model acceleration to test speeds were considerably larger than for the prototype due to the limited length of the towing tank. These characteristics lead to extreme pitch angles as the model accelerated through its take-off speed leading, in turn, to large transient motions as the model entered the constant speed portion of the run. Consequently, the model height control system was required to damp out rather more severe initial transients in comparison to full scale, which gave a good test for the control system.

Many of the runs in calm water exhibited a long-period lightly-damped oscillation in pitch and heave which is similar to the phugoid oscillation of aircraft. Even when this oscillation was stable, the long-period often led to sufficiently large transient motions so that the hull re-entered the water after take-off. In some instances, hull re-entry occurred once followed by a successful flight (e.g., Run 133) while at other times hull re-entry occurred several times followed by another take-off attempt (e.g., Run 124). In several cases, the slow pitch-heave oscillation was of smaller amplitude so that hull re-entry did not occur, but the decaying oscillation is clearly seen in the recorded motion and in the movies (e.g., Runs 131,132,133). In waves, there is some indication that this pitch-heave transient can also be excited by wave impacts on the bow. Comparing Runs 32 and 31, it would seem that the phugoid oscillation can be stabilized by decreasing the forward control gain. Comparing Runs 34 and 35, as well as Runs 85 and 87, indicates that this response can be stabilized by increasing the mean trim. Another type of pitch-heave response occurred in Runs 56 and 58 where a higher frequency oscillation was observed, probably due to the particular combination control gain settings. These observations of calm water responses show (1) automatic control of the aft flaps is not required for calm water operation or in waves, (2) acceptable pitch-heave dynamics and equilibrium conditions can be achieved through appropriate seclection of control gain, relative position between control flap and strut flap and fixed aft flap angle, and (3) a dynamic analysis of the prototype in the flying condition should be carried out to estimate the required control gains.

In order to demonstrate the model response characteristics in sea state 2, Figures B-2 through B-8 have been prepared. The observed mean

drag is shown in Figure B-2 versus the mean heave and trim conditions in calm water while the observed mean drag in waves is shown in Figure B-3. The results shown near the design mean flying height and near one degree mean trim, indicate a mean drag increase in waves of about 14 percent or less over the calm water value at the same equilibrium conditions. Assuming that power is proportional to the cube of speed in the flying mode, the corresponding speed loss at constant power would be 4.4 percent or 1.3 knots. Thus, the power required to operate at 30 knots in calm water should yield an average speed of 28.7 knots in sea state 2, flying at the design mean flying height and one degree mean trim in both cases. Consequently, the anticipated speed of 32.5 knots in sea state 2 using the calm water power for 35 knots seems quite reasonable, or perhaps even conservative.

The observed rms levels of the wave induced responses, extrapolated to full scale, are shown below based on Figures B-4 through B-8 for 30 knot operation in head seas flying at the design mean flying height and one degree mean trim.

Response	RMS	Figure
Pitch	0.55 deg	B-4
Heave	0.16 ft	B-5
Bow Acceleration	0.2 g	B-6
CG Acceleration	0.12 g	B-7
Drag	11,400 lb	B-8

Runs 35 and 59 are the two points from Table B-1 which are closest to zero mean heave and one degree mean trim in Figures B-4 through B-8. The riding comfort in the pilot's compartment which is nearly the same location as the bow accelerometer should be acceptable. These motion levels probably can be reduced somewhat by appropriate choice of control gain for the forward flaps. In any case, an analysis of the effect of control gain on wave-induced motions should be carried out to at least insure that the control is not increasing wave-induced motions.

The design load condition was tested in calm water and in head and following seas at 35 knots as shown in Runs 131 through 142 in Table B-1.

Acceptable operation is demonstrated in Runs 138 and 139 for calm water and for head seas, respectively, and in Runs 140 and 141 for calm water and for following seas, respectively. The light ship configuration tested in Runs 127 and 128 for calm water and head seas was repeated in Runs 143 and 144 for calm water and following seas indicating acceptable operation for this control system configuration.

During these tests, it was observed that significant depressions are created in the free-surface directly above the hydrofoils, caused by the suction pressure on the upper surface. These depressions are greatest and nearly constant between the struts and decrease outboard of the struts. With the propellers directly over the aft hydrofoil, the depression here will be augmented by acceleration of the fluid due to propeller thrust. Consequently, there may be some difficulty in maintaining fully wetted flow at the propeller blades due to either propeller emersion or due to ventilation. It would appear desirable therefore to fly with some trim angle in order to increase the local water depth over the aft hydrofoil. In calm water, the stern of the hull would then travel in the depression created by the aft hydrofoil and propellers and would be clear of the local water surface. In waves, the stern would be exposed to a greater number of wave impacts than with zero mean trim so that some additional mean drag will be developed. However at zero trim, propeller ventilation and the attendant loss of thrust would probably cause a greater speed reduction than this increased mean drag.

Finally, it should be noted that the light ship and design load condition were successfully operated with the same control gain for the forward flaps, but that the forward flap null and the fixed aft flap position were changed. Consequently, in subsequent test phases for the proposed vehicle, these parameters should be adjustable.

TABLE B-1

FOILBORNE WAVE TESTS
MODEL DATA SUMMARY

Run	Stbd Gain	Fwd δ_{fo} deg	Port Gain	Fwd δ_{fo} deg	Stbd Gain	Aft δ_{fo} deg	Port Gain	Aft δ_{fo} deg	Speed ft/sec	Mean Drag lb	Mean Heave in	Mean Pitch deg	RMS VALUES Pitch deg	Heave in	Bow Accel g	CG Accel g	Drag lb	Remarks
LIGHT LOAD – HEAD SEAS																		
29	4.35	11	4.35	11	0	4	0	4	14.04									Stable run
30	0.9	11	1.1	11	0	4	0	4	14.04									Stable run
31	0.9	10	1.1	10	0	3	0	3	14.04	13.38	-0.13	0.073						Stable run
32	2.3	10	2.6	10	0	3	0	3	13.95	27.40	1.03	0.63						Unstable pitch and heave
33	2.3	10	2.6	10	0	3	0	3	13.76	25.11	0.97	1.17						Unstable pitch and heave
34	0.9	10	1.1	10	0	3	0	3	14.03	23.63	0.75	0.80	0.61	0.66	0.24	0.13	9.85	Unstable pitch and heave
35	0.9	12	1.1	12	0	3	0	3	14.04	15.88	-0.04	0.86	0.52	0.50	0.19	0.10	5.02	Stable run
36	0.45	12	0.5	12	0	3	0	3	14.04	17.60	-0.42	1.14						Stable run
37	0.9	13	1.1	13	0	3	0	3	14.04	13.22	-0.55	0.94						Stable run
38	0.9	13	1.1	13	0	3	0	3	14.04	14.57	-0.35	0.97	0.57	0.54	0.19	0.12	3.71	Stable run
39	0.9	13	1.1	13	0.45	3	0.5	3	14.04	13.52	-0.36	1.13						Stable run
40	0.9	13	1.1	13	0.45	3	0.5	3	13.99	21.84	0.28	0.73	0.58	0.99	0.22	0.14	10.77	Flew for half run only
41	1.35	13	1.6	13	0.45	3	0.5	3	14.04	13.82	-0.33	1.02						Stable run
42	1.35	13	1.6	13	0.45	3	0.5	3	13.95	25.47	0.81	0.61	0.60	0.77	0.25	0.11	12.09	Flew for half run only
43	1.35	13	1.6	13	0.45	3	0.5	3	13.95	31.67	1.25	0.50	0.45	0.44	0.28	0.12	9.42	Flew for half run only
44	1.8	13	2.1	13	0.45	3	0.5	3	14.04	13.95	-0.25	0.96						Very stable run
45	1.8	13	2.1	13	0.45	3	0.5	3	13.95	29.53	1.21	0.56	0.41	0.38	0.27	0.13	8.76	Long-period pitch-heave oscil.
46	1.8	13	2.1	13	0	3	0	3	14.04	14.63	-0.08	1.60						Stable run
47	1.8	13	2.1	13	0	3	0	3	14.04	18.31	0.26	1.59	0.71	0.44	0.26	0.13	4.88	Stable run
48	1.8	13	2.1	13	0	3	0	3	14.04	13.32	-1.75	2.53						Flying high
49	1.8	13	2.1	13	0	3	0	3	13.94	23.56	-2.56	5.78	0.72	0.35	0.39	0.16	4.88	Planing on forward foil
50	1.8	7	2.1	7	0	3	0	3	14.04	15.08	-0.05	1.91						Stable run
51	1.8	7	2.1	7	0	3	0	3	13.97	18.36	0.24	1.95	0.68	0.48	0.27	0.17	5.19	Stable run with pitch-heave oscil.
52	1.8	7	2.1	7	0	3	0	3	14.04	14.52	-0.31	1.81						Stable run
53	1.8	7	2.1	7	0	3	0	3	13.97	21.66	-2.30	4.81	1.60	0.92	0.36	0.16	5.06	Planing on forward foil
54	2.3	7	2.65	7	0	3	0	3	14.04	14.83	-0.24	1.88						Stable run
55	2.3	7	2.65	7	0	3	0	3	13.95	23.03	-2.63	5.60	0.75	0.44	0.38	0.16	5.30	Planing on forward foil
56	2.3	7	2.65	7	0.25	3	0.25	3	14.04	14.33	-0.32	1.42						Stable run with high frequency pitch-heave oscillation
57	2.3	7	2.65	7	0.25	3	0.25	3	14.04	21.11	-2.90	2.73	1.22	0.88	0.47	0.23	3.48	Planing on forward foil
58	2.3	7	2.65	7	0.45	3	0.5	3	14.04	14.22	-0.38	1.30						Stable run with high frequency pitch-heave oscillation
59	2.3	7	2.65	7	0.45	3	0.5	3	14.00	18.89	0.11	1.19	0.59	0.55	0.28	0.17	5.83	Stable run
60	2.3	7	2.65	7	0	20	0	20	7.94	31.40	3.69	-0.96						No take-off
61									7.97	25.94	3.62	0.33						No take-off
62	2.3	7	2.65	10	0	10	0	10	7.96	27.53	3.55	1.47						No take-off
63	2.3	7	2.65	10	0	0	0	0	7.96	25.50	3.11	4.43						No take-off
64	2.3	7	2.65	10	0	-10	0	-10	7.96	26.61	2.34	7.05						No take-off, forward height sensor controlling
65	2.3	7	2.65	10	0	-5	0	-5	7.97	23.78	2.41	6.04						No take-off
66	2.3	7	2.65	10	0	-5	0	-5	8.96	23.03	1.70	6.34						Some rise, transom dragging
67	2.3	7	2.65	10	0	20	0	20	8.50	35.59	3.48	-0.88						No take-off
68	2.3	7	2.65	10	0	10	0	10	8.66	28.18	3.00	2.44						No take-off
69	2.3	7	2.65	10	0	10	0	10	8.85	27.91	2.81	2.44						No take-off

[Cont'd]

TABLE B-1 (Cont'd)

Run	Stbd Gain	Fwd δ_{fo} deg	Port Gain	Fwd δ_{fo} deg	Stbd Gain	Aft δ_{fo} deg	Port Gain	Aft δ_{fo} deg	Speed ft/sec	Mean Drag lb	Mean Heave in	Mean Pitch deg	RMS VALUES Pitch deg	Heave in	Bow Accel g	CG Accel g	Drag lb	Remarks
LIGHT LOAD – HEAD SEAS																		
70	2.3	7	2.65	10	0	0	0	0	9.03	21.71	1.61	5.78						Some rise, transom dragging
71	2.3	7	2.65	10	0	10	0	10	10.03	27.33	2.29	2.45						No take-off
72	2.3	7	2.65	10	0	5	0	5	10.03	18.33	1.19	4.26						Flying low, transom dragging
73	2.3	7	2.65	10	0	0	0	0	10.03	20.17	0.91	5.92						Flying low, transom dragging
74	2.3	7	2.65	10	0	0	0	0	11.03	17.76	-0.48	5.72						Flying with stern low
75	2.3	7	2.65	10	0	5	0	5	11.03	16.20	0.56	3.60						Flying low
76	2.3	7	2.65	10	0	10	0	10	11.03	25.61	1.57	1.87						Unstable in pitch and heave
77	2.3	7	2.65	10	0	7.5	0	7.5	10.03	17.38	1.28	3.52						Flying low
78	2.3	7	2.65	10	0	8.5	0	8.5	10.03									Unstable in pitch and heave
79	2.3	7	2.65	10	0	8.5	0	8.5	11.03									Stable run
80	2.3	9	2.65	12	0	8.5	0	8.5	11.03	15.15	0.16	2.16						Stable run
81	2.3	7	2.65	10	0	8.5	0	8.5	11.03	16.09	0.53	2.26						Stable run
82	2.3	9	2.65	12	0	8.5	0	8.5	11.04	19.84	0.81	2.48	0.71	0.42	0.22	0.15	4.03	Stable run, small pitch-heave oscil.
83	2.3	9	2.65	12	0	8.5	0	8.5	12.03	14.53	-0.39	1.39						Stable run
84	2.3	9	2.65	12	0	8.5	0	8.5	12.03	21.21	0.46	1.63	0.77	0.63	0.24	0.14	6.26	Stable run, pitch-heave oscil.
85	2.3	9	2.65	12	0	8.5	0	8.5	13.04	21.36	0.10	0.35						Hull re-entry, second take-off and stable flying
86	2.3	7	2.65	10	0	8.5	0	8.5	13.04	18.12	-0.05	0.59						" " " "
87	2.3	9	2.65	12	0	6.5	0	6.5	13.04	13.69	-0.61	1.34						Stable run
88	2.3	9	2.65	12	0	6.5	0	6.5	13.04	22.01	-1.77	3.12	1.52	1.53	0.34	0.18	4.92	Planing on forward foil during last part of run
89	2.3	7	2.65	7	0	3	0	3	14.04	13.34	-1.35	2.50						Stable run
90	2.3	7	2.65	7	0	3	0	3	13.04	14.71	-0.41	2.86						Stable run
91	2.3	7	2.65	7	0	3	0	3	13.04	23.99	-2.55	5.67	0.99	0.81	0.36	0.17	4.26	Planing on forward foil
92	2.3	5	2.65	5	0	3	0	3	13.04	15.51	-0.19	3.01						Stable run
93	2.3	5	2.65	5	0	3	0	3	13.04	24.17	-2.61	5.78	0.95	0.64	0.30	0.12	4.26	Planing on forward foil
94	0.9	7	1.1	7	0	3	0	3	13.04	22.83	-2.90	5.66						Planing on forward foil
95	0.9	7	1.1	7	0	3	0	3	14.04	12.95	-0.83	1.06						Stable run
96	0.9	7	1.1	7	0	3	0	3	13.04	13.83	-0.44	1.69						Stable run
97	0	-5	0	-5	0	0	0	0	2.01	0.81	3.42	-0.13						
98	0	-5	0	-5	0	0	0	0	4.01	3.92	3.57	-0.31						
99	0	-5	0	-5	0	0	0	0	6.01	11.43	3.88	-0.61						
100	0	-5	0	-5	0	0	0	0	8.03	22.92	4.16	0.41						
101	0	-5	0	-5	0	0	0	0	10.03	26.35	3.43	2.22						
102	0	-5	0	-5	0	5	0	5	2.01	0.89	3.40	-0.02						
103	0	-5	0	-5	0	5	0	5	4.01	4.11	3.50	-0.37						
105	0	-5	0	-5	0	5	0	5	6.02	11.57	3.83	-1.16						
106	0	-5	0	-5	0	5	0	5	6.07	11.52	3.85	-1.17						
107	0	-5	0	-5	0	5	0	5	8.02	25.75	4.29	-1.10						
108	0	-5	0	-5	0	5	0	5	10.03	40.41	4.17	-0.65						
109	0	-5	0	-5	0	-5	0	-5	6.02	11.57	4.04	-0.12						
110	0	-5	0	-5	0	-5	0	-5	8.02	20.97	4.17	2.45						
111	0	-5	0	-5	0	-5	0	-5	10.03	20.05	2.77	5.11						
112	0	-5	0	-5	0	-5	0	-5	10.03	19.95	2.56	5.19						
113	0	-5	0	-5	0	-10	0	-10	6.02	11.81	3.81	0.50						
114	0.9	13	1.1	13	0	3	0	3	14.03	29.71	-2.90	6.23						Planing on forward foil

[Cont'd]

TABLE B-1 (Cont'd)

Run	Stbd Gain	Fwd δ_{fo} deg	Port Gain	Fwd δ_{fo} deg	Stbd Gain	Aft δ_{fo} deg	Port Gain	Aft δ_{fo} deg	Speed ft/sec	Mean Drag lb	Mean Heave in	Mean Pitch deg	RMS VALUES Pitch deg	Heave in	Bow Accel g	CG Accel g	Drag lb	Remarks
LIGHT LOAD – HEAD SEAS																		
115	2.3	8.5	2.65	8.5	0	8.5	0	8.5	11.04	24.06	1.48	1.79						Unstable in pitch and heave
116	2.3	12	2.65	12	0	8.5	0	8.5	11.04	22.61	1.04	2.01						Unstable in pitch and heave
117	2.3	12	2.65	12	0	5	0	5	11.03	14.60	0.15	3.13						Stable run
118	2.3	12	2.65	12	0	5	0	5	11.03	16.47	0.05	2.99	0.82	0.84	0.18	0.11	4.24	Good run, hull enters water once after bow-wave impact
119	2.3	12	2.65	12	0	5	0	5	12.03	14.03	-0.36	1.99						Stable run
120	2.3	12	2.65	12	0	5	0	5	12.03	18.65	-1.50	3.67	0.90	1.05	0.23	0.10	5.76	Forward foil ventilates near start, flying continues
121	2.3	10	2.65	10	0	5	0	5	12.03	14.02	-0.41	1.86						Stable run
122	2.3	10	2.65	10	0	5	0	5	12.03	19.83	-1.16	3.56	1.02	1.17	0.25	0.11	5.19	Forward foil ventilates near start, flying re-established
123	0.9	13	1.1	13	0	3	0	3	14.04	9.99	-2.40	3.94						Stable run, sensor out of water
124	0.9	4	1.1	4	0	3	0	3	14.04	22.67	0.87	1.27						Unstable in pitch and heave
125	0.9	6	1.1	6	0	1	0	1	14.04	14.37	-0.27	2.26						Stable run
126	0.9	6	1.1	6	0	2	0	2	14.04	14.13	-0.14	1.68						Stable run
127	0.9	6	1.1	6	0	3	0	3	14.04	14.31	0.04	1.07						Stable run
128	0.9	6	1.1	6	0	3	0	3	14.04	23.39	-2.59	5.21	1.16	0.59	0.42	0.20	5.19	Forward foil ventilates, then planes
129	0.9	4	1.1	4	0	3	0	3	14.04	22.21	0.76	1.24	0.57	0.48	0.25	0.15	6.07	Hull re-enters several times following bow-wave impact
130	0.9	5	1.1	5	0	3	0	3	14.04	18.74	0.21	1.44	0.75	0.80	0.19	0.11	6.10	" " " " "
DESIGN LOAD – HEAD SEAS																		
131	0.9	6	1.1	6	0	3	0	3	16.43	23.40	-1.23	1.63						Stable run
132	0.9	7	1.1	7	0	4	0	4	16.43	22.75	-1.49	1.66						Stable run
133	0.9	7	1.1	7	0	4	0	4	16.45	24.73	-0.85	2.01						Hit trim stop, hull re-enters once on initial pitch undershoot
134	0.9	7	1.1	7	0	4	0	4	16.38	40.19	-1.16	4.64						Hit trim stop, bow foil ventilates on take-off, flies with bow foil planning
135	0.9	7	1.1	7	0	4	0	4	16.42	22.64	-0.15	1.68						Stable run
136	0.9	8	1.1	8	0	5	0	5	16.44	38.54	-0.80	3.72						Hull re-enters on initial pitch undershoot, flies with bow foil planing
137	0.9	7	1.1	7	0	5	0	5	16.40	43.86	1.32	0.90						Hull re-enters several times
138	0.9	7	1.1	7	0	4	0	4	16.45	22.77	0.19	1.55						Stable run
139	0.9	7	1.1	7	0	4	0	4	16.44	25.38	0.43	1.53	0.41	0.31	0.19	0.12	5.12	Stable run
DESIGN LOAD – FOLLOWING SEAS																		
140	0.9	7	1.1	7	0	4	0	4	16.00	24.11	0.07	2.30						Stable run
141	0.9	7	1.1	7	0	4	0	4	16.50	24.73	-0.57	2.22	0.60	0.58	0.12	0.05	4.77	Stable run, some propeller immersion
142	0.9	7	1.1	7	0	4	0	4	16.42	32.90	-1.45	4.56	2.05	1.22	0.24	0.11	9.72	Forward foil planing
LIGHT LOAD – FOLLOWING SEAS																		
143	0.9	6	1.1	6	0	3	0	3	14.08	14.37	1.23	1.73						Stable run (repeat of Run 127)
144	0.9	6	1.1	6	0	3	0	3	14.10	14.41	-0.19	1.62	0.77	0.64	0.10	0.05	3.22	Stable run, slow pitch oscillation
145	2.3	10	2.65	10	0	5	0	5	12.09	13.89	-1.18	2.50						Stable run, flying too high bow & stern
146	2.3	9	2.65	9	0	5	0	5	12.09	13.51	-1.46	2.58						" " " " " " " "
147	2.3	8	2.65	8	0	5	0	5	12.08	15.00	-0.28	2.45						Stable run, bow a little too high
148	2.3	8	2.65	8	0	6	0	6	12.08	13.90	-0.27	1.82						Stable run
149	2.3	8	2.65	8	0	6	0	6	12.06									Forward foil ventilates and hull re-enters several times
150	2.3	8	2.65	8	1.2	6	1.3	6	12.02	33.65	1.33	0.64	0.55	0.44	0.08	0.04	6.78	Did not fly
151	2.3	10	2.65	10	1.2	6	1.3	6	12.05	20.51	-0.10	1.55	0.85	1.06	0.13	0.06	8.51	Flying near middle of run, aft foil ventilates, bubble washes off, model flies on

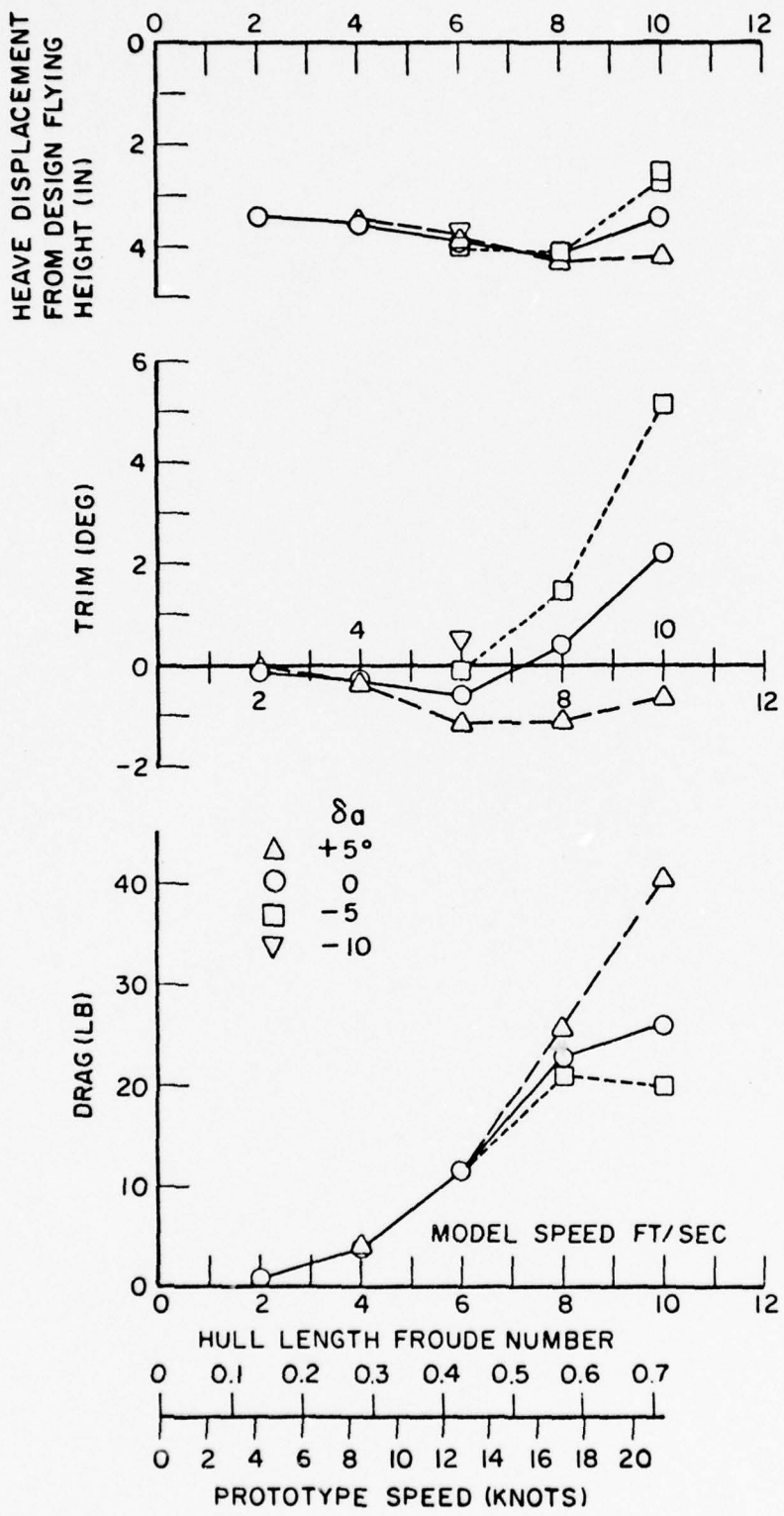

FIG. B-1. MEAN TRIM, HEAVE AND DRAG OF MODEL AT LOW SPEED IN CALM WATER FOR LIGHT SHIP CONDITION

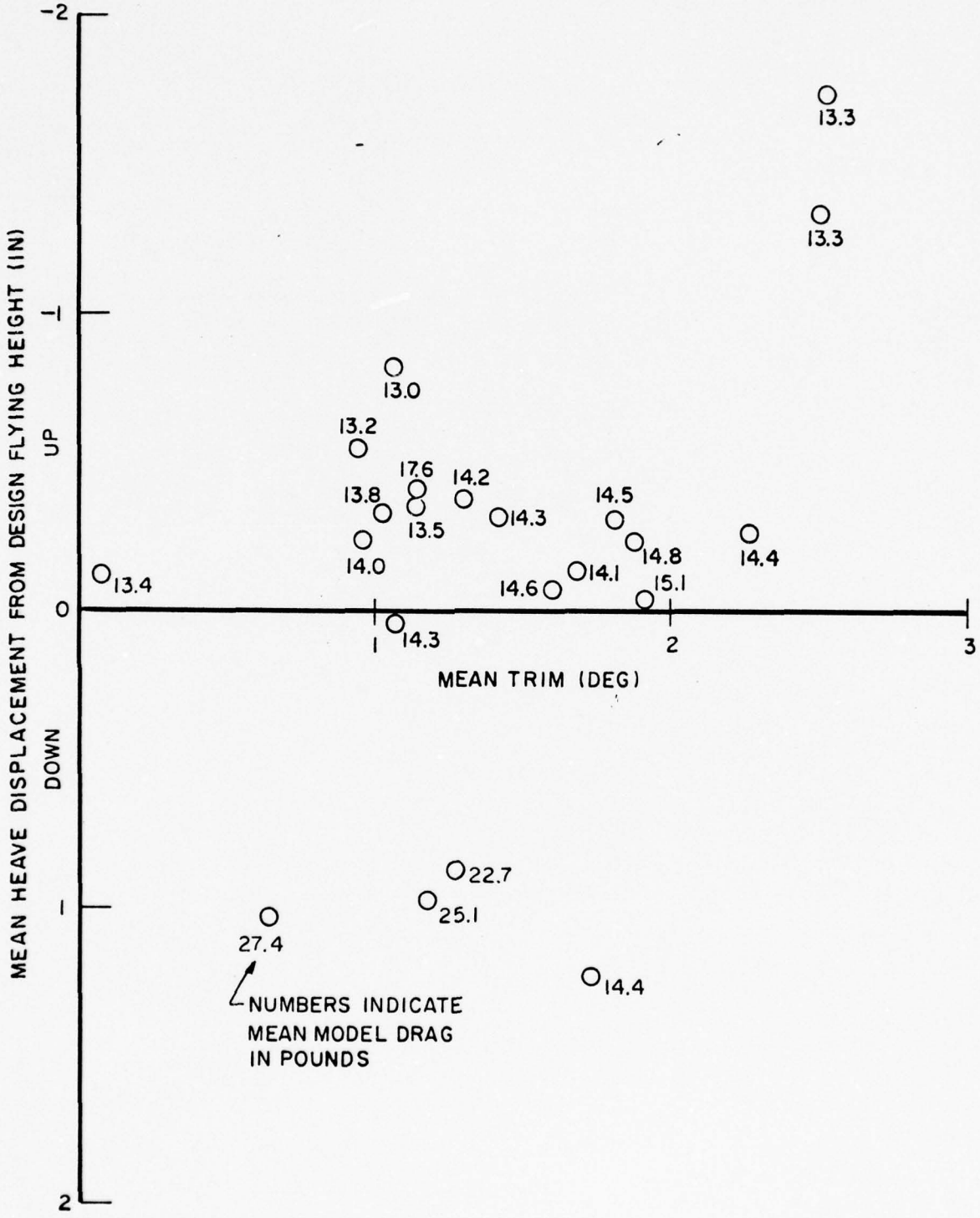

FIG. B-2. OBSERVED DRAG FOR LIGHT CONDITION IN CALM WATER AT 14 FT/SEC (30 KNOTS FULL SCALE)

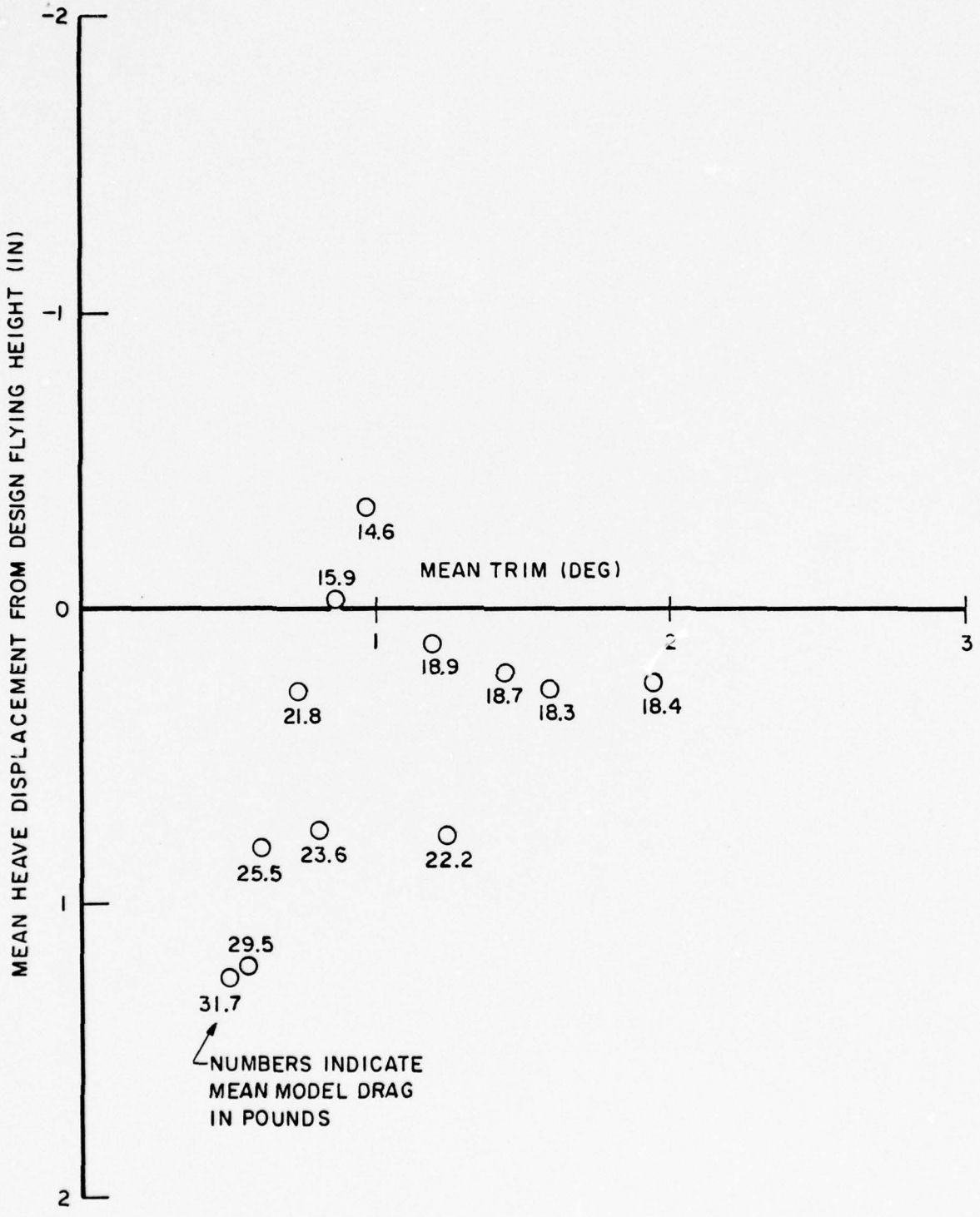

FIG. B-3. OBSERVED MEAN DRAG FOR LIGHT CONDITION IN SEA STATE 2 AT 14 FT/SEC (30 KNOTS FULL SCALE)

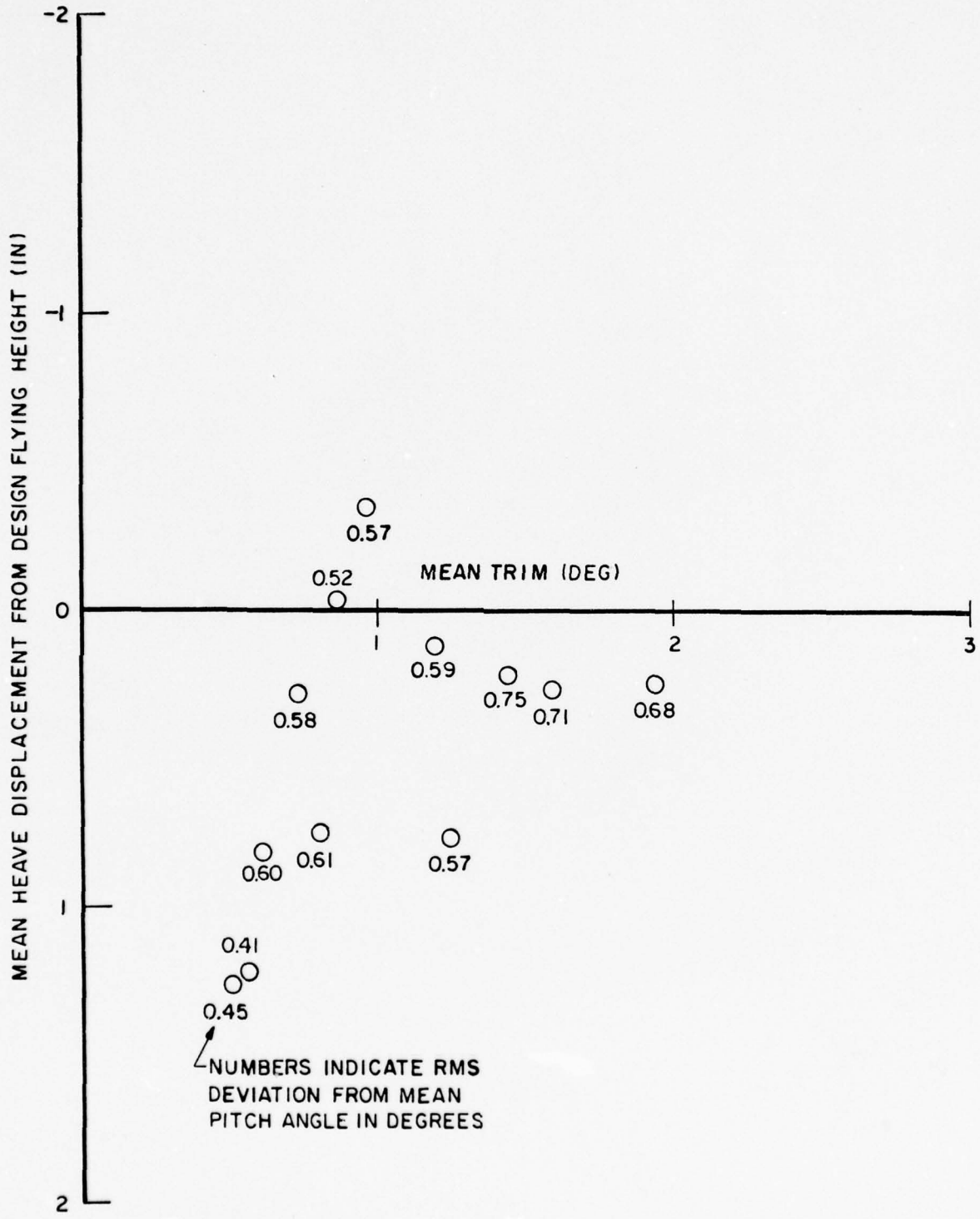

FIG. B-4. OBSERVED RMS PITCH RESPONSE FOR LIGHT CONDITION IN SEA STATE 2 AT 14 FT/SEC (30 KNOTS FULL SCALE)

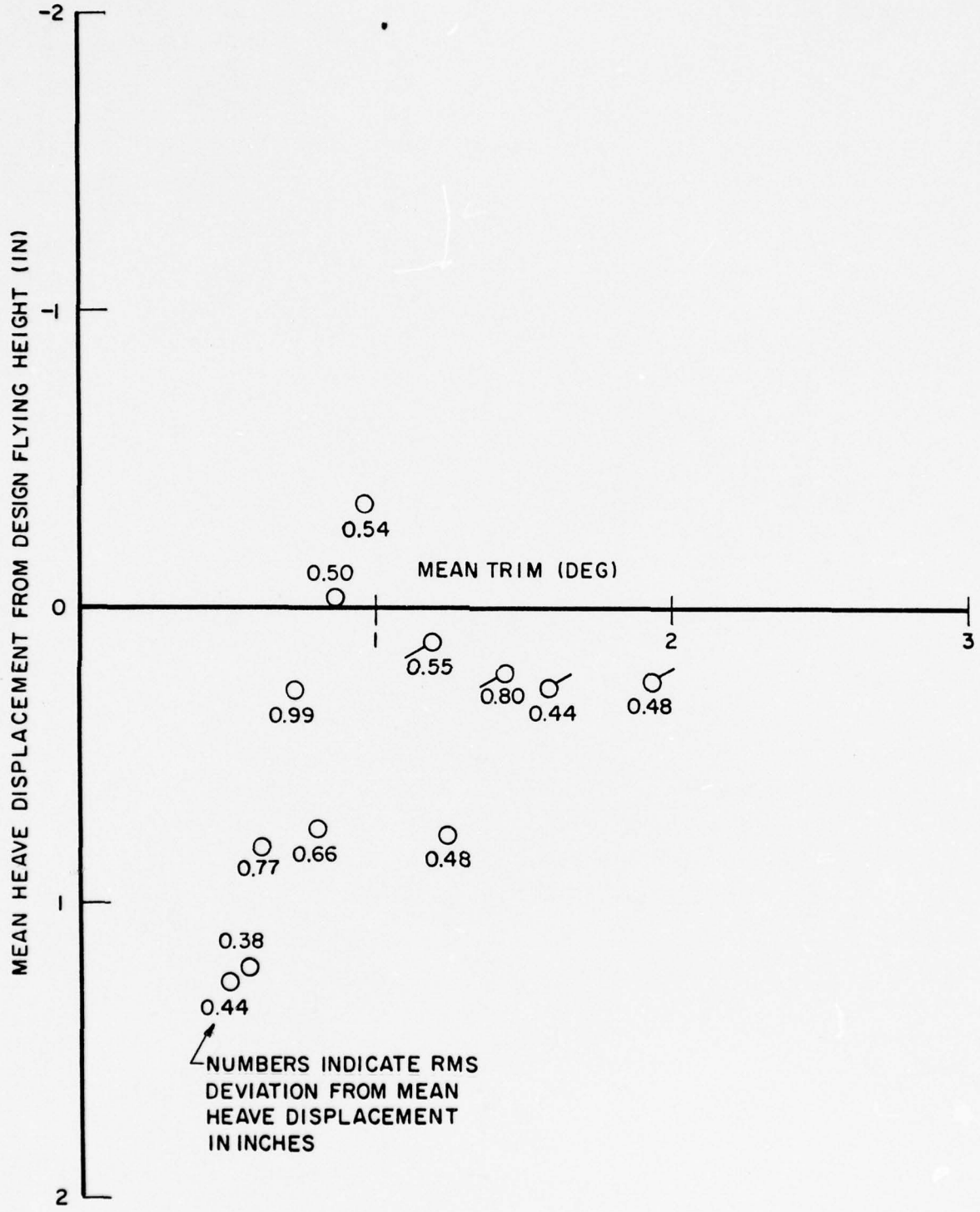

FIG. B-5. OBSERVED RMS HEAVE RESPONSE FOR LIGHT CONDITION IN SEA STATE 2 AT 14 FT/SEC (30 KNOTS FULL SCALE)

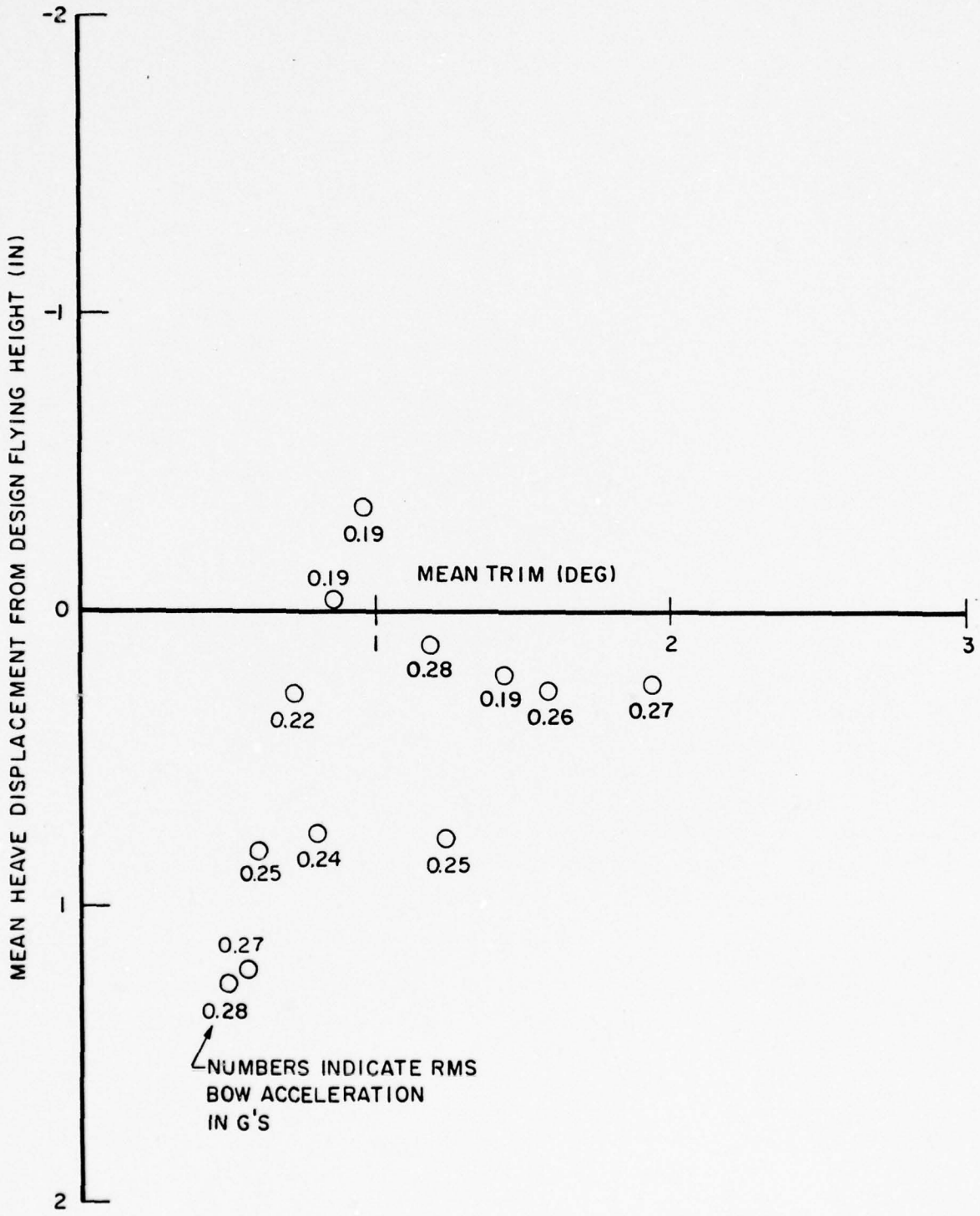

FIG. B-6. OBSERVED RMS BOW ACCELERATION FOR LIGHT CONDITION IN SEA STATE 2 AT 14 FT/SEC (30 KNOTS FULL SCALE)

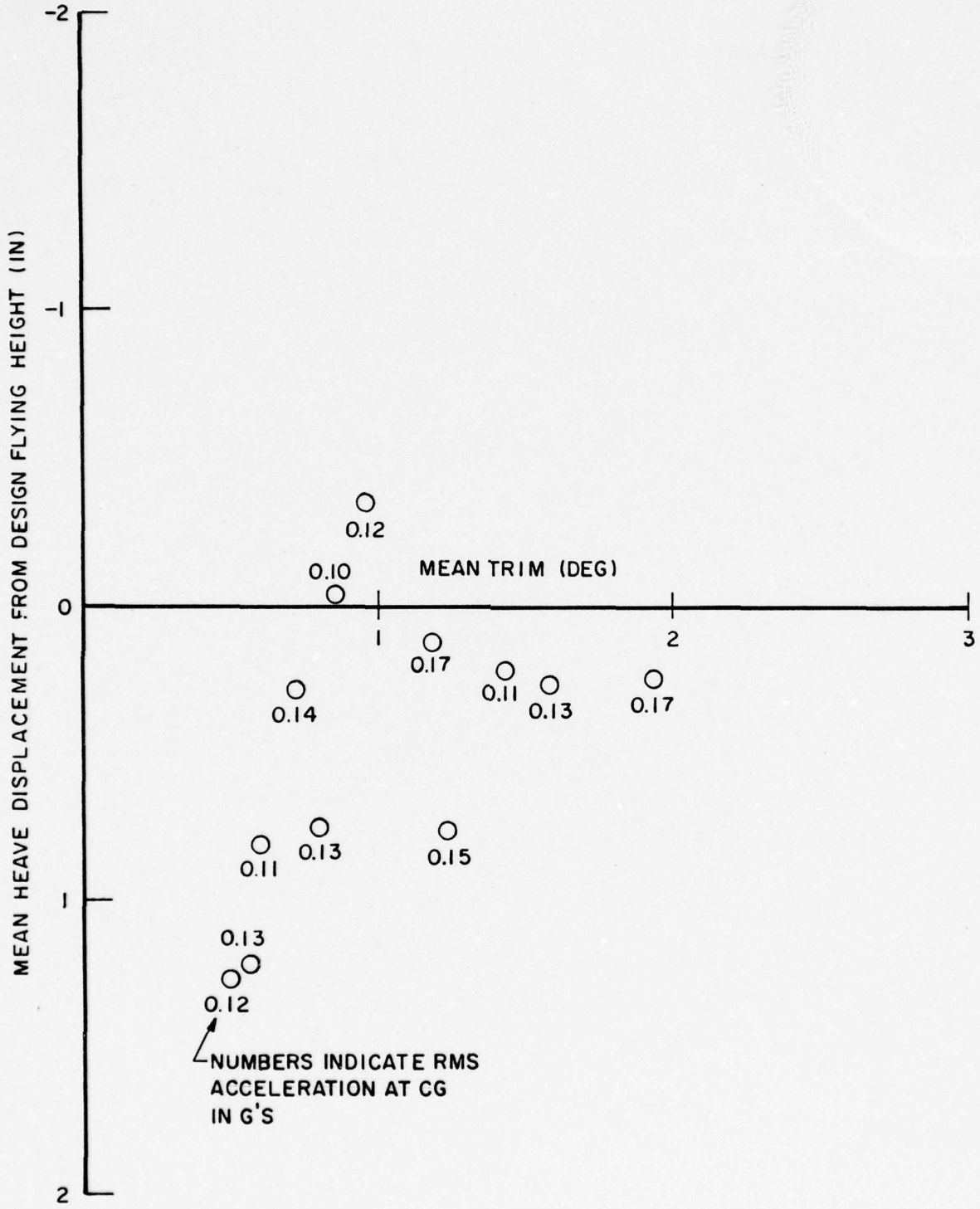

FIG. B-7. OBSERVED RMS ACCELERATION AT THE CG FOR LIGHT SHIP CONDITION IN SEA STATE 2 AT 14 FT/SEC (30 KNOTS FULL SCALE)

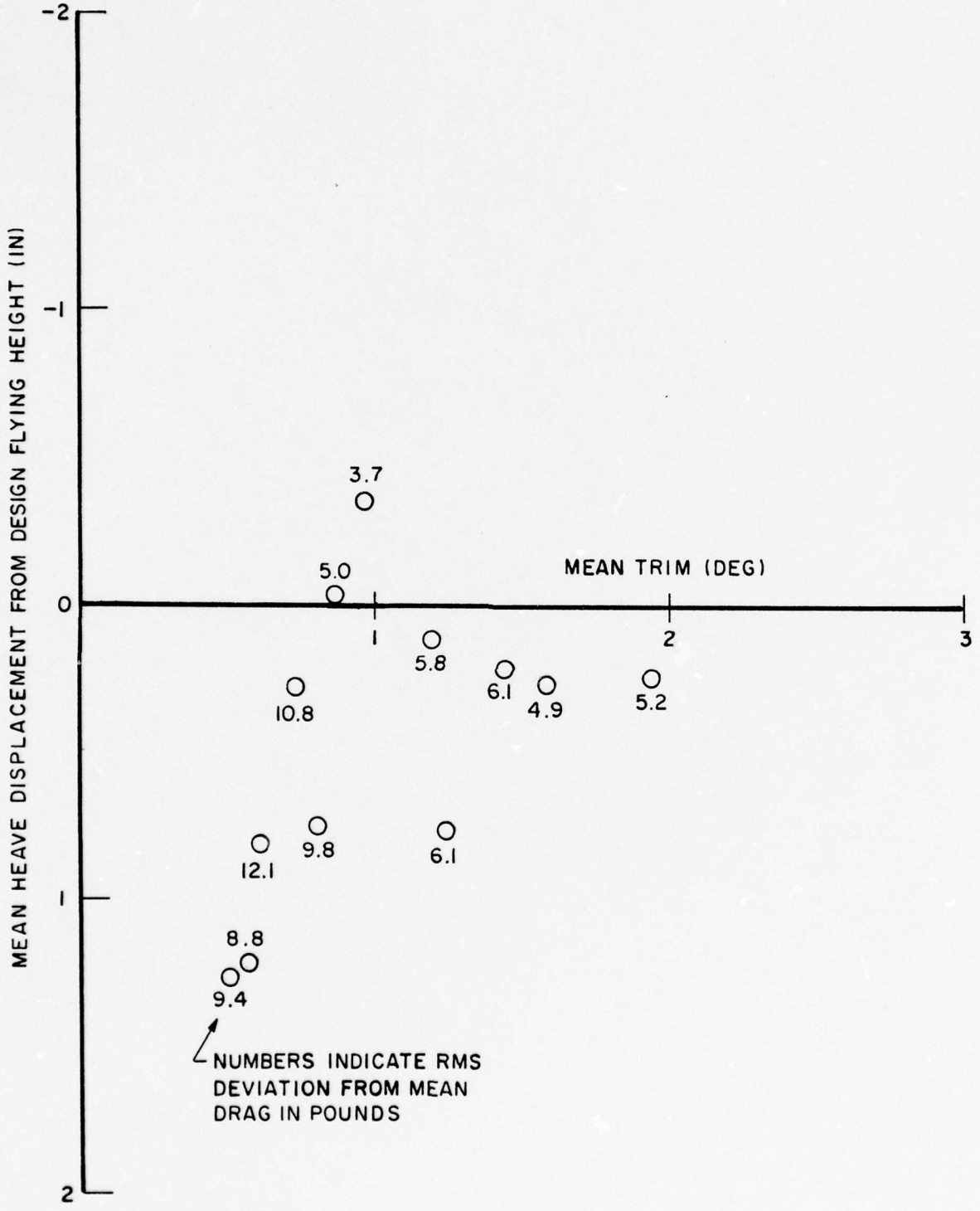

FIG. B-8. OBSERVED RMS DEVIATION IN DRAG FOR LIGHT SHIP CONDITION IN SEA STATE 2 AT 14 FT/SEC (30 KNOTS FULL SCALE)

APPENDIX C

STABILITY AND TURNING TESTS

Measurements of forward side force S'_F, aft side force S'_A, roll moment K, drag D', heave displacement and trim were obtained for the model in the light ship and design load condition traveling in a circular path, over a range of radius, speed, drift angle, roll angle and rudder angle. A diagram showing the setup and the sign conventions is given in Figure C-1. The test results are listed in Tables C-1 through C-8.

Tests were carried out at three radii, R=10,20,30 feet as shown in the Tables, where a negative radius is used to indicate turning to port and positive indicates turning to starboard. Thus, the turning rate ω about a vertical earth-fixed axis is given by

$$\omega = V/R$$

where V is the resultant speed of the model. Values of speed V, drift angle β_o, roll angle φ and rudder angle δ were chosen at random over the following ranges and increments:

$1.5 \leq V \leq 5.0$ ft/sec	$\Delta V = 0.10$ ft/sec
$-5. \leq \beta_o \leq 15.$ deg (starboard turn) $-15 \leq \beta_o \leq 5.$ deg (port turn)	$\Delta\beta = 1.$ deg
$-5. \leq \varphi \leq 5.$ deg	$\Delta\varphi = 1.$ deg
$-20 \leq \delta \leq 20.$ deg	$\Delta\delta = 2.$ deg

The speed indicated in Tables C-1 through C-8 is the observed speed obtained by measuring the time to travel a known distance during each run. The maximum available rudder angle is about 22 degrees where the rudder hits the ventilation plates over the inboard propellers. Use of a randomly selected matrix of test conditions has the advantage of covering this four-dimensional space with fewer total number of tests than a systematic test matrix, but has the disadvantage that the results cannot be plotted in any reasonable fashion.

Certain test conditions were repeated periodically as indicated in the last column of Tables C-1 through C-8 where the value 0 indicates the run is not a repeat run while a value $j \neq 0$ indicates the run belongs to the j^{th} replicate set. These runs provide additional means of judging measurement error statistics as well as goodness of fit in the least squared error curve fitting procedure. The estimated standard deviation of measurement error based on repeat runs is shown in the following table for each measured force and moment:

STANDARD DEVIATIONS

	Light Ship	Design Load
S_F' (lb)	0.0500	0.0783
S_A' (lb)	0.0565	0.0904
K (ft lb)	0.531	0.231
D' (lb)	0.231	0.203

These measurement error statistics are consistent with expectations based on experience with the instrumentation and procedures.

The least squared error curve fitting technique was used to find mathematical representations of the measured forces and moments in terms of V, ω, β_o, φ and δ. The results of this data analysis are shown in Tables C-9 through C-16. The procedure used in applying the least squared error technique is described by the following steps for each force or moment:

1) The given data were scanned for obviously erroneous points.

2) An initial fit was obtained using all remaining data points together with those first and second-order terms consistent with physical symmetry as follows:

S_F', S_A' and K: $1, \omega, \beta_o, \varphi, \delta, \tilde{V}\omega, \tilde{V}\beta_o, \tilde{V}\varphi, \tilde{V}\delta$

D': $1, \tilde{V}, \tilde{V}^2, \omega^2, \beta^2, \varphi^2, \delta^2$

where $\tilde{V} = V - V_o$, $V_o = 3.25$ ft/sec.

3) The data set was again scanned and data points whose error between measured values and values predicted by the initial fitting functions was inconsistently large, where deleted.

4) Steps 2 and 3 were repeated until the error distribution passed the Chi-Squared test of normality at the 95 percent confidence level.

5) After obtaining a trial fit, additional terms were tested up to fifth order to find terms whose correlation with the error indicated possible significant dependence.

6) One or two terms with high correlation were added while terms with low values of the Student's-t statistic for the corresponding coefficient were dropped and a new trial fit was calculated.

7) Steps 5 and 6 were repeated until one or both of the following conditions were satisfied:

a) Error correlation with the dependent variable was less than 6 percent.

b) The hypothesis that the residual error variance was not significantly larger than the measurement error variance obtained from repeat runs, passed the F-test at 95 percent confidence level.

The observed values of side forces and drag (designated by a prime) were composed of the desired hydrodynamic values (unprimed symbols) plus centrifugal force effects, such that

$$\left.\begin{aligned} S_F'+S_A' &= S_F+S_A - \frac{W_C}{g}\,\omega\, V\cos\beta_o \\ x_F S_F'+x_A S_A' &= x_F S_F+x_A S_A - x_C\,\frac{W_C}{g}\,\omega\, V\cos\beta_o \\ D' &= D + \frac{W_C}{g}\,\omega\, V\sin\beta_o \end{aligned}\right\} \qquad (C\text{-}1)$$

In order to evaluate the centrifugal force terms, a series of runs were conducted with the model raised above water with $\beta_o=0$, where it was assumed that $S_F = S_A = D = 0$. Then in terms of the observed forces, the values of W_C and x_C are given by

$$W_C = -\frac{g\omega}{V}(S'_F + S'_A)$$

$$x_C = -\frac{g\omega}{W_C V}(x_F S'_F + x_A S'_A)$$

where $x_F = -x_A = 2.5$ feet. Averaged values of these parameters from the runs in air are shown in the following table:

	Light Ship	Design Load
W_C (lb)	212	295
x_C (ft)	-0.04	+0.02

The hydrodynamic contributions to side forces and drag can then be found from Eq.(C-1) as

$$S_F = S'_F + \left(\frac{x_C - x_A}{x_F - x_A}\right)\frac{W_C}{g} V\omega\cos\beta_o = S'_F + S_{FC}$$

$$S_A = S'_A + \left(\frac{x_F - x_C}{x_F - x_A}\right)\frac{W_C}{g} V\omega\cos\beta_o = S'_A + S_{AC}$$

$$D = D' - \frac{W_C}{g} V\omega\sin\beta_o \qquad = D' - D_C$$

These corrections were made after the least squares fitting procedure by expanding each correction term in a Taylor Series Expansion at the point $(V,\omega,\beta_o,\varphi,\delta) = (V_o,0,0,0,0)$ where $V_o = 3.25$ ft/sec, as in the fitting functions. These expansions take the forms

$$S_{FC} = \left(\frac{x_C - x_A}{x_F - x_A}\right)\frac{W_C}{g}\left\{V_o\omega + \tilde{V}\omega - \frac{1}{2}V_o\omega\left(\frac{\beta_o}{57.3}\right)^2 - \frac{1}{2}\tilde{V}\omega\left(\frac{\beta_o}{57.3}\right)^2 + \frac{1}{24}V_o\omega\left(\frac{\beta_o}{57.3}\right)^4 + \ldots\right\}$$

$$= 10.53\omega + 3.24\tilde{V}\omega - .0016023\omega\beta_o^2 - .00049348\tilde{V}\omega\beta_o^2 + .40736\times10^{-7}\omega\beta_o^4 \quad \text{(Light Ship)}$$

$$= 15.01\omega + 4.62\tilde{V}\omega - .0022846\omega\beta_o^2 - .00070367\tilde{V}\omega\beta_o^2 + .57995\times10^{-7}\omega\beta_o^4 \quad \text{(Design Load)}$$

$$S_{AC} = \left(\frac{x_F - x_C}{x_F - x_A}\right) \frac{W_C}{g} \left\{V_o\omega + \tilde{V}\omega - \frac{1}{2} V_o\omega\left(\frac{\beta_o}{57.3}\right)^2 - \frac{1}{2} \tilde{V}\omega\left(\frac{\beta_o}{57.3}\right)^2 + \frac{1}{24} V_o\omega\left(\frac{\beta_o}{57.3}\right)^4 + \ldots\right\}$$

$$= 10.87\omega + 3.34\tilde{V}\omega - .0016571\omega\beta_o^2 - .00050932\tilde{V}\omega\beta_o^2 + .42035\times10^{-7}\omega\beta_o^4 \quad \text{(Light Ship)}$$

$$= 14.77\omega + 4.54V\omega - .0022481\omega\beta_o^2 - .00069148V\omega\beta_o^2 + .57067\times10^{-7}\omega\beta_o^4 \quad \text{(Design Load)}$$

$$D_C = \frac{W_C}{g} \left\{V_o\omega \left(\frac{\beta_o}{57.3}\right) + \tilde{V}\omega \left(\frac{\beta_o}{57.3}\right) - \frac{1}{6} V_o\omega \left(\frac{\beta_o}{57.3}\right)^3 - \frac{1}{6} \tilde{V}\omega \left(\frac{\beta_o}{57.3}\right)^3 + \ldots \right\}$$

$$= .37350\omega\beta_o + .11484\tilde{V}\omega\beta_o - .18980\times10^{-4}\omega\beta_o^3 - .58323\times10^{-5}\tilde{V}\omega\beta_o^3 \quad \text{(Light Ship)}$$

$$= .52011\omega\beta_o + .15987\tilde{V}\omega\beta_o - .26370\times10^{-4}\omega\beta_o^3 - .81184\times10^{-5}\tilde{V}\omega\beta_o^3 \quad \text{(Design Load)}$$

The correction coefficients and the resulting corrected coefficients are shown in Tables C-9 through C-16. In addition, terms used in fitting the data which do not have the desired symmetry were set equal to zero in the corrected coefficients. The final equations used in the following analyses are listed at the bottom of each table.

Low Speed Turning and Stability

Turning equilibrium conditions and the dynamic stability of these conditions can be obtained from the equations of motion. Using the coordinate system shown in Figure C-1 and neglecting surge, heave, roll and pitch motions yields equations of motion in side-sway and yaw in the form

$$\begin{aligned} m(\dot{v} + ru) &= Y(u,v,r,\delta,\dot{v},\dot{r}) \\ I_{zz}\dot{r} &= N(\quad " \quad) \end{aligned} \qquad \text{(C-2)}$$

For calculating turning equilibrium conditions, take $\dot{v}=\dot{r}=0$ and let $u=V\cos\beta_o$, $v=V\sin\beta_o$, $r=\omega$, so that Eqs.(C-2) become

$$\begin{aligned} Y(V\cos\beta_o, V\sin\beta_o, \omega, \delta, 0, 0) - m\omega V\cos\beta_o &= 0 \\ N(\quad " \quad) &= 0 \end{aligned} \qquad \text{(C-3)}$$

In terms of the corrected side forces $S_r(V,\omega,\beta_o,\varphi,\delta)$ and $S_A(V,\omega,\beta_o,\varphi,\delta)$, the side force and yaw moment are given by

$$Y = S_F(V,\omega,\beta_o,0,\delta) + S_A(V,\omega,\beta_o,0,\delta)$$
$$N = x_F S_F(\ \ " \ \ ) + x_A S_A(\ \ " \ \ ) \qquad \text{(C-4)}$$

Combining equations (C-3) and (C-4) gives

$$S_F(V,\omega,\beta_o,0,\delta) + S_A(V,\omega,\beta_o,0,\delta) - m\omega V\cos\beta_o = 0$$
$$x_F S_F(\ \ " \ \ ) + x_A S_A(\ \ " \ \ ) = 0 \qquad \text{(C-5)}$$

By specifying speed V and rudder angle δ, Eqs.(C-5) become two non-linear algebraic equations for determining the drift angle β_o and turning rate ω for an equilibrium turn.

If the resulting equilibrium condition is stable then the yaw rate r and the drift angle $\arctan(-v/u)$ will return to the respective equilibrium values ω and β_o after a small perturbation. This dynamic stability can be found from the equations of motion by assuming small perturbations $\tilde{v}$ and $\tilde{r}$ from the equilibrium state, i.e.,

$u = V\cos\beta_o$	$\dot{u} = 0$
$v = V\sin\beta_o + \tilde{v}$	$\dot{v} = \dot{\tilde{v}}$
$r = \omega + \tilde{r}$	$\dot{r} = \dot{\tilde{r}}$
$\delta = \delta_o$	$\dot{\delta} = 0$

The equations of motion then become

$$m\left[\dot{\tilde{v}} + (\omega+\tilde{r})V\cos\beta_o\right] = Y_o + Y_v\tilde{v} + Y_r\tilde{r} + Y_{\dot{v}}\dot{\tilde{v}} + Y_{\dot{r}}\dot{\tilde{r}}$$
$$I_{zz}\dot{\tilde{r}} = N_o + N_v\tilde{v} + N_r\tilde{r} + N_{\dot{v}}\dot{\tilde{v}} + N_{\dot{r}}\dot{\tilde{r}} \qquad \text{(C-6)}$$

where the side force and yaw moment have been expanded in a Taylor Series about the equilibrium condition, thus

$$Y_o = m\omega V\cos\beta_o \qquad N_o = 0$$

and, for example,

$$Y_v = \frac{\partial}{\partial v} Y(u,v,r,\delta,\dot{v},\dot{r}) \Big|_{\substack{u=V\cos\beta_o\ ,\ \delta=\delta_o \\ v=V\sin\beta_o\ ,\ \dot{v}=0 \\ r=\omega\ ,\ \dot{r}=0}}$$

The coefficients Y_v, Y_r, N_v, N_r can be found from Eqs.(C-4) since

$$\frac{\partial}{\partial v} = -\sin\beta_o \frac{\partial}{\partial V} - V\cos\beta_o \frac{\partial}{\partial \beta_o}$$

and

$$\frac{\partial}{\partial r} = \frac{\partial}{\partial \omega}$$

thus,

$$\begin{aligned} Y_v &= -(S_{FV_o} + S_{AV_o})\sin\beta_o - (S_{F\beta_o} + S_{A\beta_o})V\cos\beta_o \\ Y_r &= S_{F\omega_o} + S_{A\omega_o} \\ N_v &= -(x_F S_{FV_o} + x_A S_{AV_o})\sin\beta_o - (x_F S_{F\beta_o} + x_A S_{A\beta_o})V\cos\beta_o \\ N_r &= x_F S_{F\omega_o} + x_A S_{A\omega_o} \end{aligned} \qquad \text{(C-7)}$$

The added inertial coefficients $Y_{\dot{v}}, Y_{\dot{r}}, N_{\dot{v}}, N_{\dot{r}}$ were estimated as follows. It was assumed that contributions from the struts and from the hull were simply additive. The added mass of the struts was taken as

$$m' = \frac{\pi \rho \zeta^2 (c/2)^2}{\sqrt{\zeta^2 + (c/2)^2}}$$

where ζ is the strut length and c is the strut chord. The contribution to $Y_{\dot{v}}$ due to the struts is then $-4m'$ while the contribution to $Y_{\dot{r}}$ and $N_{\dot{v}}$ is $-2m'(x_{HF} + x_{HA})$ where x_{HF} and x_{HA} are the locations of the struts with respect to the CG, positive forward. The contribution to $N_{\dot{r}}$ is $-2m'(x_{HF}^2 + x_{HA}^2)$. The added mass of the hull in side-sway was estimated from Reference 9 at zero frequency which gives a contribution of $-0.33\rho\forall$ for the light ship condition and $-0.46\rho\forall$ for the design load condition. The contribution of the hull to $N_{\dot{r}}$ was estimated by assuming that the added mass $Y_{\dot{v}}$ due to the hull was uniformly distributed over the length of the hull so that

$$N_{\dot{r}} = \frac{Y_{\dot{v}} L^2}{12}$$

The resulting values are shown in the following table.

	LIGHT SHIP			DESIGN LOAD		
	Struts	Hull	Total	Struts	Hull	Total
$Y_{\dot{v}}$ (lb sec^2/ft)	-0.41	-1.25	-1.66	-0.41	-2.68	-3.09
$Y_{\dot{r}}$ (lb sec^2)	-0.16	0	-0.16	-0.20	0	-0.20
$N_{\dot{v}}$ (lb sec^2)	-0.16	0	-0.16	-0.20	0	-0.20
$N_{\dot{r}}$ (ft lb sec^2)	-1.28	-3.84	-5.12	-1.32	-8.24	-9.56

The equations of motion can now be written in the form

$$M\begin{bmatrix}\dot{v}\\ \dot{r}\end{bmatrix} = F\begin{bmatrix}\dot{v}\\ \dot{r}\end{bmatrix}$$

where

$$M = \begin{bmatrix} m-Y_{\dot{v}} & -Y_{\dot{r}} \\ -N_{\dot{v}} & I_{zz}-N_{\dot{r}} \end{bmatrix}, \quad F = \begin{bmatrix} Y_v & Y_r-mV\cos\beta_o \\ N_v & N_r \end{bmatrix}$$

and the eigenvalues of this linear system are given by the roots of the characteristic equation

$$P(\lambda) = \left|\lambda I - M^{-1}F\right| = 0 \quad .$$

The system is stable if the real parts of all eigenvalues are negative. Furthermore, the magnitude of the real part of the eigenvalues give a quantitative measure of dynamic stability at the equilibrium condition.

The turning equilibrium conditions and the least stable stability index are listed in Table C-17 for the light ship condition and in Table C-18 for the design load condition. It is seen that the turning radius is unacceptably large for both load conditions. At the same time the stability indices are very large, for example, in the light ship condition at a model speed of 3.0 ft/sec with a rudder angle of -20 degrees, the response to a small perturbation will be reduced to e^{-1} times the initial value in 3.4 seconds ($1/\sigma_i$). It is also noted that the drift angles are small. In order to explain these results, the hydrodynamic derivatives were calculated and listed in Tables C-17 and C-18. These results show that the large negative values

of N_r lead to large stabilizing yaw moments tending to make the vehicles follow a straight course and that the rudder moment is insufficient to develop large drift angles as required for reasonable turning characteristics.

In order to improve the predicted turning characteristics, the following series of calculations were carried out. First, the rudder angle dependent terms in the least squares fits were checked against empirically estimated values and new turning equilibrium and stability calculations were carried out. Secondly, the rudder geometry was changed to one having the same dimensions as the main struts (extending from hull to foils) and the corresponding turning and stability calculations were repeated. The results of these calculations are also shown in Tables C-17 and C-18. It is seen that considerable improvement in turning characteristics is obtained, with no significant change in stability. The improvement in turning characteristics is due to the increased rudder force rates in these calculations.

The empirical estimate of the rudder force rate was obtained by taking the rudder lift equal to

$$L = \frac{1}{2} \rho V_R^2 S_R C_{L\alpha R} \alpha_R$$

where

V_R = resultant inflow speed at rudder

S_R = rudder side area

$C_{L\alpha R}$ = rudder lift curve slope

α_R = angle of attack at rudder

Thus,

$$V_R^2 = V^2 - 2x_R \omega \sin\beta_o + x_R^2 \omega^2$$

$$\alpha_R = \delta_R + \arctan\left[\frac{V\sin\beta_o - x_R\omega}{V\cos\beta_o}\right]$$

Thus, the side force due to the rudder is given by

$$Y_R = \frac{1}{2} \rho S_R C_{L\alpha R} \left[V^2 - 2Vx_R\omega\sin\beta_o + x_R^2\omega^2\right] \left[\delta_R + \arctan\left(\frac{V\sin\beta_o - x_R\omega}{V\cos\beta_o}\right)\right] \qquad (C\text{-}8)$$

and the corresponding contributions to the fore and aft side forces are

$$S_{FR} = -\left(\frac{x_A - x_R}{x_F - x_A}\right) Y_R \quad \text{and} \quad S_{AR} = \left(\frac{x_F - x_R}{x_F - x_A}\right) Y_R \tag{C-9}$$

The lift curve slope for the proposed rudder was estimated from

$$C_{L\alpha R} = \frac{2\pi A_R}{A_R + 2}$$

where the aspect ratio A_R was taken as twice the geometric aspect ratio due to the end plate effect of the hull. The lift curve slope and area for the model are then

$$C_{L\alpha R} = 0.04805/\text{dec} \quad \text{and} \quad S_R = 0.10938 \text{ ft}^2$$

Differentiating Eqs.(C-9) and (C-8) with respect to δ and $V\delta$ and evaluating the results at the Taylor Series Expansion point leads to

$$S_{FR\delta} = 0.005496 \text{ lb/deg} \qquad S_{AR\delta} = 0.04946 \text{ lb/deg}$$

$$S_{FRV\delta} = 0.003382 \text{ lb sec/ft deg} \qquad S_{ARV\delta} = 0.03044 \text{ lb sec/ft deg}$$

Other terms in S_F and S_A will also be effected by the rudder; however, these effects were ignored because the struts and hull contributions are more significant and because the corrections are not straight-forward. Comparing the above values with the corresponding terms (coefficients of δ and $\tilde{V}\delta$) listed in Tables C-9, C-10, C-13 and C-14, it is seen that the least squares fit values are significantly different. These discrepancies may be due to (a) the low Reynolds number of the model as described in Appendix A, or (b) the effect of the adjacent skegs and ventilation plates. If the discrepancy is due to (a), then the full-scale rudder forces are expected to be close to the above empirical estimates. However, if the discrepancy is due to (b), then the least squares fit results should represent prototype characteristics. In either case the calculated turning characteristics shown in Tables C-17 and C-18 are not acceptable, although the larger estimated rudder characteristics do yield some improvement.

Further improvement was obtained by taking a rudder geometry identical to that of the main struts. Since this rudder extends from hull to foils, its lift curve slope was taken as the two-dimensional value of 2π/radian,

which leads to

$$S_{FR\delta} = 0.01972 \text{ lb/deg} \qquad S_{AR\delta} = 0.17748 \text{ lb/deg}$$

$$S_{FRV\delta} = 0.012136 \text{ lb sec/ft deg} \qquad S_{ARV\delta} = 0.10922 \text{ lb sec/ft deg}$$

The predicted turning characteristics using this rudder geometry are shown in Tables C-17 and C-18. The turning circle diameter for the speed range of 3 to 10 knots (full scale) varies from 6.8 lengths to 15.4 lengths. Furthermore, the turning radius approaching the higher test speed range is increasing with speed so that turning characteristics between 10 knots and take-off speed may be poor. Finally, these estimates do not include the stabilizing effect of the increased rudder force rate on Y_v and N_r and therefore may be unconservative. Consequently, the single aft rudder configuration does not appear to give acceptable turning characteristics.

Two alternative design modifications are easily available to improve turning performance. First, a bow rudder can be added at the forward foils for example, or second steering can be accomplished with control flaps on the aft struts or on all four struts. Of these the second alternative is thought to be more fruitful since the large side force rate of the struts then is utilized in directional control as well as directional stability. In order to demonstrate the effectiveness of strut flaps, turning characteristics were predicted for a simplified physical model. It was assumed that (a) side forces and yaw moments were due to struts only, i.e., contributions from hull and appendages were neglected, (b) added mass and inertia were neglected in the stability calculations, and (c) the linearized equations of motion were used. With these approximations, the equations of motion in side-sway and yaw become

$$\begin{aligned} m\dot{v} &= Y_v v + (Y_r - mu) r + Y_{\delta F}\delta_F + Y_{\delta A}\delta_A \\ I_{zz}\dot{r} &= N_v v + N_r r + N_{\delta F}\delta_F + N_{\delta A}\delta_A \end{aligned} \qquad \text{(C-10)}$$

where δ_F and δ_A are the flap deflections of the forward and aft flaps, respectively. The predicted turning characteristics are obtained by setting $\dot{v} = \dot{r} = 0$ and solving Eqs.(C-10) for r and v which leads to

$$R = \left|\frac{u}{r}\right| = \left| \frac{u\left[Y_v N_r - N_v Y_r + N_v mu\right]}{N_v(Y_{\delta F}\delta_F + Y_{\delta A}\delta_A) - Y_v(N_{\delta F}\delta_F + N_{\delta A}\delta_A)} \right| \qquad \text{(C-11)}$$

and

$$\beta_o = -\frac{v}{u} = \frac{N_r(Y_{\delta F}\delta_F + Y_{\delta A}\delta_A) - (Y_r - mu)(N_{\delta F}\delta_F + N_{\delta A}\delta_A)}{u\left[Y_v N_r - N_v(Y_r - mu)\right]}$$

The characteristic equation for the system described by Eqs.(C-10) is given by

$$P(\lambda) = \begin{vmatrix} \lambda - Y_v/m & -Y_r/m + u \\ -N_v/I_{zz} & \lambda - N_r/I_{zz} \end{vmatrix}$$

which gives eigenvalues in the form

$$\lambda_{1,2} = \left(\frac{Y_v I_{zz} + N_r m}{2mI_{zz}}\right) \pm \sqrt{\left(\frac{Y_v I_{zz} + N_r m}{2mI_{zz}}\right)^2 - \frac{Y_v N_r - N_v Y_r + N_v mu}{mI_{zz}}} \qquad \text{(C-12)}$$

For any fin i, the contribution to side force and yaw moment is given by

$$Y_i = \frac{1}{2}\rho V_i^2 A_i C_{Li} \quad , \quad N_i = x_i Y_i \qquad \text{(C-13)}$$

where

$$V_i^2 = (u - y_i r)^2 + (v + x_i r)^2$$

$$C_{L_i} = C_{L\alpha i}\left[k_i\delta_i - \arctan\left(\frac{v + x_i r}{u - y_i r}\right)\right]$$

A_i = side area

x_i, y_i = point of application of side force

$C_{L\alpha i}$ = lift curve slope

k_i = flap effectiveness coefficient

δ_i = flap angle

Differentiating Eq.(C-13) yields the contribution of the i^{th} fin to the

hydrodynamic derivatives in the form

$$Y_{\delta i} = \frac{1}{2} \rho A_i C_{L\alpha i} k_i u^2 \qquad N_{\delta i} = x_i Y_{\delta i}$$

$$Y_{vi} = -\frac{1}{u} Y_{\delta i} \qquad Y_{ri} = -\frac{1}{u} x_i Y_{\delta i} \qquad \text{(C-14)}$$

$$N_{vi} = Y_{ri} \qquad N_{ri} = -\frac{1}{u} x_i^2 Y_{\delta i}$$

The hydrodynamic derivatives are then obtained by summing these results over all fins for any configuration.

The first configuration analyzed consisted of four fixed struts and a rudder with geometry of the proposed rudder. This configuration was studied to provide a point of comparison for illustrating the improvement in turning characteristics for other configurations. The input parameters for this case are

$i = 1,2,3,4$: fixed struts
$i = 5$: rudder

$$A_i = \begin{cases} 0.17188 \text{ ft}^2; & i = 1,2,3,4 \\ 0.10938 \text{ ft}^2; & i = 5 \end{cases}$$

$$C_{L\alpha i} = \begin{cases} 2\pi/\text{rad} & ; i = 1,2,3,4 \\ 2.75331/\text{rad}; & i = 5 \end{cases}$$

$$k_i = 1; \quad i = 1,2,3,4,5$$

$$x_i = \begin{cases} 1.73 \text{ ft} & i = 1,2 \\ -2.12 \text{ ft}; & i = 3,4 \\ -2.00 \text{ ft}; & i = 5 \end{cases}$$

The mass m and yaw moment of intertia were taken as the light ship mass and pitch moment of inertia listed in Table 1. The predicted directional stability index and turning characteristics are listed in Table C-19, where it is seen that these results for this simplified configuration are reasonably representative of the results listed in Table C-17 using the estimated coefficients.

Equations (C-11),(C-12),(C-13) and (C-14) were next applied to the case of four fixed struts with an aft rudder extending from hull to foils, using the same lift curve slope and area for the rudder as for the struts. The input parameters are the same as for the previous case, except

$$A_5 = 0.17188 \text{ ft}^2$$

and

$$C_{L\alpha 5} = 2\pi/\text{rad} \quad \text{(2-D rudder)} \quad .$$

The predicted directional stability index and turning characteristics are listed in Table C-19, where again it is seen that these results for the simplified configuration are in reasonable agreement with corresponding results listed in Table C-17. Since these two cases are in reasonable agreement with the more reliable results in Table C-17, it is felt that predicted trends based on the simplified configuration are reliable.

In studying the effect of strut flaps for directional control, it was assumed that all four struts were of identical geometry, that the strut lift curve slope was 2π/rad, that the struts were located as in the proposed design, and that the flap angle forward was given by

$$\delta_F = -c_\delta \delta_A$$

In this case, the stability index and turning radius reduce to

$$\frac{\lambda_{1,2}}{u} = -\frac{\rho A_s C_{L\alpha s}}{m}\left\{1+\frac{x_F^2+x_A^2}{2r_{zz}^2} \pm \sqrt{\left(1+\frac{x_F^2+x_A^2}{2r_{zz}^2}\right)^2 - \frac{(x_F-x_A)^2}{r_{zz}^2} + \frac{m(x_F+x_A)}{\rho A_s C_{L\alpha s} r_{zz}^2}}\right\}$$

and

$$\left|\frac{R\delta_A}{x_F - x_A}\right| = \frac{1}{k(1+c_\delta)}\left|1 - \frac{m(x_F+x_A)}{\rho A_s C_{L\alpha a}(x_F-x_A)^2}\right| = \frac{59.96(\text{deg})}{k(1+c_\delta)}$$

Three steering configurations were considered:

k	0.35	0.35	0.50
c_δ	0	0.50	0.50

In the first case, only the aft flaps are used and the flap effectiveness is

84

0.35 which is a conservative estimate for a 25 percent flap. The second case uses the same flap effectiveness but with forward rudder angle equal to half the aft value and in the opposite direction. The final case uses the same flap angle ratio but the flap effectiveness of 0.50 is an optimistic estimate for a 25 percent flap. The resulting stability indices and turning characteristics are summarized in Table C-19. It is seen that aft steering alone with a low flap effectiveness is somewhat better than steering with a 2-D rudder and that the stability index is considerably smaller, but still quite adequate. Steering with fore and aft flaps gives further improvement and finally the optimistic flap effectiveness with steering fore and aft yields very acceptable turning characteristics.

Since these trends will be reduced to some extent by the stabilizing influence of the skegs and hull, it is recommended that steering with fore and aft flaps be investigated further.

Equations (C-11) and (C-12) were also used to predict the turning radius and directional stability for foilborne operation. Steering with four strut flaps was considered for which the hydrodynamic derivatives are given by Eqs.(C-14). The results described in Reference show that the lift curve slope of a surface-piercing strut at high Froude number is the same as that of a wing in infinite fluid and with aspect ratio equal to the geometric submerged aspect ratio of the strut. Thus, the lift curve slope of the struts was taken as

$$C_{L\alpha i} = \frac{2\pi(\zeta - x_i \sin\theta)}{c_s + \zeta - x_i \sin\theta} \quad ; \; i = F,A$$

and the submerged strut area is given by

$$A_{si} = c_s(\zeta - x_i \sin\theta) \quad ; \; i = F,A$$

where

ζ = foil submergence at zero trim

c_s = strut chord length

and where port and starboard struts are assumed to be the same submergence. Defining

$$C_{qi} = C_{L\alpha i} A_{si}$$

85

AD-A035 512 STEVENS INST OF TECH HOBOKEN N J DAVIDSON LAB F/G 13/10
AMPHIBIOUS HYDROFOIL LIGHTER PRELIMINARY DESIGN VERIFICATION.(U)
MAY 76 C J HENRY N00014-75-C-0384
UNCLASSIFIED SIT-DL-76-1890 NL

2 OF 2
AD A
035 512

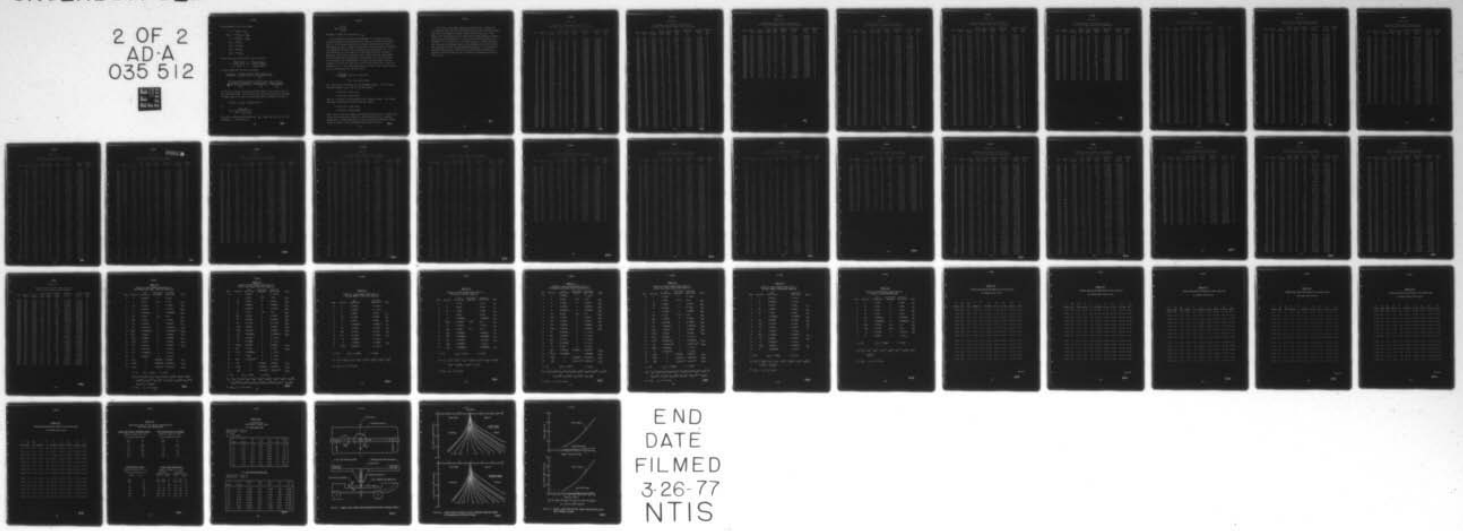

END
DATE
FILMED
3-26-77
NTIS

the hydrodynamic derivatives become

$$
\begin{aligned}
Y_v &= -\rho u(C_{qF} + C_{qA}) \\
N_v = Y_r &= -\rho u(x_F C_{qF} + x_A C_{qA} \\
N_r &= -\rho u(x_F^2 C_{qF} + x_A^2 C_{qA} \\
Y_{\delta F} &= \rho u^2 k C_{qF} \\
N_{\delta F} &= \rho u^2 k x_F C_{qF} \\
Y_{\delta A} &= \rho u^2 k C_{qA} \\
N_{\delta A} &= \rho u^2 k x_A C_{qA}
\end{aligned}
$$

The turning radius from Eq.(C-11) then is given by

$$
R' = \left| \frac{R\delta_A k(1+c_\delta)}{x_F - x_A} \right| = \left| 1 - \frac{m(C_{qF}x_F + C_{qA}x_A}{C_{qF}C_{qA}(x_F - x_A)^2} \right|
$$

and the eigenvalues from Eq.(C-12) become

$$
\frac{\lambda_{1,2}|x_F - x_A|}{u} = \frac{\rho|x_F - x_A|}{m} \left\{ \frac{C_{qF}(x_F^2 + r_{zz}^2) + C_{qA}(x_A^2 + r_{zz}^2)}{2r_{zz}^2} \right.
$$

$$
\left. \pm \sqrt{\left[\frac{C_{qF}(x_F^2 + r_{zz}^2) + C_{qA}(x_A^2 + r_{zz}^2)}{2r_{zz}^2} \right]^2 - \frac{C_{qF}C_{qA}(x_F - x_A)^2}{r_{zz}^2} + \frac{m(C_{qF}x_F + C_{qA}x_A)}{\rho r_{zz}^2}} \right\}
$$

At zero trim, $C_{qF} = C_{qA}$ and these expressions reduce to the previous ones for four identical struts. Also note that the term outside the square root above is always negative so that the directional stability boundary is given by

$$
\frac{m}{\alpha}\left(C_{qF}x_F + C_{qA}x_A\right) - C_{qF}C_{qA}(x_F - x_A)^2 = 0
$$

or

$$
C_{qF} = \frac{-x_A C_{qA}\, m/\rho}{x_F m/\rho - C_{qA}(x_F - x_A)^2}
$$

The craft is directionally unstable for C_{qF} larger than that given by this expression. It is seen that if

$$C_{qA} \geq \frac{x_F \, m/\rho}{(x_F - x_A)^2} \quad ,$$

the craft is stable for all values of C_{qF} .

The dimensionless turning radius parameter R' and the directional stability boundary were evaluated for the light ship and design load conditions in the foilborne mode using strut flaps for steering and no rudder. The results are shown in Figure C-2, where the directional stability boundary is indicated by the curve with cross-hatching on the unstable side. It is seen that there is a wide range of trim and heave conditions for stable operation. The actual turning radius can be predicted using these figures for any steering design combination. For example, at a trim of 1^o bow-up with a zero-trim foil submergence of 0.3 feet, the dimensionless turning parameter is $R'=1.41$ for light ship and $R'=1.63$ for design load. Using the definition of R' and a flap effectiveness of $k=0.35$ with a steering ratio $c_\delta = 0.5$, the turning radii are found to be

$$R = \frac{R' |x_F - x_A|}{k(1+c_\delta)\delta_A} = 29.6 \text{ feet (light ship)}$$

$$= 34.2 \text{ feet (design load)}$$

for a flap angle of 20 degrees aft and 10 degrees forward. Using a larger flap effectiveness $k=0.5$, the turning radii become

$$R = 20.7 \text{ feet (light ship)}$$

$$= 24.0 \text{ feet (design load)}$$

again at a flap angle of 20 degrees aft and 10 degrees forward. With larger flap angles forward $c_\delta=1.0$, the turning radii become

$$R = 15.6 \text{ feet (light ship)}$$

$$= 18.0 \text{ feet (design load)}$$

where $k=0.5$ and with 20 degrees of flap angle forward and aft. These values yield a turning diameter of about six vehicle lengths which is acceptable. Consequently, it would appear that the strut-flap steering should be studied further in order to insure acceptable turning characteristics.

87

The results of the model drag force analysis shown in Table C-16 for the design load condition with wheels down were used to estimate prototype drag at low speeds, as shown in Table C-20 and Figure C-3. With $\omega = \beta_o = \varphi = 0$, the equation given in Table C-16 for model drag was evaluated and the portion of drag due to skin friction was estimated based on the Schoenherr friction coefficient. The model speed and residual resistance were scaled up to prototype values and the prototype skin friction resistance was added to obtain the estimated prototype drag. At 10.7 knots the estimated prototype EHP is 2450 HP so that with 7200 HP installed, the prototype with wheels down and full load should be capable of making more than 11 knots.

88

TABLE C-1

STABILITY AND TURNING TEST RESULTS
FORWARD SIDE FORCE, LIGHT SHIP CONDITION

RUN	RADIUS FT	SPEED FT/SEC	DRIFT ANGLE DEG	ROLL ANGLE DEG	RUDDER ANGLE DEG	MEASURED VALUE LB	FITTED VALUE LB	REPEAT RUN SET
1	30	1.80	0.	1.	-8.	-0.686	0.709	0
4	30	4.28	-4.	4.	-4.	-7.034	-7.046	0
6	30	2.81	-7.	2.	-14.	-3.734	-3.823	0
5	30	3.92	-6.	-5.	-16.	-7.403	-7.497	0
8	30	3.01	-3.	1.	15.	-3.106	-3.187	0
9	30	3.01	-8.	5.	-16.	-4.662	-4.892	0
10	30	2.82	-10.	-5.	-2.	-4.566	-4.679	0
11	30	1.63	-6.	1.	10.	-0.885	-1.075	0
13	30	2.52	-7.	2.	-8.	-2.833	-2.923	0
14	30	4.94	-8.	-4.	-12.	-13.124	-13.382	0
16	30	3.02	3.	1.	15.	-1.197	-1.122	1
18	30	1.62	4.	-4.	16.	-0.034	-0.051	0
19	30	2.33	4.	1.	-20.	-0.536	-0.532	0
20	30	3.29	0.	1.	6.	-2.633	-2.543	0
23	30	4.55	5.	5.	-18.	0.018	-0.041	0
24	30	3.01	3.	1.	15.	-1.175	-1.116	1
26	-30	2.51	-6.	5.	-20.	-0.307	-0.034	0
27	-30	4.56	0.	4.	-20.	5.540	5.405	0
28	-30	3.97	5.	-5.	-16.	6.456	6.880	0
30	-30	4.26	-6.	-2.	16.	-0.498	-0.526	0
31	-30	4.19	-6.	-4.	14.	-0.438	-0.500	0
32	-30	3.02	-3.	-1.	15.	1.199	0.952	0
33	-30	4.48	-10.	-2.	16.	-4.096	-3.853	0
34	-30	1.51	3.	-3.	14.	0.887	0.796	0
36	-30	2.61	-3.	-2.	14.	1.007	0.810	0
37	-30	3.90	-10.	-3.	-18.	-3.261	-3.111	0
38	-30	2.10	-5.	-5.	16.	0.313	0.263	0
39	-30	3.58	4.	1.	14.	4.709	4.909	0
40	-30	3.00	-3.	-1.	-15.	1.053	0.960	2
42	-30	2.50	-11.	4.	-20.	-1.586	-1.347	0
43	-30	2.11	-6.	5.	-12.	-0.119	-0.060	0
44	-30	4.68	-12.	5.	4.	-4.712	-4.773	0
45	-30	3.81	-5.	3.	12.	0.258	0.169	0
46	-30	3.90	-11.	5.	-18.	-3.299	-3.367	0
47	-30	4.37	5.	-4.	-14.	8.085	8.195	0
48	-30	3.00	-3.	-1.	-15.	1.018	0.960	2
49	-30	4.50	-15.	2.	12.	-8.090	-7.919	0
50	-30	4.79	-1.	-1.	-18.	4.785	4.590	0
126	-20	3.90	-9.	-2.	-8.	-0.916	-0.545	0
129	-20	3.41	-3.	-2.	-20.	2.662	2.532	0
130	-20	2.70	0.	-5.	12.	2.808	2.466	0
131	-20	1.90	-1.	-1.	-12.	0.948	0.923	0
132	-20	4.00	-8.	1.	-16.	0.101	0.222	0
133	-20	1.80	5.	-3.	10.	1.546	1.539	0
134	-20	2.50	-14.	-2.	14.	-1.321	-1.183	0
135	-20	4.19	-8.	-3.	-20.	0.098	0.102	0
136	-20	3.00	-3.	-1.	-15.	2.250	1.966	4
137	-20	3.30	1.	-1.	-12.	4.156	4.114	0
139	-20	2.70	-5.	4.	4.	0.986	0.933	0
139	-20	2.70	-11.	3.	20.	-0.983	-1.007	0

TABLE C-1

STABILITY AND TURNING TEST RESULTS
FORWARD SIDE FORCE, LIGHT SHIP CONDITION

RUN	RADIUS FT	SPEED FT/SEC	DRIFT ANGLE DEG	ROLL ANGLE DEG	RUDDER ANGLE DEG	MEASURED VALUE LB	FITTED VALUE LB	REPEAT RUN SET
140	-20	2.10	-10.	3.	-16.	-0.395	-0.167	0
141	-20	4.49	-4.	-3.	-20.	3.986	3.698	0
142	-20	2.60	-15.	-5.	-10.	-1.557	-1.608	0
143	-20	4.19	-9.	3.	-4.	-0.443	-0.309	0
144	-20	3.00	-3.	-1.	-15.	2.244	1.966	4
145	-20	2.40	-7.	5.	10.	0.198	0.266	0
146	-20	3.49	-6.	-2.	-12.	1.153	1.122	0
147	-20	3.50	-15.	-3.	-8.	-3.515	-3.577	0
148	-20	2.80	-6.	-2.	-6.	1.075	0.878	0
150	-20	2.20	-2.	2.	4.	1.238	1.184	0
101	20	4.89	0.	-2.	-10.	-8.994	-8.683	0
102	20	4.19	13.	3.	-20.	4.028	4.227	0
103	20	3.99	8.	5.	-10.	-0.002	0.079	0
104	20	3.00	3.	1.	15.	-2.308	-2.116	3
105	20	2.90	6.	5.	10.	-1.085	-1.182	0
107	20	2.10	-5.	-3.	10.	-2.269	-1.979	0
108	20	4.49	9.	-5.	0.	-0.026	-0.006	0
109	20	2.70	-4.	-4.	-20.	-3.600	-3.556	0
110	20	3.50	0.	1.	-4.	-4.384	-4.241	0
111	20	3.40	14.	3.	-6.	2.580	2.693	0
112	20	3.00	3.	1.	15.	-2.371	-2.116	3
113	20	3.20	8.	1.	20.	-0.330	-0.249	0
115	20	2.30	6.	2.	16.	-0.713	-0.782	0
116	20	3.50	6.	1.	14.	-1.045	-1.292	0
117	20	2.80	12.	5.	-8.	0.749	0.719	0
118	20	4.99	15.	-3.	20.	5.500	5.430	0
119	20	4.20	15.	1.	-6.	5.054	4.930	0
120	20	3.00	3.	1.	15.	-2.312	-2.116	3
121	20	3.19	7.	5.	16.	-0.726	-0.853	0
122	20	4.19	2.	3.	-4.	-4.674	-4.614	0
123	20	3.79	2.	-3.	-10.	-3.652	-3.852	0
124	20	3.70	15.	2.	10.	4.048	3.958	0
125	20	3.89	-5.	4.	-20.	-8.327	-8.168	0
128	-20	3.01	-3.	-1.	-15.	2.113	1.978	4
203	10	2.49	13.	-1.	-20.	-0.647	-0.724	0
206	10	3.68	3.	-3.	8.	-7.638	-7.728	0
208	10	3.00	3.	1.	15.	-4.987	-5.127	5
209	10	2.89	-5.	-3.	-12.	-7.055	-7.135	0
210	10	1.89	-4.	-2.	-18.	-2.835	-2.754	0
211	10	3.08	5.	-5.	-10.	-4.635	-4.573	0
212	10	1.61	-3.	3.	20.	-1.855	-1.852	0
213	10	1.51	-2.	0.	20.	-1.521	-1.406	0
214	10	3.32	-1.	3.	-4.	-7.779	-7.994	0
215	10	4.00	0.	1.	-8.	-11.392	-11.133	0
216	10	3.01	3.	1.	15.	-5.101	-5.162	5
217	10	1.60	0.	2.	-14.	-1.686	-1.556	0
218	10	4.97	15.	-4.	0.	-3.041	-3.055	0
219	10	2.80	9.	1.	20.	-2.528	-2.502	0
220	10	2.00	-5.	-1.	20.	-3.236	-3.018	0
221	10	3.70	8.	5.	-4.	-4.546	-4.651	0

TABLE C-1

STABILITY AND TURNING TEST RESULTS
FORWARD SIDE FORCE, LIGHT SHIP CONDITION

RUN	RADIUS FT	SPEED FT/SEC	DRIFT ANGLE DEG	ROLL ANGLE DEG	RUDDER ANGLE DEG	MEASURED VALUE LB	FITTED VALUE LB	REPEAT RUN SET
222	10	2.90	3.	-5.	-20.	-4.916	-4.805	0
223	10	3.59	8.	4.	-10.	-4.304	-4.382	0
224	10	3.00	3.	1.	15.	-5.014	-5.127	5
226	-10	3.01	-13.	-2.	14.	1.053	1.101	0
228	-10	3.90	-1.	0.	8.	9.609	9.794	0
229	-10	3.81	-6.	-2.	12.	6.186	6.177	0
231	-10	2.20	-7.	-3.	2.	1.867	2.048	0
232	-10	3.01	-3.	-1.	-15.	4.877	5.011	6
234	-10	2.10	-6.	-4.	20.	1.941	2.045	0
235	-10	3.41	-9.	-3.	14.	3.545	3.404	0
236	-10	4.32	-5.	-2.	-10.	9.176	9.067	0
237	-10	2.00	-14.	4.	-20.	0.267	-0.070	0
238	-10	2.10	5.	-2.	-8.	3.320	3.364	0
240	-10	3.01	-3.	-1.	-15.	4.867	5.011	6
241	-10	4.69	-11.	0.	16.	5.142	5.065	0
242	-10	1.70	-9.	3.	-18.	0.756	0.622	0
243	-10	3.41	-10.	4.	-20.	2.941	2.905	0
244	-10	2.10	-5.	-1.	-14.	2.016	2.026	0
245	-10	2.70	3.	-1.	-14.	5.238	5.535	0
246	-10	2.40	4.	2.	6.	4.425	4.369	0
249	-10	2.91	-11.	3.	-16.	1.666	1.818	0
250	-10	4.40	-11.	-3.	4.	4.318	4.274	0
201	10	3.98	-5.	-5.	0.	-14.381	-14.340	0
202	10	1.69	-3.	-2.	-16.	-2.064	-2.116	0

TABLE C-2

STABILITY AND TURNING TEST RESULTS
AFT SIDE FORCE, LIGHT SHIP CONDITION

RUN	RADIUS FT	SPEED FT/SEC	DRIFT ANGLE DEG	ROLL ANGLE DEG	RUDDER ANGLE DEG	MEASURED VALUE LB	FITTED VALUE LB	REPEAT RUN SET
1	30	1.80	0.	1.	-8.	-0.036	-0.096	0
2	30	3.65	-12.	-5.	8.	-3.074	-3.380	0
3	30	2.79	-14.	2.	-4.	-3.628	-3.674	0
6	30	2.81	-7.	2.	-14.	-1.624	-1.729	0
5	30	3.92	-6.	-5.	-16.	-1.684	-1.653	0
8	30	3.01	-3.	1.	15.	-0.147	-0.124	0
7	30	3.12	-13.	2.	-8.	-4.342	-3.895	0
9	30	3.01	-8.	5.	-16.	-2.483	-2.542	0
10	30	2.82	-10.	-5.	-2.	-1.665	-1.666	0
11	30	1.63	-6.	1.	10.	-0.400	-0.578	0
12	30	4.57	-13.	1.	16.	-5.855	-5.618	0
13	30	2.52	-7.	2.	-8.	-1.603	-1.369	0
15	30	2.91	-13.	-2.	14.	-3.062	-2.818	0
16	30	3.02	3.	1.	15.	1.438	1.348	1
17	30	1.54	11.	1.	14.	1.144	0.966	0
18	30	1.62	4.	-4.	16.	0.372	0.426	0
19	30	2.33	4.	1.	-20.	0.489	0.459	0
20	30	3.29	0.	1.	6.	0.625	0.582	0
21	30	2.51	-11.	2.	14.	-2.141	-1.979	0
22	30	2.11	15.	3.	-2.	2.396	2.507	0
23	30	4.55	5.	5.	-18.	2.422	2.276	0
24	30	3.01	3.	1.	15.	1.454	1.339	1
26	-30	2.51	-6.	5.	-20.	-1.817	-1.849	0
29	-30	4.97	1.	-3.	20.	0.350	0.367	0
31	-30	4.19	-6.	-4.	14.	-2.302	-2.522	0
32	-30	3.02	-3.	-1.	15.	-0.570	-0.629	0
33	-30	4.48	-10.	-2.	16.	-5.351	-5.256	0
34	-30	1.51	3.	-3.	14.	0.394	0.181	0
35	-30	3.70	-15.	5.	-12.	-7.469	-7.647	0
36	-30	2.61	-3.	-2.	14.	-0.444	-0.431	0
37	-30	3.90	-10.	-3.	-18.	-4.681	-4.833	0
38	-30	2.10	-5.	-5.	16.	-0.335	-0.457	0
39	-30	3.58	4.	1.	14.	1.304	1.137	0
40	-30	3.00	-3.	-1.	-15.	-1.303	-1.235	2
42	-30	2.50	-11.	4.	-20.	-2.708	-3.002	0
43	-30	2.11	-6.	5.	-12.	-1.259	-1.274	0
45	-30	3.81	-5.	3.	12.	-2.152	-2.479	0
46	-30	3.90	-11.	5.	-18.	-6.606	-6.590	0
48	-30	3.00	-3.	-1.	-15.	-1.296	-1.235	2
126	-20	3.90	-9.	-2.	-8.	-4.793	-4.735	0
129	-20	3.41	-3.	-2.	-20.	-1.697	-1.947	0
130	-20	2.70	0.	-5.	12.	0.139	0.205	0
131	-20	1.90	-1.	-1.	-12.	-0.278	-0.347	0
133	-20	1.90	5.	-3.	10.	0.729	0.504	0
134	-20	2.50	-14.	-2.	14.	-3.175	-3.295	0
135	-20	4.19	-8.	-3.	-20.	-4.981	-5.178	0
136	-20	3.00	-3.	-1.	-15.	-1.337	-1.416	4
137	-20	3.30	1.	-1.	-12.	-0.471	-0.505	0
139	-20	2.70	-5.	4.	4.	-1.483	-1.534	0
139	-20	2.70	-11.	3.	20.	-2.402	-2.591	0

TABLE C-2

STABILITY AND TURNING TEST RESULTS
AFT SIDE FORCE, LIGHT SHIP CONDITION

RUN	RADIUS FT	SPEED FT/SEC	DRIFT ANGLE DEG	ROLL ANGLE DEG	RUDDER ANGLE DEG	MEASURED VALUE LB	FITTED VALUE LB	REPEAT RUN SET
140	-20	2.10	-10.	3.	-16.	-1.772	-2.037	0
141	-20	4.49	-4.	-3.	-20.	-4.185	-3.847	0
142	-20	2.60	-15.	-5.	-10.	-3.791	-3.915	0
143	-20	4.19	-9.	3.	-4.	-6.269	-6.204	0
144	-20	3.00	-3.	-1.	-15.	-1.336	-1.416	4
145	-20	2.40	-7.	5.	10.	-1.827	-1.479	0
146	-20	3.49	-6.	-2.	-12.	-2.455	-2.839	0
147	-20	3.50	-15.	-3.	-8.	-6.509	-6.235	0
148	-20	2.80	-6.	-2.	-6.	-2.021	-1.687	0
149	-20	4.69	-3.	-3.	16.	-2.683	-2.417	0
150	-20	2.20	-2.	2.	4.	-0.383	-0.510	0
101	20	4.89	0.	-2.	-10.	1.892	1.917	0
102	20	4.19	13.	3.	-20.	6.586	6.887	0
103	20	3.99	8.	5.	-10.	3.655	3.750	0
104	20	3.00	3.	1.	15.	1.459	1.564	3
105	20	2.90	6.	5.	10.	1.995	1.885	0
106	20	4.80	-2.	-4.	-8.	0.747	0.835	0
107	20	2.10	-5.	-3.	10.	-0.208	-0.237	0
108	20	4.49	9.	-5.	0.	7.989	7.765	0
109	20	2.70	-4.	-4.	-20.	-0.620	-0.434	0
110	20	3.50	0.	1.	-4.	0.515	0.702	0
111	20	3.40	14.	3.	-6.	5.432	5.531	0
112	20	3.00	3.	1.	15.	1.409	1.564	3
114	20	1.49	6.	-1.	-20.	0.288	0.331	0
115	20	2.30	6.	2.	16.	1.317	1.326	0
117	20	2.80	12.	5.	-8.	3.009	3.033	0
119	20	4.20	15.	1.	-6.	9.001	9.100	0
120	20	3.00	3.	1.	15.	1.464	1.564	3
121	20	3.19	7.	5.	16.	2.485	2.761	0
123	20	3.79	2.	-3.	-10.	1.681	1.893	0
124	20	3.70	15.	2.	10.	7.987	7.660	0
125	20	3.89	-5.	4.	-20.	-1.748	-1.937	0
128	-20	3.01	-3.	-1.	-15.	-1.356	-1.426	4
203	10	2.49	13.	-1.	-20.	3.897	3.802	0
204	10	1.49	14.	3.	4.	1.726	2.031	0
206	10	3.68	3.	-3.	8.	4.135	4.014	0
208	10	3.00	3.	1.	15.	2.219	2.404	5
209	10	2.89	-5.	-3.	-12.	-0.447	-0.451	0
210	10	1.89	-4.	-2.	-18.	-0.359	-0.300	0
211	10	3.08	5.	-5.	-10.	3.081	3.160	0
212	10	1.61	-3.	3.	20.	-0.163	-0.278	0
213	10	1.51	-2.	0.	20.	0.057	-0.008	0
214	10	3.32	-1.	3.	-4.	1.095	0.797	0
215	10	4.00	0.	1.	-8.	2.065	2.196	0
216	10	3.01	3.	1.	15.	2.339	2.422	5
217	10	1.60	0.	2.	-14.	-0.156	-0.010	0
219	10	2.80	9.	1.	20.	4.013	4.041	0
220	10	2.00	-5.	-1.	20.	-0.194	-0.223	0
221	10	3.70	8.	5.	-4.	5.417	5.171	0
222	10	2.90	3.	-5.	-20.	1.909	1.968	0

TABLE C-2

STABILITY AND TURNING TEST RESULTS
AFT SIDE FORCE, LIGHT SHIP CONDITION

RUN	RADIUS FT	SPEED FT/SEC	DRIFT ANGLE DEG	ROLL ANGLE DEG	RUDDER ANGLE DEG	MEASURED VALUE LB	FITTED VALUE LB	REPEAT RUN SET
223	10	3.59	8.	4.	-10.	4.836	4.918	0
224	10	3.00	3.	1.	15.	2.448	2.404	5
225	10	1.90	12.	-3.	-18.	2.202	1.972	0
226	-10	3.01	-13.	-2.	14.	-5.156	-5.056	0
228	-10	3.90	-1.	0.	8.	-2.230	-2.100	0
229	-10	3.81	-6.	-2.	12.	-3.896	-4.064	0
231	-10	2.20	-7.	-3.	2.	-1.802	-1.613	0
232	-10	3.01	-3.	-1.	-15.	-2.182	-2.012	6
233	-10	3.41	4.	-4.	4.	0.873	0.775	0
234	-10	2.10	-6.	-4.	20.	-1.557	-1.128	0
235	-10	3.41	-9.	-3.	14.	-4.220	-4.301	0
237	-10	2.00	-14.	4.	-20.	-3.179	-3.216	0
238	-10	2.10	5.	-2.	-8.	0.493	0.556	0
239	-10	4.79	-14.	-5.	0.	-12.001	-11.981	0
240	-10	3.01	-3.	-1.	-15.	-2.160	-2.012	6
242	-10	1.70	-9.	3.	-18.	-1.561	-1.503	0
243	-10	3.41	-10.	4.	-20.	-6.537	-6.437	0
244	-10	2.10	-5.	-1.	-14.	-1.364	-1.259	0
245	-10	2.70	3.	-1.	-14.	-0.047	-0.030	0
246	-10	2.40	4.	2.	6.	0.297	0.294	0
247	-10	4.91	-10.	-4.	-14.	-10.870	-10.901	0
249	-10	2.91	-11.	3.	-16.	-4.849	-4.783	0
250	-10	4.40	-11.	-3.	4.	-8.817	-8.942	0
201	10	3.98	-5.	-5.	0.	0.248	-0.016	0
202	10	1.69	-3.	-2.	-16.	-0.191	-0.180	0

TABLE C-3

STABILITY AND TURNING TEST RESULTS
FULL MOMENT, LIGHT LOAD CONDITION

RUN	RADIUS FT	SPEED FT/SEC	DRIFT ANGLE DEG	ROLL ANGLE DEG	RUDDER ANGLE DEG	MEASURED VALUE FT-LB	FITTED VALUE FT-LB	REPEAT RUN SET
1	30	1.80	0.	1.	-8.	-7.030	-7.012	0
2	30	3.65	-12.	-5.	8.	33.720	34.069	0
3	30	2.79	-14.	2.	-7.	-10.940	-11.978	0
4	30	4.28	-4.	4.	-4.	-26.130	-26.550	0
8	30	3.01	-3.	1.	15.	-6.910	-7.004	0
7	30	3.12	-13.	2.	-8.	-10.940	-11.803	0
10	30	2.82	-10.	-5.	-2.	35.480	35.797	0
11	30	1.63	-6.	1.	10.	-3.430	-3.345	0
12	30	4.57	-13.	1.	16.	-2.680	-3.293	0
13	30	2.52	-7.	2.	-8.	-8.940	-9.865	0
15	30	2.91	-13.	-2.	14.	11.700	12.478	0
16	30	3.02	3.	1.	15.	-8.110	-8.168	1
17	30	1.54	11.	1.	14.	-6.760	-6.923	0
18	30	1.62	4.	-4.	16.	23.540	23.537	0
20	30	3.29	0.	1.	6.	-4.450	-4.257	0
21	30	2.51	-11.	2.	14.	-8.330	-9.296	0
22	30	2.11	15.	3.	-2.	-20.040	-21.036	0
23	30	4.55	5.	5.	-18.	-33.550	-33.363	0
24	30	3.01	3.	1.	15.	-8.160	-8.160	1
26	-30	2.51	-6.	5.	-20.	-26.970	-27.651	0
27	-30	4.56	0.	4.	-20.	-23.700	-24.020	0
28	-30	3.97	5.	-5.	-16.	33.820	34.158	0
29	-30	4.97	1.	-3.	20.	21.740	21.838	0
30	-30	4.26	-6.	-2.	16.	16.070	16.740	0
31	-30	4.19	-6.	-4.	14.	27.330	27.372	0
32	-30	3.02	-3.	-1.	15.	8.010	8.073	0
33	-30	4.48	-10.	-2.	16.	18.170	18.291	0
35	-30	3.70	-15.	5.	-12.	-23.960	-24.921	0
36	-30	2.61	-3.	-2.	14.	11.060	11.456	0
37	-30	3.90	-10.	-3.	-18.	20.090	21.105	0
38	-30	2.10	-5.	-5.	16.	35.010	35.095	0
39	-30	3.58	4.	1.	14.	-3.940	-4.291	0
40	-30	3.00	-3.	-1.	-15.	7.110	7.984	2
41	-30	4.96	-8.	-1.	-12.	6.370	7.008	0
42	-30	2.50	-11.	4.	-20.	-22.950	-24.289	0
43	-30	2.11	-6.	5.	-12.	-26.970	-27.674	0
45	-30	3.81	-5.	3.	12.	-18.010	-18.768	0
46	-30	3.90	-11.	5.	-18.	-28.490	-28.661	0
47	-30	4.37	5.	-4.	-14.	27.100	27.428	0
48	-30	3.00	-3.	-1.	-15.	8.140	7.984	2
49	-30	4.50	-15.	2.	12.	-4.010	-4.843	0
50	-30	4.79	-1.	-1.	-18.	4.240	4.088	0
126	-20	3.90	-9.	-2.	-8.	13.430	13.963	0
127	-20	4.70	-5.	2.	8.	-12.610	-11.763	0
129	-20	3.41	-3.	-2.	-20.	11.880	11.971	0
130	-20	2.70	0.	-5.	12.	32.610	31.836	0
131	-20	1.90	-1.	-1.	-12.	7.690	7.604	0
132	-20	4.00	-8.	1.	-16.	-4.390	-4.145	0
133	-20	1.80	5.	-3.	10.	17.410	17.528	0
134	-20	2.50	-14.	-2.	14.	16.100	16.759	0

TABLE C-3

STABILITY AND TURNING TEST RESULTS
ROLL MOMENT, LIGHT LOAD CONDITION

RUN	RADIUS FT	SPEED FT/SEC	DRIFT ANGLE DEG	ROLL ANGLE DEG	RUDDER ANGLE DEG	MEASURED VALUE FT-LB	FITTED VALUE FT-LB	REPEAT RUN SET
135	-20	4.19	-8.	-3.	-20.	20.960	21.120	0
136	-20	3.00	-3.	-1.	-15.	8.120	8.233	4
137	-20	3.30	1.	-1.	-12.	7.440	7.450	0
139	-20	2.70	-5.	4.	4.	-24.450	-24.664	0
139	-20	2.70	-11.	3.	20.	-17.730	-17.750	0
140	-20	2.10	-10.	3.	-16.	-18.960	-18.529	0
141	-20	4.49	-4.	-3.	-20.	24.560	23.646	0
142	-20	2.60	-15.	-5.	-10.	37.800	37.495	0
143	-20	4.19	-9.	3.	-4.	-17.850	-17.069	0
144	-20	3.00	-3.	-1.	-15.	8.430	8.233	4
145	-20	2.40	-7.	5.	10.	-27.350	-27.274	0
146	-20	3.49	-6.	-2.	-12.	12.240	12.771	0
147	-20	3.50	-15.	-3.	-8.	21.970	22.157	0
149	-20	4.69	-3.	-3.	16.	21.140	19.912	0
150	-20	2.20	-2.	2.	4.	-9.600	-9.374	0
101	20	4.89	0.	-2.	-10.	12.900	13.200	0
102	20	4.19	13.	3.	-20.	-22.820	-23.384	0
103	20	3.99	8.	5.	-10.	-34.790	-33.660	0
104	20	3.00	3.	1.	15.	-8.420	-8.400	3
105	20	2.90	6.	5.	10.	-30.970	-30.785	0
106	20	4.80	-2.	-4.	-8.	28.770	28.344	0
107	20	2.10	-5.	-3.	10.	21.030	20.898	0
109	20	2.70	-4.	-4.	-20.	27.880	27.760	0
110	20	3.50	0.	1.	-4.	-4.640	-4.645	0
111	20	3.40	14.	3.	-6.	-21.110	-21.611	0
112	20	3.00	3.	1.	15.	-8.620	-8.400	3
113	20	3.20	8.	1.	20.	-9.770	-9.652	0
114	20	1.49	6.	-1.	-20.	3.070	2.994	0
116	20	3.50	6.	1.	14.	-6.130	-6.111	0
117	20	2.80	12.	5.	-8.	-34.360	-34.207	0
118	20	4.99	15.	-3.	20.	13.780	14.837	0
119	20	4.20	15.	1.	-6.	-12.990	-13.614	0
120	20	3.00	3.	1.	15.	-8.340	-8.400	3
121	20	3.19	7.	5.	16.	-31.990	-31.561	0
122	20	4.19	2.	3.	-4.	-20.600	-19.493	0
123	20	3.79	2.	-3.	-10.	19.820	19.822	0
124	20	3.70	15.	2.	10.	-15.530	-15.879	0
125	20	3.89	-5.	4.	-20.	-23.850	-23.428	0
128	-20	3.01	-3.	-1.	-15.	7.930	8.237	4
203	10	2.49	13.	-1.	-20.	0.440	0.326	0
204	10	1.49	14.	3.	4.	-18.010	-16.833	0
205	10	4.78	-2.	-2.	16.	13.030	13.070	0
206	10	3.68	3.	-3.	8.	15.420	15.217	0
207	10	4.98	-3.	-1.	14.	7.010	6.119	0
208	10	3.00	3.	1.	15.	-9.000	-9.146	5
209	10	2.89	-5.	-3.	-12.	15.940	17.011	0
210	10	1.89	-4.	-2.	-18.	14.010	13.202	0
211	10	3.08	5.	-5.	-10.	28.840	28.695	0
212	10	1.61	-3.	3.	20.	-20.570	-20.230	0
213	10	1.51	-2.	0.	20.	-0.530	-0.579	0

TABLE C-3

STABILITY AND TURNING TEST RESULTS
ROLL MOMENT, LIGHT LOAD CONDITION

RUN	RADIUS FT	SPEED FT/SEC	DRIFT ANGLE DEG	ROLL ANGLE DEG	RUDDER ANGLE DEG	MEASURED VALUE FT-LB	FITTED VALUE FT-LB	REPEAT RUN SET
214	10	3.32	-1.	3.	-4.	-22.450	-21.907	0
215	10	4.00	0.	1.	-8.	-6.610	-5.758	0
216	10	3.01	3.	1.	15.	-9.530	-9.157	5
217	10	1.60	0.	2.	-14.	-14.490	-14.071	0
218	10	4.97	15.	-4.	0.	18.240	17.544	0
219	10	2.80	9.	1.	20.	-9.670	-9.912	0
220	10	2.00	-5.	-1.	20.	6.470	6.403	0
221	10	3.70	8.	5.	-4.	-36.610	-36.588	0
222	10	2.90	3.	-5.	-20.	32.320	32.336	0
223	10	3.59	8.	4.	-10.	-27.150	-27.704	0
224	10	3.00	3.	1.	15.	-9.180	-9.146	5
225	10	1.90	12.	-3.	-18.	15.450	15.212	0
226	-10	3.01	-13.	-2.	14.	18.600	18.160	0
227	-10	4.99	-2.	5.	18.	-28.750	-28.056	0
228	-10	3.90	-1.	0.	8.	2.050	1.706	0
229	-10	3.81	-6.	-2.	12.	14.500	13.941	0
230	-10	1.80	-7.	2.	0.	-9.600	-8.695	0
231	-10	2.20	-7.	-3.	2.	19.310	19.498	0
232	-10	3.01	-3.	-1.	-15.	9.310	8.985	6
233	-10	3.41	4.	-4.	4.	29.490	28.764	0
234	-10	2.10	-6.	-4.	20.	29.590	29.524	0
235	-10	3.41	-9.	-3.	14.	22.490	21.440	0
236	-10	4.32	-5.	-2.	-10.	19.070	17.606	0
237	-10	2.00	-14.	4.	-20.	-21.590	-20.943	0
238	-10	2.10	5.	-2.	-8.	14.290	14.581	0
240	-10	3.01	-3.	-1.	-15.	9.550	8.985	6
241	-10	4.69	-11.	0.	16.	4.950	5.683	0
242	-10	1.70	-9.	3.	-18.	-16.010	-15.300	0
243	-10	3.41	-10.	4.	-20.	-22.860	-22.659	0
244	-10	2.10	-5.	-1.	-14.	8.140	8.613	0
245	-10	2.70	3.	-1.	-14.	8.070	7.828	0
246	-10	2.40	4.	2.	6.	-9.450	-9.415	0
247	-10	4.91	-10.	-4.	-14.	30.130	30.710	0
248	-10	3.01	-3.	-1.	-15.	7.720	8.985	6
249	-10	2.91	-11.	3.	-16.	-17.200	-16.904	0
250	-10	4.40	-11.	-3.	4.	23.570	23.327	0
201	10	3.98	-5.	-5.	0.	30.510	31.344	0
202	10	1.69	-3.	-2.	-16.	10.600	9.673	0

97<

TABLE C-4

STABILITY AND TURNING TEST RESULTS
DRAG FORCE, LIGHT SHIP CONDITION

RUN	RADIUS FT	SPEED FT/SEC	DRIFT ANGLE DEG	ROLL ANGLE DEG	RUDDER ANGLE DEG	MEASURED VALUE LB	FITTED VALUE LB	REPEAT RUN SET
1	30	1.80	0.	1.	-6.	3.783	3.956	0
2	30	3.65	-12.	-5.	8.	17.152	16.784	0
3	30	2.79	-14.	2.	-4.	9.457	9.000	0
6	30	2.61	-7.	2.	-14.	9.613	9.624	0
5	30	3.92	-6.	-5.	-16.	20.205	20.190	0
8	30	3.01	-3.	1.	15.	10.930	11.367	0
7	30	3.12	-13.	2.	-6.	11.666	11.569	0
9	30	3.01	-8.	5.	-16.	10.466	10.657	0
10	30	2.52	-10.	-5.	-2.	9.752	9.964	0
11	30	1.63	-6.	1.	10.	3.014	3.121	0
13	30	2.52	-7.	2.	-8.	7.347	7.617	0
15	30	2.91	-13.	-2.	14.	10.634	10.386	0
16	30	3.02	3.	1.	15.	11.926	11.767	1
17	30	1.54	11.	1.	14.	3.058	3.244	0
18	30	1.62	4.	-4.	16.	3.232	3.387	0
19	30	2.33	4.	1.	-20.	6.862	6.860	0
20	30	3.29	0.	1.	6.	13.480	13.687	0
21	30	2.51	-11.	2.	14.	7.566	7.335	0
22	30	2.11	15.	3.	-2.	5.925	6.148	0
23	30	4.55	5.	5.	-18.	28.197	27.564	0
24	30	3.01	3.	1.	15.	11.877	11.687	1
26	-30	2.51	-6.	5.	-20.	7.977	8.185	0
28	-30	3.97	5.	-5.	-16.	19.344	19.816	0
29	-30	4.97	1.	-3.	20.	32.384	32.734	0
30	-30	4.26	-6.	-2.	16.	23.827	23.993	0
31	-30	4.19	-6.	-4.	14.	22.936	22.982	0
32	-30	3.02	-3.	-1.	15.	11.609	11.685	0
33	-30	4.43	-10.	-2.	16.	27.128	26.857	0
34	-30	1.51	3.	-3.	14.	2.661	2.624	0
35	-30	3.70	-15.	5.	-12.	17.375	17.975	0
36	-30	2.61	-3.	-2.	14.	8.579	8.593	0
37	-30	3.90	-10.	-3.	-13.	20.174	20.438	0
38	-30	2.10	-5.	-5.	16.	5.446	5.362	0
39	-30	3.58	4.	1.	14.	16.423	16.441	0
40	-30	3.00	-3.	-1.	-15.	11.536	11.602	2
41	-30	4.96	-8.	-1.	-12.	33.609	32.756	0
42	-30	2.50	-11.	4.	-20.	8.058	8.134	0
43	-30	2.11	-6.	5.	-12.	5.519	5.596	0
44	-30	4.63	-12.	5.	4.	29.396	28.860	0
45	-30	3.81	-5.	3.	12.	18.751	18.998	0
46	-30	3.90	-11.	5.	-18.	20.049	20.272	0
47	-30	4.37	5.	-4.	-14.	23.626	24.170	0
48	-30	3.00	-3.	-1.	-15.	11.724	11.602	2
49	-30	4.50	-15.	2.	12.	27.023	27.172	0
50	-30	4.79	-1.	-1.	-18.	30.935	30.322	0
126	-20	3.90	-9.	-2.	-8.	19.969	20.373	0
129	-20	3.41	-3.	-2.	-20.	15.455	15.455	0
130	-20	2.70	0.	-5.	12.	8.770	8.961	0
131	-20	1.90	-1.	-1.	-12.	4.569	4.538	0
132	-20	4.00	-8.	1.	-16.	21.434	21.820	0

TABLE C-4

STABILITY AND TURNING TEST RESULTS
DRAG FORCE, LIGHT SHIP CONDITION

RUN	RADIUS FT	SPEED FT/SEC	DRIFT ANGLE DEG	ROLL ANGLE DEG	RUDDER ANGLE DEG	MEASURED VALUE LB	FITTED VALUE LB	REPEAT RUN SET
133	-20	1.80	5.	-3.	10.	3.932	3.746	0
134	-20	2.50	-14.	-2.	14.	8.453	8.370	0
135	-20	4.19	-8.	-3.	-20.	23.873	23.275	0
136	-20	3.00	-3.	-1.	-15.	11.915	11.766	4
137	-20	3.30	1.	-1.	-12.	13.683	13.912	0
139	-20	2.70	-5.	4.	4.	9.409	9.510	0
139	-20	2.70	-11.	3.	20.	9.580	9.666	0
140	-20	2.10	-10.	3.	-16.	5.309	5.911	0
141	-20	4.49	-4.	-3.	-20.	27.204	27.044	0
142	-20	2.60	-15.	-5.	-10.	9.120	9.119	0
143	-20	4.19	-9.	3.	-4.	23.346	23.646	0
144	-20	3.00	-3.	-1.	-15.	11.891	11.766	4
145	-20	2.40	-7.	5.	10.	7.378	7.418	0
146	-20	3.49	-6.	-2.	-12.	15.849	16.137	0
147	-20	3.50	-15.	-3.	-3.	16.330	16.775	0
148	-20	2.80	-6.	-2.	-6.	10.484	10.186	0
149	-20	4.69	-3.	-3.	16.	28.816	29.377	0
150	-20	2.20	-2.	2.	4.	6.045	6.192	0
101	20	4.59	0.	-2.	-10.	31.971	31.878	0
102	20	4.19	13.	3.	-20.	24.038	24.503	0
103	20	3.99	8.	5.	-10.	21.408	21.292	0
104	20	3.00	3.	1.	15.	11.957	11.772	3
105	20	2.90	6.	5.	10.	11.072	11.063	0
106	20	4.80	-2.	-4.	-8.	30.830	30.666	0
107	20	2.10	-5.	-3.	10.	5.444	5.578	0
108	20	4.49	9.	-5.	0.	27.957	27.564	0
109	20	2.70	-4.	-4.	-20.	9.427	9.604	0
110	20	3.50	0.	1.	-4.	15.330	15.698	0
111	20	3.40	14.	3.	-6.	15.935	15.776	0
112	20	3.00	3.	1.	15.	11.304	11.772	3
113	20	3.20	8.	1.	20.	14.223	14.008	0
114	20	1.49	6.	-1.	-20.	2.367	2.649	0
115	20	2.30	6.	2.	16.	6.771	7.018	0
116	20	3.50	6.	1.	14.	16.503	16.368	0
117	20	2.30	12.	5.	-8.	10.627	10.814	0
118	20	4.99	15.	-3.	20.	35.600	35.479	0
119	20	4.50	15.	1.	-6.	23.174	24.126	0
120	20	3.00	3.	1.	15.	11.710	11.772	3
121	20	3.19	7.	5.	16.	13.705	13.690	0
122	20	4.19	2.	3.	-4.	23.862	23.755	0
123	20	3.79	2.	-3.	-10.	18.999	19.100	0
124	20	3.70	15.	2.	10.	19.273	18.949	0
128	-20	3.01	-3.	-1.	-15.	12.043	11.846	4
203	10	2.42	13.	-1.	-20.	9.029	9.313	0
204	10	1.49	14.	3.	4.	3.152	3.775	0
205	10	4.73	-2.	-2.	16.	31.552	32.096	0
206	10	3.63	3.	-3.	8.	20.173	19.467	0
208	10	3.00	3.	1.	15.	12.692	12.584	5
209	10	2.89	-5.	-3.	-12.	11.004	11.308	0
210	10	1.39	-4.	-2.	-13.	4.776	4.685	0

TABLE C-4

STABILITY AND TURNING TEST RESULTS
DRAG FORCE, LIGHT SHIP CONDITION

RUN	RADIUS FT	SPEED FT/SEC	DRIFT ANGLE DEG	ROLL ANGLE DEG	RUDDER ANGLE DEG	MEASURED VALUE LB	FITTED VALUE LB	REPEAT RUN SET
211	10	3.08	5.	-5.	-10.	13.999	14.122	0
212	10	1.61	-3.	3.	20.	3.127	2.942	0
213	10	1.51	-2.	0.	20.	2.963	2.916	0
214	10	3.32	-1.	3.	-4.	13.961	14.327	0
215	10	4.00	0.	1.	-8.	21.274	22.027	0
216	10	3.01	3.	1.	15.	12.912	12.670	5
217	10	1.60	0.	2.	-14.	3.126	3.119	0
218	10	4.97	15.	-4.	0.	37.922	38.370	0
219	10	2.30	9.	1.	20.	11.924	11.788	0
220	10	2.00	-5.	-1.	20.	5.289	5.195	0
221	10	3.70	8.	5.	-4.	19.306	19.368	0
222	10	2.90	3.	-5.	-20.	12.468	12.600	0
223	10	3.59	8.	4.	-10.	18.321	18.407	0
224	10	3.00	3.	1.	15.	12.730	12.584	5
225	10	1.90	12.	-3.	-18.	5.299	5.376	0
226	-10	3.01	-13.	-2.	14.	13.326	13.450	0
227	-10	4.99	-2.	5.	18.	37.473	37.229	0
228	-10	3.90	-1.	0.	8.	21.648	21.152	0
229	-10	3.81	-6.	-2.	12.	21.054	20.731	0
230	-10	1.30	-7.	2.	0.	5.591	4.760	0
231	-10	2.20	-7.	-3.	2.	6.677	6.713	0
232	-10	3.01	-3.	-1.	-15.	12.884	12.663	6
233	-10	3.41	4.	-4.	4.	14.301	14.598	0
235	-10	3.41	-9.	-3.	14.	17.348	16.761	0
236	-10	4.32	-5.	-2.	-10.	26.973	26.340	0
237	-10	2.00	-14.	4.	-20.	6.273	6.381	0
238	-10	2.10	5.	-2.	-8.	5.713	5.301	0
239	-10	4.79	-14.	-5.	0.	32.921	33.552	0
240	-10	3.01	-3.	-1.	-15.	12.989	12.663	6
241	-10	4.69	-11.	0.	16.	33.190	33.344	0
242	-10	1.70	-9.	3.	-18.	4.443	4.478	0
243	-10	3.41	-10.	4.	-20.	18.247	17.951	0
244	-10	2.10	-5.	-1.	-14.	6.325	6.268	0
245	-10	2.70	3.	-1.	-14.	9.706	9.493	0
246	-10	2.40	4.	2.	6.	7.790	7.630	0
247	-10	4.91	-10.	-4.	-14.	35.247	35.125	0
248	-10	3.01	-3.	-1.	-15.	12.127	12.663	6
249	-10	2.91	-11.	3.	-16.	12.954	13.035	0
250	-10	4.40	-11.	-3.	4.	28.619	28.313	0
201	10	3.98	-5.	-5.	0.	21.587	21.950	0
202	10	1.69	-3.	-2.	-16.	3.642	3.700	0

100<

TABLE C-5

STABILITY AND TURNING TEST RESULTS
FORWARD SIDE FORCE, DESIGN LOAD CONDITION

RUN	RADIUS FT	SPEED FT/SEC	DRIFT ANGLE DEG	ROLL ANGLE DEG	RUDDER ANGLE DEG	MEASURED VALUE LB	FITTED VALUE LB	REPEAT RUN SET
76	-30	4.92	-4.	2.	-2.	4.265	4.039	0
78	-30	3.25	-7.	-3.	0.	-0.654	-0.643	0
80	-30	3.00	-3.	-1.	-15.	1.152	1.209	2
83	-30	2.31	3.	-3.	-2.	2.170	2.018	0
85	-30	2.01	5.	-3.	2.	1.928	1.703	0
86	-30	2.30	-2.	-5.	10.	0.935	1.161	0
87	-30	1.92	5.	4.	-4.	1.745	1.416	0
88	-30	3.01	-3.	-1.	-15.	1.225	1.217	2
89	-30	1.71	-15.	-3.	4.	-0.662	-0.784	0
90	-30	4.51	-4.	-5.	4.	0.419	0.280	0
91	-30	4.81	-12.	5.	12.	-3.676	-3.545	0
92	-30	4.01	-1.	2.	-6.	4.380	4.496	0
93	-30	4.11	-6.	-4.	4.	-0.695	-0.650	0
94	-30	4.60	0.	-3.	18.	5.166	5.010	0
95	-30	3.61	-2.	-2.	6.	2.331	2.368	0
96	-30	2.99	-3.	-1.	-15.	1.190	1.201	2
98	-30	1.91	-14.	1.	2.	-0.976	-1.017	0
99	-30	2.10	-15.	1.	20.	-1.392	-1.559	0
100	-30	3.33	5.	-4.	10.	6.459	6.716	0
51	30	3.25	-5.	3.	-18.	-4.791	-5.046	0
52	30	4.36	-1.	2.	10.	-5.659	-5.802	0
54	30	3.40	2.	-5.	-6.	-2.435	-2.802	0
53	30	3.34	0.	-1.	-12.	-3.032	-3.167	0
56	30	3.00	3.	1.	15.	-1.205	-1.096	1
57	30	4.60	12.	5.	-12.	7.793	7.766	0
58	30	1.47	5.	-2.	2.	-0.108	-0.274	0
59	30	3.70	-3.	1.	-8.	-5.630	-5.699	0
61	30	3.40	3.	-3.	20.	-1.653	-1.789	0
62	30	4.80	0.	-5.	10.	-9.368	-9.187	0
63	30	4.10	9.	-3.	-4.	1.353	1.213	0
64	30	3.00	3.	1.	15.	-1.201	-1.096	1
65	30	4.50	15.	-1.	-6.	8.033	8.396	0
66	30	4.70	-5.	-1.	12.	-11.939	-11.694	0
67	30	4.66	0.	-4.	14.	-8.160	-8.112	0
68	30	4.30	14.	5.	-4.	7.945	8.059	0
69	30	4.40	1.	-3.	-3.	-5.629	-5.928	0
70	30	2.80	0.	1.	12.	-2.111	-2.000	0
71	30	3.10	-5.	-3.	-10.	-4.906	-5.136	0
72	30	3.00	3.	1.	15.	-1.131	-1.096	1
73	30	4.70	15.	1.	-6.	8.367	8.346	0
74	30	3.80	10.	2.	-12.	2.776	2.796	0
75	30	3.70	7.	-3.	20.	0.236	0.248	0
97	-30	4.51	-3.	3.	3.	4.637	4.475	0
151	20	3.49	-4.	3.	16.	-6.673	-7.092	0
152	20	3.00	3.	1.	15.	-2.317	-2.330	3
153	20	2.80	12.	3.	4.	1.038	1.115	0
154	20	2.40	3.	-5.	0.	-0.319	-0.217	0
155	20	2.20	10.	-4.	-12.	0.142	0.066	0
156	20	3.90	4.	-1.	-2.	-3.723	-3.937	0
157	20	4.20	-3.	-5.	-4.	-12.200	-11.8[illegible]	0

TABLE C-5

STABILITY AND TURNING TEST RESULTS
FORWARD SIDE FORCE, DESIGN LOAD CONDITION

RUN	RADIUS FT	SPEED FT/SEC	DRIFT ANGLE DEG	ROLL ANGLE DEG	RUDDER ANGLE DEG	MEASURED VALUE LB	FITTED VALUE LB	REPEAT RUN SET
158	20	1.80	12.	-5.	16.	0.335	0.431	0
159	20	3.01	7.	3.	16.	-0.874	-0.651	0
160	20	3.00	3.	1.	15.	-2.473	-2.330	3
162	20	4.41	2.	2.	2.	-6.133	-6.146	0
163	20	4.81	3.	0.	-16.	-7.244	-7.230	0
164	20	3.70	-4.	1.	-2.	-3.143	-3.250	0
165	20	2.80	-2.	-1.	2.	-3.996	-3.863	0
166	20	1.90	10.	1.	0.	-0.070	-0.168	0
167	20	4.01	4.	-1.	4.	-3.966	-4.174	0
168	20	3.00	3.	1.	15.	-2.410	-2.330	3
169	20	2.30	9.	3.	10.	-0.097	-0.104	0
170	20	4.60	13.	-2.	-14.	2.664	2.492	0
171	20	3.09	0.	2.	2.	-3.807	-3.800	0
172	20	2.70	2.	-1.	20.	0.053	0.061	0
173	20	4.32	11.	-4.	-13.	0.001	-0.117	0
174	20	3.11	-3.	1.	16.	-5.116	-5.264	0
175	20	3.91	-2.	-2.	6.	-4.362	-8.396	0
176	-20	3.05	-3.	-1.	-15.	2.254	2.516	4
178	-20	1.50	-3.	5.	16.	0.187	0.134	0
180	-20	2.91	4.	5.	-4.	5.108	5.089	0
181	-20	3.79	-4.	-1.	12.	3.545	3.449	0
182	-20	2.70	-7.	-1.	6.	0.644	0.767	0
183	-20	3.21	-10.	-3.	-16.	-0.817	-0.730	0
184	-20	3.01	-3.	-1.	-15.	2.444	2.446	4
185	-20	4.22	2.	-4.	16.	8.565	8.340	0
186	-20	2.30	-2.	-3.	4.	1.777	1.743	0
187	-20	3.60	-13.	-3.	-6.	-3.010	-2.862	0
189	-20	3.30	-11.	-3.	-13.	-1.393	-1.324	0
190	-20	3.40	-6.	-4.	14.	1.490	1.473	0
192	-20	3.00	-3.	-1.	-15.	2.396	2.429	4
193	-20	1.50	-3.	-5.	-8.	0.636	0.556	0
194	-20	4.69	-4.	2.	2.	6.945	6.746	0
196	-20	4.09	-2.	5.	8.	7.126	7.124	0
195	-20	2.90	4.	-4.	-3.	4.473	4.568	0
197	-20	4.00	3.	-3.	-12.	8.257	8.243	0
198	-20	1.70	-8.	-1.	10.	0.212	0.540	0
199	-20	1.90	-15.	-2.	2.	-0.676	-0.691	0
200	-20	3.00	-3.	-1.	-15.	2.569	2.429	4
276	-10	4.31	-6.	4.	12.	11.916	12.164	0
277	-10	3.31	-1.	5.	14.	9.967	9.030	0
279	-10	4.99	-4.	-3.	-6.	16.378	16.013	0
280	-10	3.00	-3.	-1.	-15.	5.809	6.024	6
281	-10	2.10	-15.	-5.	6.	0.376	0.514	0
282	-10	1.91	4.	-2.	14.	3.195	3.102	0
284	-10	4.99	5.	1.	20.	27.157	27.083	0
283	-10	4.69	1.	-1.	-16.	19.586	19.523	0
286	-10	3.21	-12.	4.	-12.	3.405	3.244	0
285	-10	3.41	-15.	-2.	-20.	1.174	1.154	0
287	-10	2.60	-3.	2.	-8.	4.435	4.531	0
289	-10	4.80	4.	-1.	16.	22.873	23.116	0

TABLE C-5

STABILITY AND TURNING TEST RESULTS
FORWARD SIDE FORCE, DESIGN LOAD CONDITION

RUN	RADIUS FT	SPEED FT/SEC	DRIFT ANGLE DEG	ROLL ANGLE DEG	RUDDER ANGLE DEG	MEASURED VALUE LB	FITTED VALUE LB	REPEAT RUN SET
288	-10	3.01	-3.	-1.	-15.	5.964	6.068	6
290	-10	4.60	-9.	-3.	-16.	8.788	8.801	0
291	-10	3.21	-12.	2.	-20.	2.680	2.962	0
292	-10	4.60	-11.	-5.	-13.	5.775	5.752	0
293	-10	2.50	1.	-3.	8.	4.901	5.147	0
294	-10	4.01	-1.	0.	8.	12.877	12.946	0
296	-10	3.01	-3.	-1.	-15.	5.905	6.068	6
297	-10	3.61	0.	-3.	-12.	11.143	11.511	0
298	-10	4.70	2.	3.	-8.	22.493	22.201	0
299	-10	2.60	-15.	-5.	18.	1.007	0.844	0
300	-10	2.50	-11.	-4.	-18.	1.974	1.678	0
251	10	2.39	10.	-2.	-16.	-1.887	-1.931	0
252	10	1.69	-5.	0.	-20.	-2.634	-2.398	0
253	10	4.27	15.	1.	0.	-2.637	-2.660	0
254	10	1.60	6.	4.	12.	-1.396	-1.321	0
255	10	3.00	5.	1.	2.	-5.233	-5.228	0
256	10	3.00	3.	1.	15.	-6.034	-6.098	5
259	10	2.19	0.	2.	-16.	-3.952	-3.623	0
260	10	3.88	-1.	-3.	-18.	-14.592	-14.681	0
261	10	1.69	0.	0.	3.	-2.254	-1.936	0
262	10	2.50	0.	1.	0.	-5.093	-4.956	0
263	10	3.98	3.	2.	-2.	-11.275	-11.224	0
264	10	2.98	3.	1.	15.	-6.076	-6.010	5
265	10	1.50	7.	-3.	-12.	-1.157	-1.134	0
266	10	2.19	3.	-3.	-6.	-3.351	-2.999	0
267	10	2.89	5.	1.	-20.	-4.853	-4.858	0
268	10	2.40	9.	-1.	2.	-2.107	-2.157	0
270	10	2.61	14.	2.	10.	-1.018	-1.002	0
271	10	1.90	13.	5.	0.	-0.767	-0.770	0
272	10	2.99	3.	1.	15.	-6.032	-6.054	5
273	10	4.09	6.	4.	-8.	-8.572	-8.705	0

TABLE C-6

STABILITY AND TURNING TEST RESULTS
AFT SIDE FORCE, DESIGN LOAD CONDITION

RUN	RADIUS FT	SPEED FT/SEC	DRIFT ANGLE DEG	ROLL ANGLE DEG	RUDDER ANGLE DEG	MEASURED VALUE LB	FITTED VALUE LB	REPEAT RUN SET
78	-30	3.25	-7.	-3.	0.	-1.961	-2.064	0
79	-30	1.61	-12.	-3.	-20.	-1.274	-1.444	0
80	-30	3.00	-3.	-1.	-15.	-1.266	-1.200	2
81	-30	4.99	-7.	-5.	0.	-5.581	-5.338	0
82	-30	2.61	-15.	1.	16.	-3.723	-3.447	0
83	-30	2.31	3.	-3.	-2.	0.499	0.648	0
85	-30	2.01	5.	-3.	2.	0.832	0.830	0
86	-30	2.30	-2.	-5.	10.	0.022	0.113	0
87	-30	1.92	5.	4.	-4.	0.469	0.553	0
88	-30	3.01	-3.	-1.	-15.	-1.266	-1.209	2
89	-30	1.71	-15.	-3.	4.	-1.768	-1.880	0
90	-30	4.51	-4.	-5.	4.	-1.995	-2.135	0
93	-30	4.11	-6.	-4.	4.	-2.522	-2.902	0
94	-30	4.60	0.	-3.	18.	0.492	0.399	0
95	-30	3.61	-2.	-2.	6.	-0.801	-0.791	0
96	-30	2.99	-3.	-1.	-15.	-1.240	-1.191	2
98	-30	1.91	-14.	1.	2.	-2.076	-1.950	0
99	-30	2.10	-15.	1.	20.	-2.460	-2.430	0
100	-30	3.83	5.	-4.	10.	2.549	2.557	0
51	30	3.25	-5.	3.	-18.	-1.837	-2.029	0
54	30	3.40	2.	-5.	-6.	1.349	1.666	0
53	30	3.34	0.	-1.	-12.	0.114	0.239	0
55	30	1.61	10.	3.	12.	1.018	1.152	0
56	30	3.00	3.	1.	15.	1.059	1.246	1
57	30	4.60	12.	5.	-12.	6.760	6.838	0
58	30	1.49	5.	-2.	2.	0.514	0.516	0
59	30	3.70	-3.	1.	-8.	-0.819	-0.890	0
60	30	2.40	15.	-5.	8.	3.494	3.457	0
61	30	3.40	3.	-3.	20.	2.053	2.034	0
62	30	4.30	0.	-5.	10.	2.973	2.648	0
63	30	4.10	9.	-3.	-4.	5.633	5.754	0
64	30	3.00	3.	1.	15.	1.159	1.246	1
65	30	4.30	14.	5.	-4.	7.445	7.673	0
69	30	4.40	1.	-3.	-8.	2.209	1.897	0
70	30	2.30	0.	1.	12.	0.198	0.376	0
71	30	3.10	-5.	-3.	-10.	-1.299	-0.907	0
72	30	3.00	3.	1.	15.	1.116	1.246	1
73	30	4.70	15.	1.	-6.	11.275	11.091	0
75	30	3.70	7.	-3.	20.	3.959	4.032	0
97	-30	4.51	-3.	3.	8.	-3.625	-2.986	0
151	20	3.49	-4.	3.	16.	-0.545	-0.902	0
152	20	3.00	3.	1.	15.	1.306	1.415	3
154	20	2.40	8.	-5.	0.	1.990	1.892	0
155	20	2.20	10.	-4.	-12.	1.646	1.646	0
156	20	3.90	4.	-1.	-2.	3.042	3.007	0
157	20	4.20	-3.	-5.	-4.	0.112	0.537	0
158	20	1.30	12.	-5.	16.	1.632	1.427	0
159	20	3.01	7.	3.	16.	2.000	2.306	0
160	20	3.00	3.	1.	15.	1.194	1.415	3
161	20	3.10	14.	1.	-16.	4.442	4.507	0

TABLE C-6

STABILITY AND TURNING TEST RESULTS
AFT SIDE FORCE, DESIGN LOAD CONDITION

RUN	RADIUS FT	SPEED FT/SEC	DRIFT ANGLE DEG	ROLL ANGLE DEG	RUDDER ANGLE DEG	MEASURED VALUE LB	FITTED VALUE LB	REPEAT RUN SET
162	20	4.41	2.	2.	2.	2.589	2.274	0
163	20	4.51	3.	2.	-16.	3.422	3.238	0
164	20	3.70	-4.	1.	-4.	-1.002	-1.022	0
165	20	2.30	-2.	-1.	2.	-0.115	0.016	0
166	20	1.20	10.	1.	0.	1.249	1.441	0
167	20	4.01	4.	-1.	4.	3.615	3.360	0
168	20	3.00	3.	1.	15.	1.176	1.415	3
169	20	2.30	9.	3.	10.	1.942	1.689	0
171	20	3.09	0.	2.	2.	0.190	0.422	0
172	20	2.70	9.	-1.	20.	2.499	2.660	0
173	20	4.39	11.	-4.	-18.	8.131	7.856	0
174	20	3.11	-3.	1.	16.	-0.166	-0.163	0
176	-20	3.05	-3.	-1.	-15.	-1.653	-1.421	4
178	-20	1.60	-8.	5.	16.	-0.755	-0.640	0
180	-20	2.91	4.	5.	-4.	0.383	0.243	0
181	-20	3.79	-4.	-1.	12.	-1.730	-2.083	0
182	-20	2.70	-7.	-1.	6.	-1.649	-1.628	0
183	-20	3.51	-10.	-3.	-16.	-3.565	-3.669	0
184	-20	3.01	-3.	-1.	-15.	-1.404	-1.379	4
186	-20	2.30	-2.	-3.	4.	-0.245	-0.179	0
187	-20	3.60	-13.	-3.	-6.	-5.739	-5.772	0
189	-20	3.30	-11.	-3.	-13.	-4.043	-4.303	0
191	-20	1.60	-13.	-5.	18.	-1.109	-1.274	0
192	-20	3.00	-3.	-1.	-15.	-1.476	-1.368	4
193	-20	1.50	-3.	-5.	-8.	-0.114	-0.187	0
196	-20	4.09	-2.	5.	8.	-2.433	-2.553	0
195	-20	2.90	4.	-4.	-3.	1.060	1.019	0
197	-20	4.00	3.	-3.	-12.	0.287	0.736	0
198	-20	1.70	-8.	-1.	10.	-0.620	-0.726	0
199	-20	1.90	-15.	-2.	2.	-2.137	-2.202	0
200	-20	3.00	-3.	-1.	-15.	-1.242	-1.368	4
276	-10	4.31	-6.	4.	12.	-6.389	-6.691	0
277	-10	3.31	-1.	5.	14.	-1.173	-1.347	0
278	-10	2.50	5.	5.	14.	1.148	1.042	0
279	-10	4.99	-4.	-3.	-6.	-7.202	-7.050	0
280	-10	3.00	-3.	-1.	-15.	-2.049	-1.960	6
281	-10	2.10	-15.	-5.	6.	-3.068	-3.042	0
282	-10	1.91	4.	-2.	14.	0.801	0.842	0
283	-10	4.69	1.	-1.	-16.	-2.224	-2.392	0
286	-10	3.21	-12.	4.	-12.	-6.589	-6.494	0
285	-10	3.41	-15.	-2.	-20.	-7.958	-8.388	0
287	-10	2.60	-3.	2.	-8.	-1.645	-1.472	0
288	-10	3.01	-3.	-1.	-15.	-2.098	-1.976	6
290	-10	4.60	-9.	-3.	-16.	-10.143	-10.175	0
291	-10	3.21	-12.	2.	-20.	-6.291	-6.400	0
292	-10	4.60	-11.	-5.	-18.	-11.059	-11.177	0
293	-10	2.50	1.	-3.	8.	0.479	0.325	0
294	-10	4.01	-1.	0.	8.	-2.127	-2.260	0
295	-10	3.31	3.	3.	-10.	-0.067	-0.270	0
296	-10	3.01	-3.	-1.	-15.	-2.066	-1.976	6

TABLE C-6

STABILITY AND TURNING TEST RESULTS
AFT SIDE FORCE, DESIGN LOAD CONDITION

RUN	RADIUS FT	SPEED FT/SEC	DRIFT ANGLE DEG	ROLL ANGLE DEG	RUDDER ANGLE DEG	MEASURED VALUE LB	FITTED VALUE LB	REPEAT RUN SET
297	-10	3.81	0.	-3.	-12.	-1.478	-1.342	0
299	-10	2.60	-15.	-5.	18.	-4.133	-3.875	0
300	-10	2.50	-11.	-4.	-18.	-3.379	-2.824	0
251	10	2.39	10.	-2.	-16.	2.468	2.403	0
252	10	1.69	-5.	0.	-20.	-0.705	-0.840	0
254	10	1.60	6.	4.	12.	0.743	0.753	0
255	10	3.00	5.	1.	2.	2.673	2.548	0
256	10	3.00	3.	1.	15.	2.150	2.010	5
257	10	5.06	8.	5.	4.	9.990	9.972	0
258	10	1.50	15.	-2.	6.	1.816	2.102	0
259	10	2.19	0.	2.	-16.	-0.261	-0.068	0
260	10	3.38	-1.	-3.	-18.	0.756	0.960	0
261	10	1.69	0.	0.	-6.	0.086	0.036	0
262	10	2.50	0.	1.	0.	0.360	0.466	0
263	10	3.98	3.	2.	-2.	3.686	3.444	0
264	10	2.98	3.	1.	15.	2.083	1.979	5
265	10	1.50	7.	-3.	-12.	0.687	0.553	0
266	10	2.19	3.	-3.	-6.	1.004	0.828	0
267	10	2.89	5.	1.	-20.	1.665	1.852	0
268	10	2.40	9.	-1.	2.	2.658	2.544	0
269	10	1.59	10.	4.	6.	1.301	1.344	0
270	10	2.61	14.	2.	10.	4.737	4.529	0
271	10	1.90	13.	5.	0.	2.403	2.164	0
272	10	2.99	3.	1.	15.	2.101	1.994	5
273	10	4.09	6.	4.	-8.	4.452	4.607	0
275	10	4.30	2.	-4.	-18.	3.432	3.455	0

TABLE C-7

STABILITY AND TURNING TEST RESULTS
ROLL MOMENT, DESIGN LOAD CONDITION

RUN	RADIUS FT	SPEED FT/SEC	DRIFT ANGLE DEG	ROLL ANGLE DEG	RUDDER ANGLE DEG	MEASURED VALUE FT-LB	FITTED VALUE FT-LB	REPEAT RUN SET
76	-30	4.92	-4.	2.	-2.	-12.220	-12.080	0
77	-30	4.72	-11.	-2.	14.	17.900	17.935	0
78	-30	3.25	-7.	-3.	0.	23.220	23.430	0
79	-30	1.61	-12.	-3.	-20.	17.420	17.421	0
80	-30	3.00	-3.	-1.	-15.	7.380	7.402	2
81	-30	4.99	-7.	-5.	0.	43.500	43.193	0
82	-30	2.61	-15.	1.	16.	-3.780	-4.120	0
83	-30	2.31	3.	-3.	-2.	19.940	20.172	0
84	-30	2.50	-14.	-4.	16.	27.710	27.486	0
85	-30	2.01	5.	-3.	2.	16.200	16.395	0
86	-30	2.30	-2.	-5.	10.	35.850	35.966	0
87	-30	1.92	5.	4.	-4.	-23.520	-23.555	0
88	-30	3.01	-3.	-1.	-15.	6.880	7.410	2
89	-30	1.71	-15.	-3.	4.	21.210	21.618	0
90	-30	4.51	-4.	-5.	4.	40.700	40.185	0
91	-30	4.81	-12.	5.	12.	-28.100	-28.127	0
92	-30	4.01	-1.	2.	-6.	-14.320	-13.901	0
93	-30	4.11	-6.	-4.	4.	27.990	28.661	0
94	-30	4.60	0.	-3.	18.	21.960	22.761	0
95	-30	3.61	-2.	-2.	6.	10.890	11.313	0
96	-30	2.99	-3.	-1.	-15.	7.160	7.395	2
98	-30	1.91	-14.	1.	2.	-4.710	-5.631	0
99	-30	2.10	-15.	1.	20.	-1.670	-1.578	0
100	-30	3.83	5.	-4.	10.	23.380	23.642	0
51	30	3.25	-5.	3.	-18.	-19.530	-19.516	0
52	30	4.36	-1.	2.	10.	-11.810	-11.238	0
53	30	3.34	0.	-1.	-12.	2.710	2.638	0
55	30	1.61	10.	3.	12.	-20.180	-20.615	0
56	30	3.00	3.	1.	15.	-8.080	-8.266	1
58	30	1.49	5.	-2.	2.	9.230	9.399	0
59	30	3.70	-3.	1.	-8.	-3.420	-3.339	0
61	30	3.40	3.	-3.	20.	20.720	20.494	0
63	30	4.10	9.	-3.	-4.	17.640	16.980	0
64	30	3.00	3.	1.	15.	-8.090	-8.266	1
65	30	4.80	15.	-1.	-6.	-6.560	-6.921	0
66	30	4.70	-5.	-1.	12.	5.830	5.653	0
67	30	4.68	0.	-4.	14.	29.640	29.517	0
68	30	4.30	14.	5.	-4.	-39.490	-39.638	0
69	30	4.40	1.	-3.	-8.	20.110	20.581	0
70	30	2.80	0.	1.	12.	-7.430	-7.464	0
71	30	3.10	-5.	-3.	-10.	22.230	21.880	0
72	30	3.00	3.	1.	15.	-7.860	-8.266	1
73	30	4.70	15.	1.	-6.	-17.650	-17.528	0
74	30	3.80	10.	2.	-12.	-15.150	-15.509	0
75	30	3.70	7.	-3.	20.	15.190	15.182	0
97	-30	4.51	-3.	3.	8.	-19.240	-19.863	0
151	20	3.49	-4.	3.	16.	-16.880	-16.822	0
152	20	3.00	3.	1.	15.	-8.320	-8.393	3
153	20	2.80	12.	3.	4.	-23.990	-23.828	0
154	20	2.40	8.	-5.	0.	30.330	30.182	0

TABLE C-7

STABILITY AND TURNING TEST RESULTS
ROLL MOMENT, DESIGN LOAD CONDITION

RUN	RADIUS FT	SPEED FT/SEC	DRIFT ANGLE DEG	ROLL ANGLE DEG	RUDDER ANGLE DEG	MEASURED VALUE FT-LB	FITTED VALUE FT-LB	REPEAT RUN SET
155	20	2.20	10.	-4.	-12.	22.440	22.472	0
156	20	3.90	4.	-1.	-2.	5.320	4.387	0
159	20	3.01	7.	3.	16.	-19.300	-19.681	0
160	20	3.00	3.	1.	15.	-8.340	-8.393	3
161	20	3.10	14.	1.	-16.	-7.760	-8.163	0
162	20	4.41	2.	2.	2.	-13.210	-13.193	0
163	20	4.81	3.	0.	-16.	-3.600	-3.365	0
164	20	3.70	-4.	1.	-2.	-6.870	-6.618	0
165	20	2.80	-2.	-1.	2.	2.950	3.111	0
166	20	1.90	10.	1.	0.	-4.800	-4.947	0
167	20	4.01	4.	-1.	4.	4.560	4.359	0
168	20	3.00	3.	1.	15.	-8.020	-8.393	3
169	20	2.30	9.	3.	10.	-21.950	-21.987	0
170	20	4.60	13.	-2.	-14.	1.840	2.261	0
171	20	3.09	0.	2.	2.	-11.020	-11.242	0
172	20	2.70	9.	-1.	20.	4.820	4.786	0
173	20	4.39	11.	-4.	-18.	19.350	19.129	0
174	20	3.11	-3.	1.	16.	-3.540	-3.356	0
175	20	3.90	-2.	-2.	6.	14.240	14.360	0
176	-20	3.05	-3.	-1.	-15.	8.110	7.571	4
178	-20	1.60	-8.	5.	16.	-32.180	-31.676	0
180	-20	2.91	4.	5.	-4.	-34.640	-34.180	0
181	-20	3.79	-4.	-1.	12.	8.440	8.914	0
182	-20	2.70	-7.	-1.	6.	4.360	4.755	0
183	-20	3.21	-10.	-3.	-16.	20.150	20.594	0
184	-20	3.01	-3.	-1.	-15.	7.710	7.538	4
185	-20	4.29	2.	-4.	16.	30.140	29.450	0
186	-20	2.30	-2.	-3.	4.	17.570	17.568	0
187	-20	3.60	-13.	-3.	-6.	27.200	26.521	0
188	-20	4.60	5.	5.	16.	-34.860	-34.416	0
189	-20	3.30	-11.	-3.	-18.	20.420	21.131	0
190	-20	3.40	-6.	-4.	14.	27.620	27.755	0
192	-20	3.00	-3.	-1.	-15.	7.750	7.530	4
194	-20	4.69	-4.	2.	2.	-11.580	-12.059	0
196	-20	4.09	-2.	5.	8.	-33.560	-33.718	0
195	-20	2.90	4.	-4.	-8.	22.880	23.734	0
197	-20	4.00	3.	-3.	-12.	16.480	16.780	0
198	-20	1.70	-8.	-1.	10.	7.420	7.251	0
199	-20	1.90	-15.	-2.	2.	11.420	11.517	0
200	-20	3.00	-3.	-1.	-15.	7.450	7.530	4
276	-10	4.31	-6.	4.	12.	-21.520	-21.663	0
277	-10	3.31	-1.	5.	17.	-33.460	-33.547	0
279	-10	4.99	-4.	-3.	-6.	22.680	23.005	0
280	-10	3.00	-3.	-1.	-15.	8.210	7.938	6
282	-10	1.91	4.	-2.	14.	13.400	13.520	0
284	-10	4.99	5.	1.	20.	-9.190	-9.620	0
283	-10	4.69	1.	-1.	-16.	7.540	7.654	0
286	-10	3.21	-12.	4.	-12.	-23.550	-23.918	0
285	-10	3.41	-15.	-2.	-20.	20.080	19.827	0
287	-10	2.60	-3.	2.	-8.	-13.010	-13.023	0

TABLE C-7

STABILITY AND TURNING TEST RESULTS
ROLL MOMENT, DESIGN LOAD CONDITION

RUN	RADIUS FT	SPEED FT/SEC	DRIFT ANGLE DEG	ROLL ANGLE DEG	RUDDER ANGLE DEG	MEASURED VALUE FT-LB	FITTED VALUE FT-LB	REPEAT RUN SET
289	-10	4.80	4.	-1.	16.	5.700	6.170	0
288	-10	3.04	-3.	-1.	-15.	7.990	7.948	6
290	-10	4.60	-9.	-3.	-16.	25.240	25.112	0
291	-10	3.21	-12.	2.	-20.	-6.980	-6.825	0
293	-10	2.50	1.	-3.	8.	21.400	21.268	0
294	-10	4.01	-1.	0.	8.	1.020	1.008	0
295	-10	3.31	3.	3.	-10.	-21.090	-21.279	0
296	-10	3.01	-3.	-1.	-15.	7.680	7.948	6
297	-10	3.81	0.	-3.	-12.	23.290	22.540	0
298	-10	4.70	2.	3.	-8.	-18.900	-18.644	0
299	-10	2.60	-15.	-5.	18.	36.620	36.462	0
251	10	2.39	10.	-2.	-16.	8.300	7.917	0
252	10	1.69	-5.	0.	-20.	-0.130	-0.263	0
253	10	4.27	15.	1.	0.	-13.420	-13.173	0
254	10	1.60	6.	4.	12.	-26.920	-26.901	0
255	10	3.00	5.	1.	2.	-9.520	-9.481	0
256	10	3.00	3.	1.	15.	-8.960	-8.801	5
257	10	5.06	8.	5.	4.	-41.060	-41.398	0
259	10	2.19	0.	2.	-16.	-14.330	-14.129	0
260	10	3.88	-1.	-3.	-18.	17.070	17.112	0
261	10	1.69	0.	0.	-6.	-0.520	-0.711	0
262	10	2.50	0.	1.	0.	-8.030	-7.831	0
263	10	3.98	3.	2.	-2.	-13.760	-13.894	0
264	10	2.98	3.	1.	15.	-9.000	-8.777	5
265	10	1.50	7.	-3.	-12.	16.110	15.982	0
266	10	2.19	3.	-3.	-6.	19.820	19.746	0
267	10	2.89	5.	1.	-20.	-5.780	-5.760	0
268	10	2.40	9.	-1.	2.	4.620	4.622	0
269	10	1.59	10.	4.	6.	-24.120	-24.079	0
270	10	2.61	14.	2.	10.	-14.480	-14.065	0
271	10	1.90	13.	5.	0.	-34.730	-34.560	0
272	10	2.99	3.	1.	15.	-9.380	-8.789	5
273	10	4.09	6.	4.	-8.	-33.460	-33.003	0
274	10	4.69	13.	-4.	-2.	21.560	21.678	0

TABLE C-8

STABILITY AND TURNING TEST RESULTS
DRAG FORCE, DESIGN LOAD CONDITION

RUN	RADIUS FT	SPEED FT/SEC	DRIFT ANGLE DEG	ROLL ANGLE DEG	RUDDER ANGLE DEG	MEASURED VALUE LB	FITTED VALUE LB	REPEAT RUN SET
77	-30	4.72	-11.	-2.	14.	33.535	33.304	0
78	-30	3.25	-7.	-3.	0.	14.846	15.193	0
79	-30	1.61	-12.	-3.	-20.	3.967	4.167	0
80	-30	3.00	-3.	-1.	-15.	12.724	12.872	2
81	-30	4.99	-7.	-5.	0.	36.274	36.198	0
82	-30	2.61	-15.	1.	16.	10.612	10.644	0
83	-30	2.31	3.	-3.	-2.	7.115	7.248	0
84	-30	2.50	-14.	-4.	16.	9.676	9.563	0
86	-30	2.30	-2.	-5.	10.	7.171	7.307	0
87	-30	1.92	5.	4.	-4.	5.160	5.132	0
88	-30	3.01	-3.	-1.	-15.	12.965	12.959	2
89	-30	1.71	-15.	-3.	4.	4.492	4.578	0
90	-30	4.51	-4.	-5.	4.	29.484	29.076	0
92	-30	4.01	-1.	2.	-6.	22.890	22.967	0
93	-30	4.11	-6.	-4.	4.	24.429	24.361	0
94	-30	4.60	0.	-3.	18.	30.607	30.097	0
95	-30	3.61	-2.	-2.	6.	18.361	18.474	0
96	-30	2.99	-3.	-1.	-15.	12.759	12.786	2
98	-30	1.91	-14.	1.	2.	5.577	5.660	0
99	-30	2.10	-15.	1.	20.	6.984	7.119	0
100	-30	3.83	5.	-4.	10.	19.673	20.267	0
52	30	4.36	-1.	2.	10.	26.911	26.809	0
54	30	3.40	2.	-5.	-6.	16.563	16.624	0
53	30	3.34	0.	-1.	-12.	15.631	15.788	0
55	30	1.61	10.	3.	12.	3.844	3.877	0
56	30	3.00	3.	1.	15.	13.086	12.861	1
57	30	4.60	12.	5.	-12.	31.032	31.499	0
58	30	1.49	5.	-2.	2.	3.280	3.149	0
59	30	3.70	-3.	1.	-8.	18.516	19.112	0
60	30	2.40	15.	-5.	8.	9.180	9.052	0
61	30	3.40	3.	-3.	20.	17.001	16.848	0
62	30	4.80	0.	-5.	10.	33.454	33.107	0
63	30	4.10	9.	-3.	-4.	24.536	24.923	0
64	30	3.00	3.	1.	15.	12.926	12.861	1
65	30	4.80	15.	-1.	-6.	36.251	35.137	0
66	30	4.70	-5.	-1.	12.	30.827	30.924	0
67	30	4.68	0.	-4.	14.	30.718	31.465	0
68	30	4.30	14.	5.	-4.	27.700	27.740	0
69	30	4.40	1.	-3.	-8.	27.671	27.757	0
70	30	2.80	0.	1.	12.	10.565	11.001	0
71	30	3.10	-5.	-3.	-10.	13.238	13.450	0
72	30	3.00	3.	1.	15.	12.699	12.861	1
73	30	4.70	15.	1.	-6.	34.413	33.594	0
74	30	3.80	10.	2.	-12.	21.018	21.364	0
75	30	3.70	7.	-3.	20.	20.032	20.292	0
97	-30	4.51	-3.	3.	8.	29.454	29.453	0
151	20	3.49	-4.	3.	16.	16.584	17.036	0
152	20	3.00	3.	1.	15.	13.393	13.105	3
153	20	2.80	12.	3.	4.	12.160	11.958	0
154	20	2.40	8.	-5.	0.	8.853	8.793	0

TABLE C-8

STABILITY AND TURNING TEST RESULTS
DRAG FORCE, DESIGN LOAD CONDITION

RUN	RADIUS FT	SPEED FT/SEC	DRIFT ANGLE DEG	ROLL ANGLE DEG	RUDDER ANGLE DEG	MEASURED VALUE LB	FITTED VALUE LB	REPEAT RUN SET
155	20	2.20	10.	-4.	-12.	7.468	7.587	0
156	20	3.90	4.	-1.	-2.	22.522	22.399	0
157	20	4.20	-3.	-5.	-4.	25.398	25.338	0
158	20	1.80	12.	-5.	16.	5.222	5.403	0
159	20	3.01	7.	3.	16.	13.567	13.485	0
160	20	3.00	3.	1.	15.	13.381	13.105	3
161	20	3.10	14.	1.	-16.	15.030	15.241	0
162	20	4.41	2.	2.	2.	27.995	28.167	0
163	20	4.81	3.	0.	-16.	34.658	34.109	0
165	20	2.80	-2.	-1.	2.	10.922	11.030	0
166	20	1.90	10.	1.	0.	5.423	5.465	0
167	20	4.01	4.	-1.	4.	23.700	23.705	0
168	20	3.00	3.	1.	15.	13.023	13.105	3
169	20	2.30	9.	3.	10.	8.036	7.878	0
170	20	4.60	13.	-2.	-14.	33.749	33.333	0
171	20	3.09	0.	2.	2.	13.156	13.492	0
172	20	2.70	9.	-1.	20.	11.196	11.292	0
173	20	4.39	11.	-4.	-18.	30.369	30.206	0
174	20	3.11	-3.	1.	16.	13.579	13.690	0
175	20	3.90	-2.	-2.	6.	21.672	21.734	0
176	-20	3.05	-3.	-1.	-15.	13.808	13.588	4
178	-20	1.60	-8.	5.	16.	4.097	4.139	0
180	-20	2.91	4.	5.	-4.	12.256	12.118	0
181	-20	3.79	-4.	-1.	12.	21.215	21.157	0
182	-20	2.70	-7.	-1.	6.	10.721	10.826	0
183	-20	3.21	-10.	-3.	-16.	16.054	15.737	0
184	-20	3.01	-3.	-1.	-15.	13.469	13.231	4
185	-20	4.29	2.	-4.	16.	25.478	26.093	0
186	-20	2.30	-2.	-3.	4.	7.495	7.442	0
187	-20	3.60	-13.	-3.	-6.	20.377	20.081	0
188	-20	4.60	5.	5.	16.	30.089	30.342	0
189	-20	3.30	-11.	-3.	-18.	17.168	16.807	0
190	-20	3.40	-6.	-4.	14.	16.856	17.066	0
191	-20	1.60	-13.	-5.	18.	4.052	4.173	0
192	-20	3.00	-3.	-1.	-15.	13.141	13.142	4
193	-20	1.50	-3.	-5.	-8.	3.275	3.074	0
194	-20	4.69	-4.	2.	2.	32.326	32.770	0
196	-20	4.09	-2.	5.	8.	24.819	24.822	0
195	-20	2.90	4.	-4.	-8.	11.194	11.584	0
197	-20	4.00	3.	-3.	-12.	22.234	22.560	0
198	-20	1.70	-8.	-1.	10.	4.360	4.335	0
199	-20	1.90	-15.	-2.	2.	5.811	5.807	0
200	-20	3.00	-3.	-1.	-15.	13.099	13.142	4
276	-10	4.31	-6.	4.	12.	31.889	32.081	0
277	-10	3.31	-1.	5.	14.	17.992	18.155	0
278	-10	2.50	5.	5.	14.	9.603	9.845	0
280	-10	3.00	-3.	-1.	-15.	14.996	14.539	6
281	-10	2.10	-15.	-5.	6.	7.759	7.777	0
282	-10	1.91	4.	-2.	14.	5.582	5.400	0
284	-10	4.99	5.	1.	20.	37.997	38.201	0

TABLE C-8

STABILITY AND TURNING TEST RESULTS
DRAG FORCE, DESIGN LOAD CONDITION

RUN	RADIUS FT	SPEED FT/SEC	DRIFT ANGLE DEG	ROLL ANGLE DEG	RUDDER ANGLE DEG	MEASURED VALUE LB	FITTED VALUE LB	REPEAT RUN SET
285	-10	3.41	-15.	-2.	-20.	21.540	21.486	0
287	-10	2.60	-3.	2.	-8.	11.308	11.071	0
288	-10	3.01	-3.	-1.	-15.	15.043	14.637	6
290	-10	4.60	-9.	-3.	-16.	36.652	36.717	0
292	-10	4.60	-11.	-5.	-18.	36.764	37.181	0
293	-10	2.50	1.	-3.	8.	9.298	9.350	0
294	-10	4.01	-1.	0.	8.	26.028	25.760	0
295	-10	3.31	3.	3.	-10.	17.883	17.155	0
296	-10	3.01	-3.	-1.	-15.	14.938	14.637	6
297	-10	3.81	0.	-3.	-12.	22.664	22.577	0
299	-10	2.60	-15.	-5.	18.	11.939	12.223	0
300	-10	2.50	-11.	-4.	-18.	10.927	10.777	0
251	10	2.39	10.	-2.	-16.	9.770	10.038	0
252	10	1.69	-5.	0.	-20.	4.311	4.426	0
253	10	4.27	15.	1.	0.	32.384	32.925	0
254	10	1.60	6.	4.	12.	4.111	3.962	0
255	10	3.00	5.	1.	2.	14.852	14.406	0
256	10	3.00	3.	1.	15.	14.596	14.242	5
258	10	1.50	15.	-2.	6.	4.165	4.348	0
259	10	2.19	0.	2.	-16.	7.122	7.277	0
260	10	3.88	-1.	-3.	-18.	23.664	23.509	0
261	10	1.69	0.	0.	-6.	4.551	4.324	0
262	10	2.50	0.	1.	0.	9.634	9.423	0
263	10	3.98	3.	2.	-2.	25.181	24.933	0
264	10	2.98	3.	1.	15.	14.533	14.052	5
265	10	1.50	7.	-3.	-12.	3.781	3.911	0
266	10	2.19	3.	-3.	-6.	7.820	7.784	0
267	10	2.89	5.	1.	-20.	13.686	13.672	0
268	10	2.40	9.	-1.	2.	9.683	9.784	0
269	10	1.59	10.	4.	6.	4.173	4.125	0
270	10	2.61	14.	2.	10.	12.156	12.121	0
271	10	1.90	13.	5.	0.	6.027	6.058	0
272	10	2.99	3.	1.	15.	14.656	14.147	5
273	10	4.09	6.	4.	-8.	26.480	26.860	0
274	10	4.69	13.	-4.	-2.	39.247	39.725	0
275	10	4.30	2.	-4.	-18.	30.134	29.985	0

TABLE C-9

RESULTS OF LEAST SQUARED ERROR CURVE FIT
FOR FORWARD SIDE FORCE, LIGHT SHIP CONDITION

Term	Function	LSF Coefficient	Centrifugal Component	Corrected Coefficient	Label
0	1	-0.058132	0	0.(sym.)	
1	ω	-22.062	10.53	-11.53	a_{FF1}
2	β_o	0.41918	0	0.41918	a_{FF2}
3	φ	-0.010711	0	-0.010711	a_{FF3}
4	δ	-0.0033509	0	-0.0033509	a_{FF4}
5	$\tilde{V}\omega$	-7.7000	3.24	-4.46	a_{FF5}
6	$\tilde{V}\beta_o$	0.32300	0	0.32300	a_{FF6}
7	$\tilde{V}\varphi$	0.030918	0	0.030918	a_{FF7}
8	$\tilde{V}\delta$	-0.0051919	0	-0.0051919	a_{FF8}
9	$\beta_o^3\delta^2$	0.70386×10^{-6}	0	0.70386×10^{-6}	a_{FF16}
10	$\tilde{V}^2\beta_o$	0.028352	0	0.028352	a_{FF9}
11	$\tilde{V}^3\beta_o$	-0.028903	0	-0.028903	a_{FF12}
12	$\omega^3\beta_o^2$	0.044411	0	0.044411	a_{FF14}
13	$\tilde{V}^2\varphi$	0.022745	0	0.022745	a_{FF10}
14	$\varphi\delta$	-0.0015105	0	0.(sym.)	
15	$\tilde{V}\varphi^4$	0.00028323	0	0.(sym.)	
16	$\tilde{V}$	-0.022383	0	0.(sym.)	
17	$\omega\beta_o^2$	0	-.0016023	-.0016023	a_{FF11}
18	$\tilde{V}\omega\beta_o^2$	0	-.00049348	-.00049348	a_{FF13}
19	$\omega\beta_o^4$	0	$.40736\times10^{-7}$	$.40736\times10^{-7}$	a_{FF15}

$n = 124 \qquad \sigma_e/\sigma_y = 0.0391 \qquad r = 0.0365$

$$S_{FF} = a_{FF1}\omega + a_{FF2}\beta_o + a_{FF3}\varphi + a_{FF4}\delta + a_{FF5}\tilde{V}\omega + a_{FF6}\tilde{V}\beta_o + a_{FF7}\tilde{V}\varphi + a_{FF8}\tilde{V}\delta + a_{FF9}\tilde{V}^2\beta_o + a_{FF10}\tilde{V}^2\varphi + a_{FF11}\omega\beta_o^2 + a_{FF12}\tilde{V}^3\beta_o + a_{FF13}\tilde{V}\omega\beta_o^2 + a_{FF14}\omega^3\beta_o^2 + a_{FF15}\omega\beta_o^4 + a_{FF16}\beta_o^3\delta^2$$

$\tilde{V} = V - V_o$, $V_o = 3.25$ ft/sec

TABLE C-10

RESULTS OF LEAST SQUARED ERROR CURVE FIT
FOR AFT SIDE FORCE, LIGHT SHIP CONDITION

Term	Function	LSF Coefficient	Centrifugal Component	Corrected Coefficient	Label
0	1	0.022474	0	0. (sym.)	
1	ω	3.9495	10.87	14.82	a_{AF1}
2	β_o	0.26273	0	0.26273	a_{AF2}
3	φ	-0.092457	0	-0.092457	a_{AF3}
4	δ	0.023447	0	0.023447	a_{AF4}
5	$\tilde{V}\omega$	2.1713	3.34	5.51	a_{AF5}
6	$\tilde{V}\beta_o$	0.15362	0	0.15362	a_{AF6}
7	$\tilde{V}\varphi$	-0.033784	0	-0.033784	a_{AF7}
8	$\tilde{V}\delta$	0.011194	0	0.011194	a_{AF8}
9	$\omega^2\beta_o$	0.96358	0	0.96358	a_{AF10}
10	$\tilde{V}^2\beta_o$	0.022608	0	0.022608	a_{AF9}
11	β_o^3	0.00025053	0	0.00025053	a_{AF12}
12	$\omega\beta_o$	0.037675	0	0. (sym.)	
13	$\tilde{V}^2$	-0.048996	0	0. (sym.)	
14	$\tilde{V}\omega\beta_o\varphi$	-0.035593	0	-0.035593	a_{AF14}
15	$\tilde{V}^4\omega$	0.11974	0	0.11974	a_{AF15}
16	$\tilde{V}\beta_o^2$	0.00084482	0	0. (sym.)	
17	ω^2	1.6755	0	0. (sym.)	
18	$\beta_o^2\varphi\delta$	0.13236×10^{-4}	0	0. (sym.)	
19	$\omega\beta_o^2$	0	-.0016571	-.0016571	a_{AF11}
20	$\tilde{V}\omega\beta_o^2$	0	-.00050932	-.00050932	a_{AF13}
21	$\omega\beta_o^4$	0	$.42035\times10^{-7}$	$.42035\times10^{-7}$	a_{AF16}

$n = 125$ $\quad \sigma_e/\sigma_y = 0.0534$ $\quad r = 0.0494$

$$S_{AF} = a_{AF1}\omega + a_{AF2}\beta_o + a_{AF3}\varphi + a_{AF4}\delta + a_{AF5}\tilde{V}\omega + a_{AF6}\tilde{V}\beta_o + a_{AF7}\tilde{V}\varphi + a_{AF8}\tilde{V}\delta + a_{AF9}\tilde{V}^2\beta_o$$
$$+ a_{AF10}\omega^2\beta_o + a_{AF11}\omega\beta_o^2 + a_{AF12}\beta_o^3 + a_{AF13}\tilde{V}\omega\beta_o^2 + a_{AF14}\tilde{V}\omega\beta_o\varphi + a_{AF15}\tilde{V}^4\omega + a_{AF16}\omega\beta_o^4$$

$\tilde{V} = V - V_o$, $V_o = 3.25$ ft/sec

114

TABLE C-11

RESULTS OF LEAST SQUARED ERROR CURVE FIT
FOR ROLL MOMENT, LIGHT SHIP CONDITION

Term	Function	LSF Coefficient	Corrected Coefficient	Label
0	1	-0.20705	0. (sym.)	
1	$\tilde{V}$	-0.23550	0. (sym.)	
2	ω	-4.8376	-4.8376	b_{F1}
3	β_o	-0.22245	-0.22245	b_{F2}
4	φ	-7.0858	-7.0858	b_{F3}
5	δ	0.0027219	0.0027219	b_{F4}
6	$\tilde{V}\omega$	0.55416	0.55416	b_{F5}
7	$\tilde{V}\beta_o$	-0.11643	-0.11643	b_{F6}
8	$\tilde{V}\varphi$	-0.15428	-0.15428	b_{F7}
9	φ^2	0.058910	0. (sym.)	
10	φ^3	0.016578	0.016578	b_{F8}
11	$\tilde{V}\beta_o\varphi$	-0.0076122	0. (sym.)	

$n = 138$ $\quad \sigma_e/\sigma_y = 0.00095$ $\quad r = 0.0295$

$$K_F = b_{F1}\omega + b_{F2}\beta_o + b_{F3}\varphi + b_{F4}\delta + b_{F5}\tilde{V}\omega + b_{F6}\tilde{V}\beta_o + b_{F7}\tilde{V}\varphi + b_{F8}\varphi^3$$

$\tilde{V} = V - V_o$, $V_o = 3.25$ ft/sec

TABLE C-12

RESULTS OF LEAST SQUARED ERROR CURVE FIT
FOR DRAG, LIGHT SHIP CONDITION

Term	Function	LSF Coefficient	Centrifugal Component	Corrected Coefficient	Label
0	1	13.214		13.214	C_{Fo}
1	$\tilde{V}$	8.3761		8.3761	C_{F1}
2	$\tilde{V}^2$	1.3818		1.3818	C_{F2}
3	ω^2	10.657		10.657	C_{F3}
4	δ^2	0.00099552		0.00099552	C_{F8}
5	$\tilde{V}\omega\beta_o$	0.042045	6.58	6.62	C_{F9}
6	$\omega\varphi$	-0.52712		-0.52712	C_{F5}
7	$\omega\beta_o$	0.36551	21.4	21.77	C_{F4}
8	$\beta_o\varphi$	0.0065249		0.0065249	C_{F6}
9	$\tilde{V}\delta^2$	0.00078682		0.00078682	C_{F11}
10	$\tilde{V}\omega\delta$	-0.021834		-0.021834	C_{F10}
11	$\beta_o\varphi^2$	0.0010384		0. (sym.)	
12	$\beta_o\delta$	0.00068065		0.00068065	C_{F7}

$n = 141$ $\qquad \sigma_e/\sigma_y = 0.00121$ $\qquad r = 0.0333$

$$X_F = c_{Fo} + c_{F1}\tilde{V} + c_{F2}\tilde{V}^2 + c_{F3}\omega^2 + c_{F4}\omega\beta_o + c_{F5}\omega\varphi + c_{F6}\beta_o\varphi + c_{F7}\beta_o\delta + c_{F8}\delta^2 + c_{F9}\tilde{V}\omega\beta_o + c_{F10}\tilde{V}\omega\delta + c_{F11}\tilde{V}\delta^2$$

$\tilde{V} = V - V_o$, $V_o = 3.25$ ft/sec

TABLE C-13

RESULTS OF LEAST SQUARED ERROR CURVE FIT
FOR FORWARD SIDE FORCE, DESIGN LOAD CONDITION

Term	Function	LSF Coefficient	Centrifugal Component	Corrected Coefficient	Label
0	1	0.082651	0	0. (sym.)	
1	ω	-27.085	15.01	-12.08	a_{GF1}
2	β_o	0.47342	0	0.47342	a_{GF2}
3	φ	0.096794	0	0.096794	a_{GF3}
4	δ	0.0033340	0	0.0033340	a_{GF4}
5	$\tilde{V}\omega$	-9.9324	4.62	-5.31	a_{GF5}
6	$\tilde{V}\beta_o$	0.30976	0	0.30976	a_{GF6}
7	$\tilde{V}\varphi$	0.17007	0	0.17007	a_{GF7}
8	$\tilde{V}^2\varphi$	0.063486	0	0.063486	a_{GF9}
9	$\tilde{V}^2\beta_o$	0.029706	0	0.029706	a_{GF8}
10	$\varphi\delta$	-0.0015872	0	0. (sym.)	
11	$\tilde{V}\omega\delta$	0.013665	0	0. (sym.)	
12	$\beta_o\varphi$	0.14795	0	0. (sym.)	
13	β_o^2	-0.0022098	0	0. (sym.)	
14	ω^2	-2.1530	0	0. (sym.)	
15	$\omega\beta_o^2$	0.0064187	-.0022846	-.0022846	a_{GF10}
16	$\tilde{V}^2\beta_o\varphi^2$	0.00048853	0	0.00048853	a_{GF12}
17	$\tilde{V}\omega\beta_o^2$	0	-.00070367	-.00070367	a_{GF11}
18	$\omega\beta_o^4$	0	$+.57995\times10^{-7}$	$+.57995\times10^{-7}$	a_{GF13}

n = 131 $\quad \sigma_e/\sigma_y = 0.00071 \quad$ r = 0.0250

$$S_{FG} = a_{GF1}\omega + a_{GF2}\beta_o + a_{GF3}\varphi + a_{GF4}\delta + a_{GF5}\tilde{V}\omega + a_{GF6}\tilde{V}\beta_o + a_{GF7}\tilde{V}\varphi + a_{GF8}\tilde{V}^2\beta_o + a_{GF9}\tilde{V}^2\varphi + a_{GF10}\omega\beta_o^2 + a_{GF11}\tilde{V}\omega\beta_o^2 + a_{GF12}\tilde{V}^2\beta_o\varphi^2 + a_{GF13}\omega\beta_o^4$$

$\tilde{V} = V - V_o$, $V_o = 3.25$ ft/sec

117

TABLE C-14

RESULTS OF LEAST SQUARED ERROR CURVE FIT
FOR AFT SIDE FORCE, DESIGN LOAD CONDITION

Term	Function	LSF Coefficient	Centrifugal Component	Corrected Coefficient	Label
0	1	0.10118	0	0. (sym.)	
1	ω	3.2357	14.77	18.01	a_{GA1}
2	β_o	0.29605	0	0.29605	a_{GA2}
3	φ	-0.12390	0	-0.12390	a_{GA3}
4	δ	0.020674	0	0.020674	a_{GA4}
5	$\tilde{V}\omega$	2.1073	4.54	6.65	a_{GA5}
6	$\tilde{V}\beta_o$	0.18505	0	0.18505	a_{GA6}
7	$\tilde{V}\varphi$	-0.076448	0	-0.076448	a_{GA7}
8	$\tilde{V}\delta$	0.0085706	0	0.0085706	a_{GA8}
9	$\tilde{V}^2\beta_o$	0.038321	0	0.038321	a_{GA9}
10	$\omega^2\beta_o$	0.97679	0	0.97679	a_{GA10}
11	$\tilde{V}\omega\varphi$	-0.094531	0	0. (sym.)	
12	$\omega\varphi^2\delta^2$	-0.00031661	0	-0.00031661	a_{GA14}
13	β_o^5	0.59012×10^{-6}	0	0.59012×10^{-6}	a_{GA15}
14	$\omega\beta_o\varphi^2$	-0.0034932	0	0. (sym.)	
15	δ^2	-0.00035454	0	0. (sym.)	
16	$\omega\beta_o^2$	0	-.0022481	-.0022481	a_{GA11}
17	$\tilde{V}\omega\beta_o^2$	0	-.00069148	-.00069148	a_{GA12}
18	$\omega\beta_o^4$	0	$.57067\times10^{-7}$	$.57067\times10^{-7}$	a_{GA13}

$n = 126$ $\quad \sigma_e/\sigma_y = 0.00388$ $\quad r = 0.0584$

$$S_{AG} = a_{GA1}\omega + a_{GA2}\beta_o + a_{GA3}\varphi + a_{GA4}\delta + a_{GA5}\tilde{V}\omega + a_{GA6}\tilde{V}\beta_o + a_{GA7}\tilde{V}\varphi + a_{GA8}\tilde{V}\delta + a_{GA9}\tilde{V}^2\beta_o + a_{GA10}\omega^2\beta_o + a_{GA11}\omega\beta_o^2 + a_{GA12}\tilde{V}\omega\beta_o^2 + a_{GA13}\omega\beta_o^4 + a_{GA14}\omega\varphi^2\delta^2 + a_{GA15}\beta_o^5$$

$\tilde{V} = V - V_o$, $V_o = 3.25$ ft/sec

118

TABLE C-15

RESULTS OF LEAST SQUARED ERROR CURVE FIT
FOR ROLL MOMENT, DESIGN LOAD CONDITION

Term	Function	LSF Coefficient	Corrected Coefficient	Label
0	1	-0.57113	0.(sym.)	
1	$\tilde{V}$	-0.093479	0.(sym.)	
2	ω	-2.3679	-2.3679	b_{G1}
3	β_o	-0.29593	-0.29593	b_{G2}
4	φ	-7.0001	-7.0001	b_{G3}
5	δ	0.0076453	0.0076453	b_{G4}
6	$\tilde{V}\omega$	-0.53892	-0.53892	b_{G5}
7	$\tilde{V}\beta_o$	-0.17704	-0.17704	b_{G6}
8	$\tilde{V}\varphi$	-0.20422	-0.20422	b_{G7}
9	φ^2	0.064162	0.(sym.)	
10	$\omega\beta_o\varphi$	-0.028073	-0.028073	b_{G10}
11	$\omega^2\varphi$	-0.89555	-0.89555	b_{G9}
12	$\varphi\delta$	-0.0040134	0.(sym.)	
13	$V^2\beta_o$	-0.022661	-0.022661	b_{G8}
14	δ^2	0.00049747	0.(sym.)	

$n = 134$ $\qquad \sigma_e/\sigma_y = 0.00035$ $\qquad r = 0.0177$

$$K_G = b_{G1}\omega + b_{G2}\beta_o + b_{G3}\varphi + b_{G4}\delta + b_{G5}\tilde{V}\omega + b_{G6}\tilde{V}\beta_o + b_{G7}\tilde{V}\varphi + b_{G8}\tilde{V}^2\beta_o + b_{G9}\omega^2\varphi + b_{G10}\omega\beta_o\varphi$$

$\tilde{V} = V - V_o$, $V_o = 3.25$ ft/sec

TABLE C-16

RESULTS OF LEAST SQUARED ERROR CURVE FIT
FOR DRAG, DESIGN LOAD CONDITION

Term	Function	LSF Coefficient	Centrifugal Component	Corrected Coefficient	Label
0	1	14.636	0	14.636	c_{Go}
1	$\tilde{V}$	9.1695	0	9.1695	c_{G1}
2	$\tilde{V}^2$	1.4477	0	1.4477	c_{G2}
3	ω^2	16.534	0	16.534	c_{G3}
4	β_o^2	0.0019425	0	0.0019425	c_{G4}
5	δ^2	0.00066378	0	0.00066378	c_{G5}
6	$\tilde{V}\omega\beta_o$	0.18519	9.16	9.35	c_{G8}
7	$\omega\beta_o$	0.51194	29.8	30.31	c_{G6}
8	$\omega\varphi$	-0.39150	0	-0.39150	c_{G7}
9	ω^3	-5.4868	0	0.(sym.)	

$n = 136$ $\qquad \sigma_e/\sigma_y = 0.00094$ $\qquad r = 0.0297$

$$X_G = c_{Go} + c_{G1}\tilde{V} + c_{G2}\tilde{V}^2 + c_{G3}\omega^2 + c_{G4}\beta_o^2 + c_{G5}\delta^2 + c_{G6}\omega\beta_o + c_{G7}\omega\varphi + c_{G8}\tilde{V}\omega\beta_o$$

$\tilde{V} = V - V_o$, $V_o = 3.25$ ft/sec

120

TABLE C-17

TURNING EQUILIBRIUM AND STABILITY FOR LIGHT SHIP

LSF Rudder Coefficients

V	δ_R	β_o	ω	R	Y_v	Y_r	N_v	N_r	σ_i
ft/sec	deg	deg	rad/sec	ft	lb sec/ft	lb sec	lb sec	ft lb sec	sec^{-1}
1.50	-20.	1.21	.000	8727.	-0.242	2.574	-0.122	-25.06	-0.04
2.00	-20.	1.36	.010	202.	-0.450	2.292	-0.051	-35.51	-0.08
2.50	-20.	1.19	.018	138.	-0.919	2.579	-0.279	-47.38	-0.16
3.00	-20.	1.00	.024	126.	-1.705	3.071	-0.858	-59.76	-0.29
3.50	-20.	0.87	.027	128.	-2.819	3.596	-1.733	-72.22	-0.47
4.00	-20.	0.77	.029	136.	-4.230	4.157	-2.738	-84.77	-0.71
4.50	-20.	0.70	.030	150.	-5.860	4.933	-3.599	-97.86	-0.99
5.00	-20.	0.65	.029	171.	-7.592	6.285	-3.935	-112.39	-1.31
3.25	0.	0.00	.000	-99.	-2.216	3.290	-1.271	-65.88	-0.37
3.25	-5.	0.23	.006	503.	-2.216	3.293	-1.271	-65.88	-0.37
3.25	-10.	0.46	.013	251.	-2.217	3.301	-1.269	-65.90	-0.38
3.25	-15.	0.70	.019	168.	-2.219	3.314	-1.267	-65.94	-0.38
3.25	-20.	0.93	.026	126.	-2.222	3.333	-1.267	-65.99	-0.38
3.25	-25.	1.16	.032	101.	-2.228	3.358	-1.269	-66.05	-0.38

(Cont'd)

TABLE C-17

TURNING EQUILIBRIUM AND STABILITY FOR LIGHT SHIP

Estimated Rudder Coefficients

V	δ_R	β_o	ω	R	Y_v	Y_r	N_v	N_r	σ_i
ft/sec	deg	deg	rad/sec	ft	lb sec/ft	lb sec	lb sec	ft lb sec	sec^{-1}
1.50	-20.	-0.71	-.009	166.	-0.239	2.587	-0.122	-25.09	-0.04
2.00	-20.	1.50	.015	130.	-0.452	2.310	-0.051	-35.56	-0.08
2.50	-20.	2.17	.030	83.	-0.933	2.655	-0.278	-47.59	-0.16
3.00	-20.	2.24	.042	72.	-1.727	3.194	-0.853	-60.09	-0.30
3.50	-20.	2.17	.050	70.	-2.845	3.746	-1.722	-72.62	-0.48
4.00	-20.	2.08	.055	73.	-4.259	4.319	-2.721	-85.21	-0.72
4.50	-20.	2.01	.056	80.	-5.892	5.096	-3.578	-98.30	-1.00
5.00	-20.	1.95	.054	92.	-7.625	6.437	-3.914	-112.81	-1.31
3.25	0.	0.00	.000	-99.	-2.216	3.290	-1.271	-65.88	-0.37
3.25	-5.	0.56	.012	279.	-2.217	3.301	-1.268	-65.91	-0.38
3.25	-10.	1.11	.023	140.	-2.221	3.336	-1.262	-66.00	-0.38
3.25	-15.	1.66	.035	93.	-2.230	3.393	-1.256	-66.15	-0.38
3.25	-20.	2.21	.046	70.	-2.246	3.473	-1.258	-66.36	-0.38
3.25	-25.	2.74	.058	56.	-2.274	3.574	-1.280	-66.63	-0.39

(Cont'd)

TABLE C-17

TURNING EQUILIBRIUM AND STABILITY FOR LIGHT SHIP

2-D Rudder Coefficients

V	δ_R	β_o	ω	R	Y_v	Y_r	N_v	N_r	σ_i
ft/sec	deg	deg	rad/sec	ft	lb sec/ft	lb sec	lb sec	ft lb sec	sec^{-1}
1.50	-20.	-2.47	-.032	47.	-0.254	2.720	-0.120	-25.44	-0.04
2.00	-20.	5.02	.054	37.	-0.529	2.754	-0.049	-36.73	-0.10
2.50	-20.	7.06	.103	24.	-1.131	3.895	-0.250	-50.61	-0.20
3.00	-20.	7.35	.142	21.	-2.003	5.026	-0.768	-64.31	-0.35
3.50	-20.	7.21	.170	21.	-3.182	5.928	-1.567	-77.50	-0.56
4.00	-20.	7.01	.187	21.	-4.646	6.670	-2.497	-90.39	-0.81
4.50	-20.	6.84	.193	23.	-6.318	7.465	-3.304	-103.54	-1.10
5.00	-20.	6.71	.188	27.	-8.073	8.676	-3.622	-117.85	-1.42
3.25	0.	0.00	.000	-99.	-2.216	3.290	-1.271	-65.88	-0.37
3.25	-5.	1.99	.042	78.	-2.230	3.437	-1.235	-66.27	-0.38
3.25	-10.	3.91	.082	40.	-2.279	3.869	-1.154	-67.38	-0.39
3.25	-15.	5.70	.120	27.	-2.379	4.565	-1.093	-69.01	-0.41
3.25	-20.	7.30	.157	21.	-2.554	5.506	-1.139	-70.96	-0.45
3.25	-25.	8.67	.195	17.	-2.823	6.678	-1.369	-73.05	-0.50

TABLE C-18

TURNING EQUILIBRIUM AND STABILITY FOR DESIGN LOAD

LSF Rudder Coefficients

V	δ_R	β_o	ω	R	Y_v	Y_r	N_v	N_r	σ_i
ft/sec	deg	deg	rad/sec	ft	lb sec/ft	lb sec	lb sec	ft lb sec	sec^{-1}
1.50	-20.	1.38	-.005	299.	-0.168	3.568	0.252	-22.97	-0.03
2.00	-20.	1.31	.009	212.	-0.515	4.274	-0.040	-37.91	-0.06
2.50	-20.	1.13	.015	172.	-1.092	4.953	-0.492	-52.88	-0.11
3.00	-20.	0.97	.016	183.	-1.950	5.622	-1.090	-67.83	-0.20
3.50	-20.	0.85	.017	204.	-3.141	6.290	-1.818	-82.77	-0.32
4.00	-20.	0.76	.017	231.	-4.716	6.957	-2.658	-97.71	-0.48
4.50	-20.	0.68	.017	260.	-6.725	7.625	-3.594	-112.66	-0.68
5.00	-20.	0.62	.017	292.	-9.219	8.293	-4.612	-127.60	-0.94
3.25	0.	0.00	.000	-99.	-2.501	5.930	-1.441	-75.23	-0.25
3.25	-5.	0.23	.004	770.	-2.501	5.932	-1.441	-75.23	-0.25
3.25	-10.	0.45	.008	385.	-2.501	5.937	-1.441	-75.24	-0.25
3.25	-15.	0.68	.013	257.	-2.501	5.945	-1.440	-75.27	-0.25
3.25	-20.	0.91	.017	193.	-2.501	5.956	-1.439	-75.30	-0.25
3.25	-25.	1.14	.021	154.	-2.501	5.971	-1.438	-75.34	-0.25

(Cont'd)

TABLE C-18

TURNING EQUILIBRIUM AND STABILITY FOR DESIGN LOAD

Estimated Rudder Coefficients

V ft/sec	δ_R deg	β_o deg	ω rad/sec	R ft	Y_v lb sec/ft	Y_r lb sec	N_v lb sec ft	N_r lb sec	σ_i sec^{-1}
1.50	-20.	-0.82	-.001	1091.	-0.168	3.586	0.252	-22.91	-0.03
2.00	-20.	1.39	.014	142.	-0.515	4.288	-0.039	-37.95	-0.06
2.50	-20.	2.01	.030	84.	-1.093	5.028	-0.488	-53.09	-0.11
3.00	-20.	2.14	.039	77.	-1.953	5.738	-1.081	-68.16	-0.20
3.50	-20.	2.10	.044	80.	-3.145	6.423	-1.803	-83.15	-0.32
4.00	-20.	2.01	.046	86.	-4.720	7.095	-2.639	-98.11	-0.48
4.50	-20.	1.90	.048	94.	-6.729	7.760	-3.572	-113.04	-0.68
5.00	-20.	1.79	.049	103.	-9.224	8.423	-4.586	-127.98	-0.94
3.25	0.	0.00	.000	-99.	-2.501	5.930	-1.441	-75.23	-0.25
3.25	-5.	0.53	.010	311.	-2.501	5.940	-1.440	-75.25	-0.25
3.25	-10.	1.07	.021	156.	-2.502	5.968	-1.438	-75.33	-0.25
3.25	-15.	1.60	.031	104.	-2.502	6.016	-1.433	-75.47	-0.25
3.25	-20.	2.13	.042	78.	-2.504	6.083	-1.427	-75.66	-0.25
3.25	-25.	2.66	.052	63.	-2.506	6.168	-1.418	-75.90	-0.25

(Cont'd)

TABLE C-18

TURNING EQUILIBRIUM AND STABILITY FOR DESIGN LOAD

2-D Rudder Coefficients

V	δ_R	β_o	Ω	R	Y_v	Y_r	N_v	N_r	σ_i
ft/sec	deg	deg	rad/sec	ft	lb sec/ft	lb sec	lb sec	ft lb sec	sec^{-1}
1.50	-20.	-2.94	-.005	305.	-0.168	3.595	0.253	-22.97	-0.03
2.00	-20.	4.92	.050	40.	-0.520	4.666	-0.019	-39.05	-0.06
2.50	-20.	6.96	.103	24.	-1.122	6.152	-0.386	-56.29	-0.12
3.00	-20.	7.37	.133	23.	-2.003	7.282	-0.897	-72.54	-0.21
3.50	-20.	7.27	.151	23.	-3.210	8.144	-1.554	-88.05	-0.33
4.00	-20.	6.98	.161	25.	-4.794	8.857	-2.337	-103.14	-0.50
4.50	-20.	6.64	.167	27.	-6.810	9.492	-3.226	-118.01	-0.71
5.00	-20.	6.28	.170	29.	-9.309	10.090	-4.202	-132.78	-0.97
3.25	0.	0.00	.000	-99.	-2.501	5.930	-1.441	-75.23	-0.25
3.25	-5.	1.91	.037	87.	-2.503	6.053	-1.430	-75.57	-0.25
3.25	-10.	3.79	.074	44.	-2.512	6.414	-1.392	-76.60	-0.26
3.25	-15.	5.61	.109	30.	-2.530	6.988	-1.322	-78.23	-0.26
3.25	-20.	7.35	.143	23.	-2.563	7.738	-1.208	-80.36	-0.27
3.25	-25.	8.99	.174	19.	-2.614	8.622	-1.043	-82.88	-0.28

TABLE C-19

DIRECTIONAL STABILITY AND TURNING CHARACTERISTICS
FOR SIMPLIFIED CONDIGURATION

FOUR FIXED STRUTS & PROPOSED RUDDER

Stability Index σ_i = -5.4u

Turning Characteristics

δ_5 deg	R ft
- 5	409
-10	204
-15	136
-20	102
-25	82

FOUR FIXED STRUTS & 2-D RUDDER

Stability Index σ_i = -5.8u

Turning Characteristics

δ_5 deg	R ft
- 5	154
-10	77
-15	51
-20	38
-25	31

STRUT FLAPS AFT ONLY

Stability Index σ_i = -1.3u

Turning Characteristics

k=0.35 c_δ = 0

$\delta_{3,4}$ deg	R ft
- 5	132
-10	66
-15	44
-20	33
-25	26

STRUT FLAPS FORE AND AFT

Stability Index σ_i = -1.3u

Turning Characteristics k=0.35 c_δ=0.5			Turning Characteristics k=0.5 c_δ=0.5		
$\delta_{1,2}$ deg	$\delta_{3,4}$ deg	R ft	$\delta_{1,2}$ deg	$\delta_{3,4}$ deg	R ft
2.5	- 5	88	2.5	- 5	62
5.0	-10	44	5.0	-10	31
7.5	-15	29	7.5	-15	20
10.0	-20	22	10.0	-20	15
12.5	-25	18	12.5	-25	12

TABLE C-20

LOW SPEED DRAG
DESIGN LOAD — WHEELS DOWN

(a) Model Drag λ=13

Wetted length = 5.5 ft
Wetted area = 28.4ft^2
$\tilde{V} = V - V_o$
V_o = 3.25 ft/sec

V ft/sec	$\tilde{V}$ ft/sec	X_G lb	R_e 10^5	C_f 10^{-3}	X_f lb	$X_G - X_f$ lb
1.5	-1.75	3.0	8.03	4.602	0.3	2.7
2.0	-1.25	5.4	10.7	4.355	0.5	4.9
2.5	-0.75	8.6	13.4	4.170	0.7	7.9
3.0	-0.25	12.4	16.0	4.035	1.0	11.4
3.5	0.25	17.0	18.7	3.921	1.3	15.7
4.0	0.75	22.0	21.4	3.824	1.7	20.6
4.5	1.25	28.4	24.1	3.742	2.1	26.3
5.0	1.75	35.1	26.8	3.673	2.5	32.6

(b) Estimated Prototype Drag

Wetted length = 71.5 ft
Wetted area = 4800 ft^2

V knots	V ft/sec	$X_G - X_f$ lb	R_e 10^7	C_f 10^{-3}	X_f lb	X_G lb
3.2	5.41	5,900	3.27	2.438	340	6,240
4.3	7.21	10,800	4.36	2.335	580	11,380
5.3	9.01	17,400	5.45	2.260	880	18,280
6.4	10.82	25,000	6.54	2.201	1,230	26,230
7.5	12.62	34,500	7.63	2.153	1,640	36,140
8.5	14.42	45,200	8.72	2.112	2,100	47,300
9.6	16.22	57,800	9.81	2.078	2,610	60,410
10.7	18.03	71,600	10.9	2.048	3,180	74,780

128

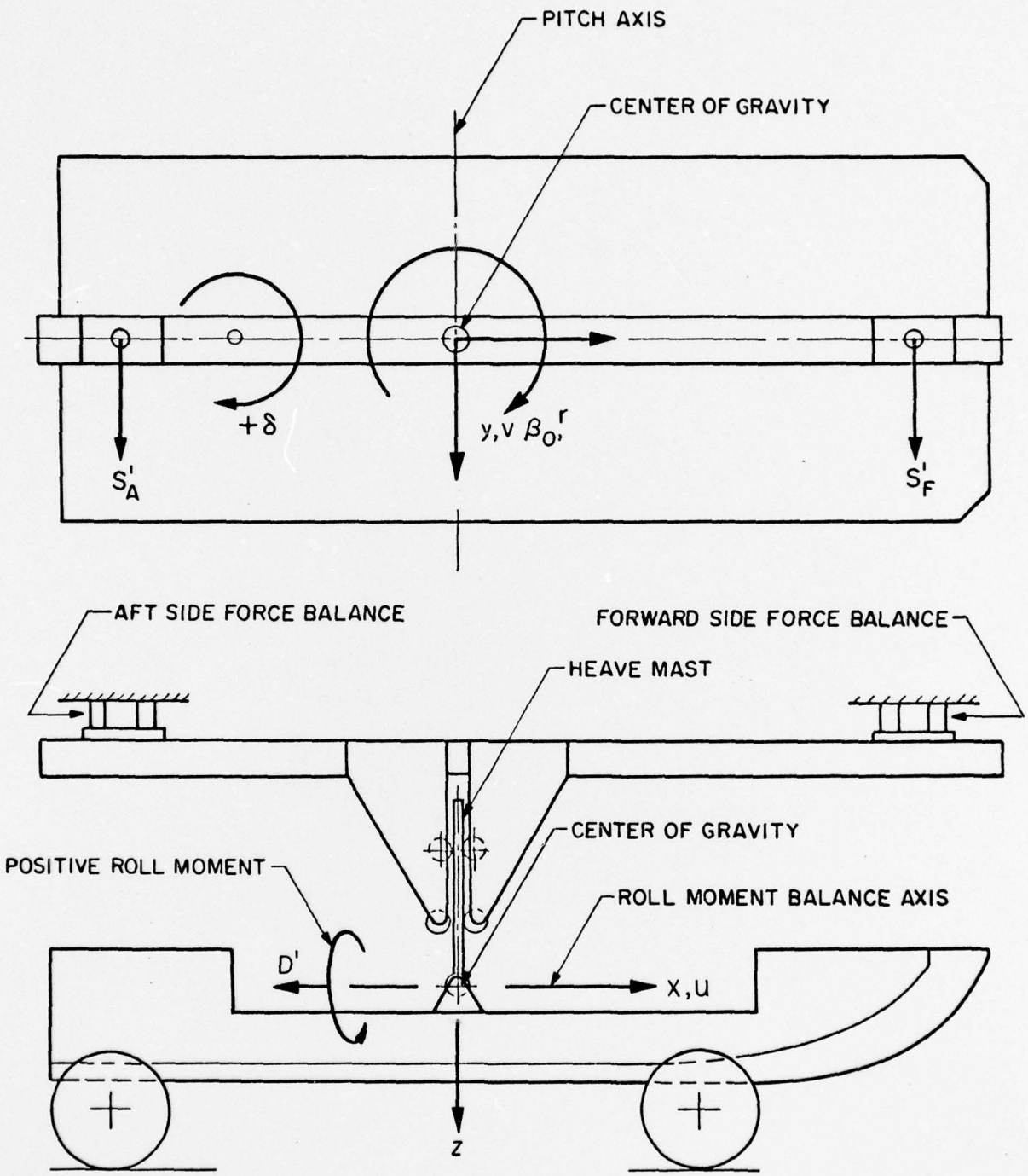

FIG. C-I. MODEL SETUP AND SIGN CONVENTIONS FOR TURNING TESTS

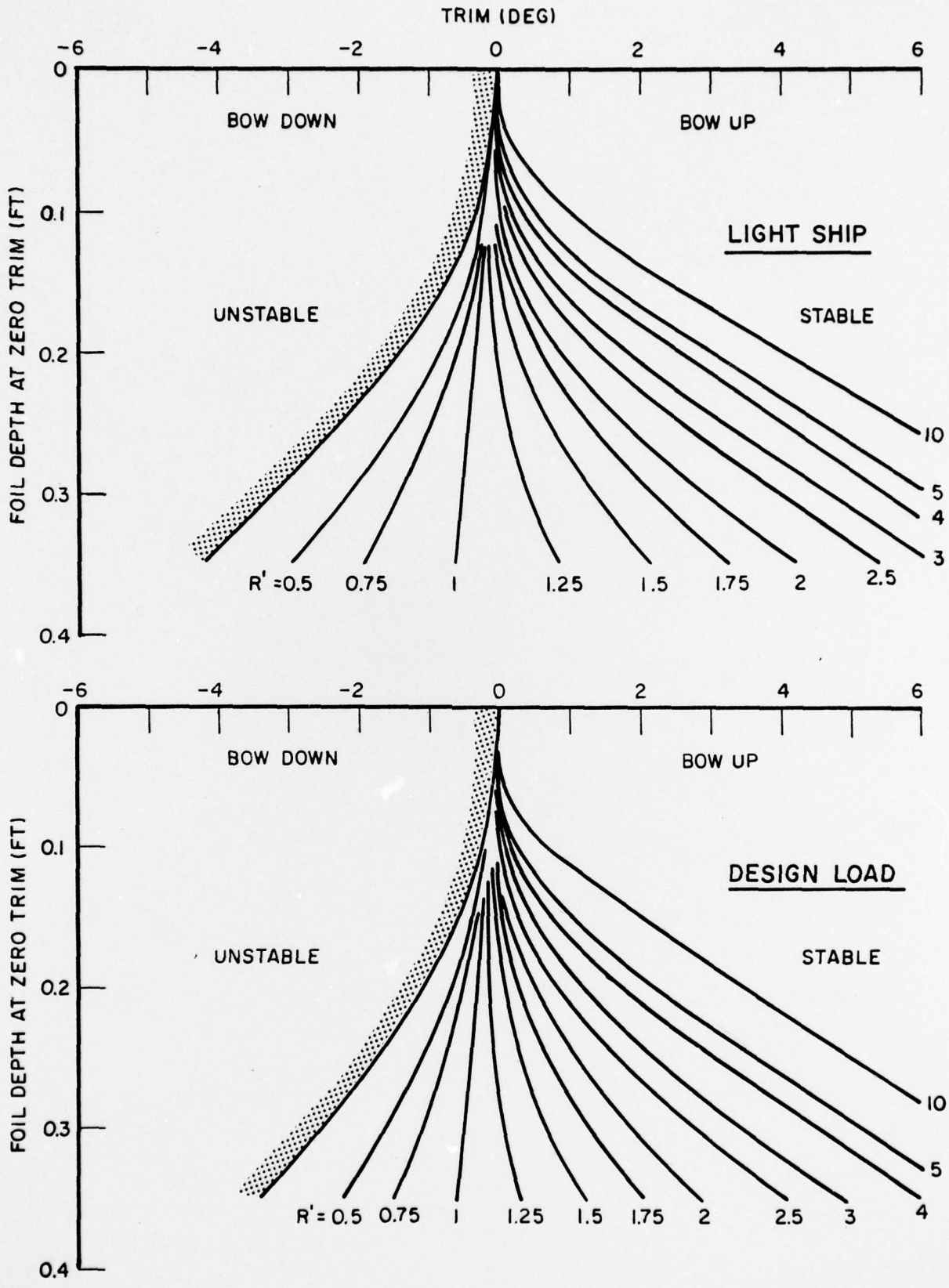

FIG. C-2. DIRECTIONAL STABILITY AND TURNING RADIUS WHEN FOILBORNE WITH STRUT FLAPS

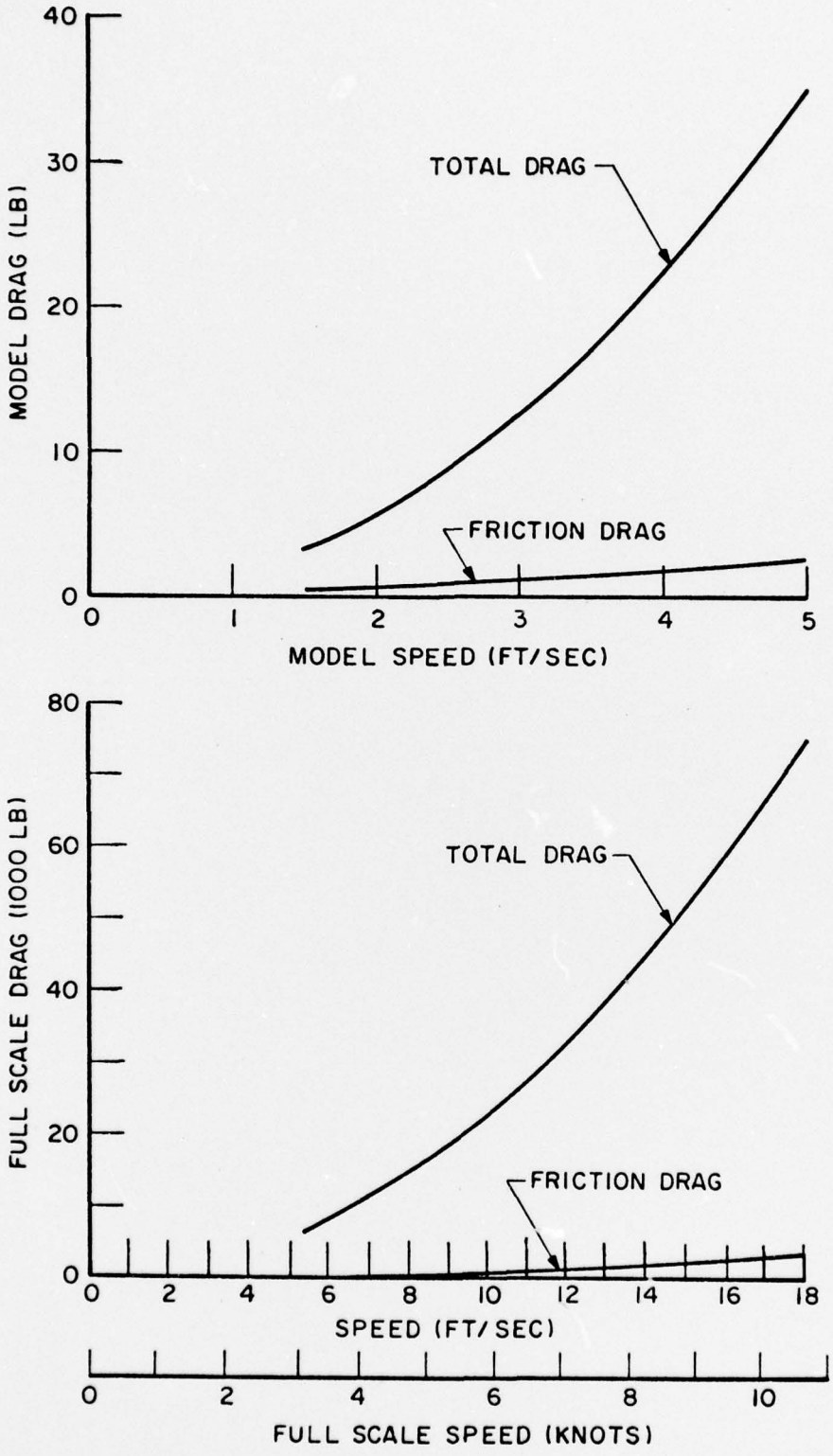

FIG. C-3. MODEL AND PROTOTYPE DRAG FOR DESIGN LOAD WITH WHEELS DOWN